ANALYSIS OF SPATIAL-TEMPORAL VARIATIONS OF DROUGHT IN OKLAHOMA

A Dissertation

by

LIYAN TIAN

Submitted to the Office of Graduate and Professional Studies of
Texas A&M University
in partial fulfillment of the requirements for the degree of

DOCTOR OF PHILOSOPHY

Chair of Committee,	Steven M. Quiring
Committee Members,	Oliver W. Frauenfeld
	Brendan Roark
	Huilin Gao
Head of Department,	David M. Cairns

August 2017

Major Subject: Geography

ABSTRACT

Drought is a recurrent natural hazard that has impacts on agriculture, hydrology, ecosystem, and social-economy. A comprehensive analysis of drought is valuable for drought assessment and mitigation. Oklahoma is a state that frequently experiences drought. The goal of this dissertation is to analyze the spatial-temporal patterns of drought in Oklahoma. Specifically, it developed a new drought index and evaluated it against a number of widely-used drought indices. Then, the spatial-temporal patterns of drought in Oklahoma were investigated using the most suitable drought index. Finally, the impacts of climate oscillations on the drought were quantified and used to develop drought forecasts.

A new drought index called the Precipitation Evapotranspiration Difference Condition Index (PEDCI) was developed. It overcomes a number of the limitations of other drought indices. The comparison of PEDCI and six widely used drought indices (Palmer's Drought Severity Index, Z-Index, Standardized Precipitation Evapotranspiration Index (SPEI), Standardized Precipitation Index, percent normal, and percentiles) demonstrated that the performance of drought indices varies temporally and spatially. The SPEI is the drought index that is the most representative of soil moisture conditions. The correlations with winter wheat yield indicated that drought indices such as SPEI, Z-Index and PEDCI, which are based on precipitation and evapotranspiration, are most appropriate for representing the impact of drought conditions on crop yield.

Oklahoma was divided into four regions (southeast, southwest, northeast, and northwest Oklahoma) for the spatial and temporal analysis of drought. Drought frequency in northwest Oklahoma is higher than in other regions, and the frequency in spring is higher than in other seasons. There is a decadal-scale drought cycle in Oklahoma. Droughts are caused by both decreases in precipitation and increases in evapotranspiration, especially in recent years.

Finally, drought is influenced by multiple climate oscillations. Seven regression models were developed for producing drought forecasts. The CCA-based regression model using multiple teleconnections at different lags was more skillful than the other drought forecast models. While skill is limited in some seasons, this method has promise for providing drought early warning in Oklahoma.

ACKNOWLEDGEMENTS

I would like to sincerely thank my committee chair, Dr. Steven Quiring. Thanks Dr. Quiring for his great guidance, encouragement, patience and support during my doctoral degree program. I would also like to give my wholehearted thanks to my committee members, Dr. Frauenfeld, Dr. Gao, and Dr. Roark for being on my committee and their support and suggestions throughout the work on this research.

Thanks also go to my friends and colleagues in the Climate Science Lab. Thanks everyone for the suggestions and comments on my research as well as numerous help during my time at Texas A&M University. I also want to give my appreciation to all of the faculty and staff in the Geography Department for their kindness and help which made my time at Texas A&M University a great experience.

I also want to extend my gratitude to all members of the Support Women in Geography (SWIG) group for their meaningful support and help.

Finally, thanks to my parents and boyfriend for their tremendous encouragement and love throughout these years.

CONTRIBUTORS AND FUNDING SOURCES

Contributors

Part 1, faculty committee recognition

This work was supervised by a dissertation committee consisting of Professor Steven Quiring [advisor], Professor Oliver Frauenfeld and Professor Brendan Roark of the Department of Geography and Professor Huilin Gao of the Department of Civil Engineering.

Part 2, student/advisor contributions

Assistance with the analyses in Chapter 5 were provided by Zachary Leasor and Dr. Quiring of the Department of Geography and were published in 2016. Assistance with the analyses in Chapter 3 were provided by Shanshui Yuan and Dr. Quiring of the Department of Geography and will be submitted to Agricultural and Forest Meteorology in May 2017. All other work for the dissertation was completed by the student under the advisement of Steven Quiring of the Department of Geography.

Funding Sources

This work was supported by Department of Interior's South Central Climate Science Center Project "Developing Effective Tools for Communicating Drought Information". Dr. Mark Shafer, University of Oklahoma, is the Principal Investigator (PI) of this project.

NOMENCLATURE

AMO	Atlantic Multidecadal Oscillation
AWC	Available Water Content
CCA	Canonical Correlation Analysis
CDL	Cropland Data Layer
CPC	Climate Prediction Center
CRU TS	Climatic Research Unit Time-Series
EA	East Atlantic pattern
EDI	Effective Drought Index
ENSO	El Niño-Southern Oscillation
EOF	Empirical Orthogonal Function
FAO	Food and Agricultural Organization
HSS	Heidke Skill Score
IPCC	Intergovernmental Panel on Climate Change
MCDW	Monthly Climatic Data for the World
MDO	Monthly Drought Outlooks
NAO	North Atlantic Oscillation
NARR	North America Regional Reanalysis
NASMD	North American Soil Moisture Database
NASS	National Agricultural Statistics Service
NCDC	National Climatic Data Center

NDI	NOAA Drought Index
NLDAS	North American Land Data Assimilation System
PCA	Principal Component Analysis
PDO	Pacific Decadal Oscillation
PDSI	Palmer's Drought Severity Index
PED	Difference between Precipitation and PET
PEDCI	Precipitation Evapotranspiration Difference Condition Index
PET	Potential Evapotranspiration
PNA	Pacific-North American pattern
PRISM	Parameter elevation Regression on Independent Slopes Model
SPEI	Standardized Precipitation Evapotranspiration Index
SPEI1	SPEI at 1-month scale
SPEI3	SPEI at 3-month scale
SPEI6	SPEI at 6-month scale
SPI	Standardized Precipitation Index
SST	Sea Surface Temperature
SYRS	Standardized Yield Residuals Series
USDA	United States Department of Agriculture
VDI	Vegetation Condition Index
WMO	World Meteorological Organization
WP	West Pacific Pattern
WWR	World Weather Records

TABLE OF CONTENTS

Page

LIST OF FIGURES

Page

LIST OF TABLES

Page

CHAPTER I

INTRODUCTION

1.1 Introduction

Drought is a recurring natural hazard that has an impact on many aspects of human life (Heim, 2002). It can cause significant damage to agriculture, ecosystems and society (A. K. Mishra & Singh, 2010). A comprehensive drought characterization is essential for drought management and mitigation (Zargar, Sadiq, Naser, & Khan, 2011). It can improve drought early warning and drought risk analysis, thereby minimizing the damage caused by drought (Zargar et al., 2011).

Drought indices are widely used tools to characterize drought conditions. Drought indices quantitatively measure drought conditions using variables such as precipitation, evapotranspiration, soil moisture, and streamflow (Heim, 2002; Zargar et al., 2011). Since the development of drought indices can be based on different indicators, more than 150 drought indices have been developed (Niemeyer, 2008). These drought indices have been developed for different places, objectives, and applications (Zargar et al., 2011). Since the performance of drought indices varies by region and application, it is important to identify the most suitable drought index for a specific region and application so that drought conditions can be accurately measured.

Once the most appropriate drought index for a particular region and application has been identified, the spatial-temporal patterns of drought can be quantified. Unlike

other natural hazards such as floods, which typically occur in a certain region and have a well-defined return period, droughts are more complex (Vicente-Serrano, 2006). Drought onset is usually slow, and the impact of droughts can affect a large area for a long period of time (A. K. Mishra & Singh, 2010). Knowledge of the temporal behavior of droughts and their spatial patterns is vital for the drought management and mitigation (Vicente-Serrano, 2006).

Generally, the complicated spatial-temporal patterns of droughts are controlled by atmospheric circulation patterns (Vicente-Serrano, 2006). Among these atmospheric patterns, El Niño-Southern Oscillation (ENSO) is regarded as the major factor causing drought (Trenberth et al., 2014). However, it is necessary to investigate the impacts of multiple atmospheric circulation patterns on drought (Stevens & Ruscher, 2014). The relationships between drought conditions and atmospheric circulation patterns can be used as the basis for drought forecasting.

This doctoral research will analyze the spatial-temporal patterns of drought in Oklahoma. It will develop a new drought index and evaluate it against a number of widely-used drought indices to identify the best drought index for agricultural drought monitoring in Oklahoma. This drought index will then be used to analyze the spatial-temporal patterns of drought in Oklahoma and to investigate the relationship between drought and multiple climate oscillations. This dissertation will focus on three research questions: 1) What is the best drought index for agricultural drought monitoring in Oklahoma? 2) What are the primary spatial-temporal patterns of drought in Oklahoma? 3) What causes drought in Oklahoma?

Specifically, it will:

(1) Establish a new drought index;

(2) Identify the best drought index for agricultural drought monitoring in Oklahoma;

(3) Analyze the spatial-temporal patterns of drought in Oklahoma;

(4) Investigate the impacts of climate oscillations on the spatial-temporal variations of drought in Oklahoma.

1.2 Study Area

Oklahoma is a state that frequently experiences drought. For example, the 1998 drought caused about $2.0 billion in agricultural losses in Oklahoma (Graumann, Lott, McCown, & Ross, 1998). Recently, the 2011 drought caused $1.6 billion in agricultural losses in Oklahoma (Stotts, 2011). Oklahoma is located in a temperate region and experiences occasional extremes of temperature and precipitation typical of a continental climate. Weather patterns within the state vary dramatically over relatively small regions in a short time. The climate of the eastern part of Oklahoma is heavily influenced by southerly winds bringing moisture from the Gulf of Mexico. The climate of the western part of Oklahoma is semi-arid. There are strong precipitation and temperatures gradients from east to west. The average annual temperature in the southeast areas is about 16 °C with an annual rainfall over 1200 mm, while, in the western areas, the average annual temperature is about 14 °C, with an annual rainfall of ~500 mm (Illston, Basara, & Crawford, 2004).

This region contains the Oklahoma Mesonet, the densest network of continuously-monitoring in situ soil moisture stations in the United States. The Oklahoma Mesonet consists of 121 meteorological stations across Oklahoma. The stations are evenly distributed across Oklahoma (Figure 1.1). The stations measure ten variables including rainfall, temperature, soil moisture, humidity, pressure, solar radiation, soil temperature, leaf wetness, wind speed and direction every 15 minutes (Brock et al., 1995). This study will use soil moisture observations from these stations to evaluate the drought indices.

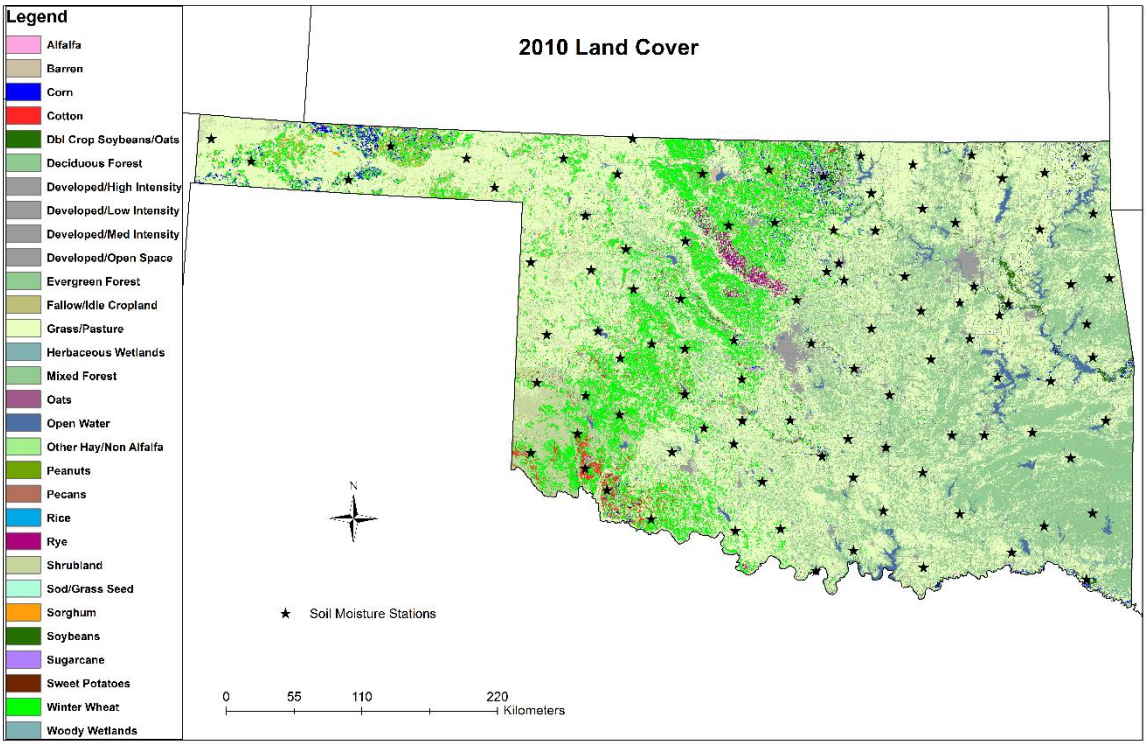

Figure 1.1 Dominant land cover in Oklahoma. Stars indicate the location of Oklahoma Mesonet stations that are used in this study.

CHAPTER II

DEVELOPMENT OF A NEW DROUGHT INDEX

2.1 Introduction

Drought is one of the most complex natural hazards, which has impacts on agriculture, hydrology, environment, society and economy. It is difficult to have a single definition of drought because of the broad impacts of drought as well as the differences in water demand in different regions around the world (William M Alley, 1985; A. Dai, Trenberth, & Qian, 2004; Keyantash & Dracup, 2002; Wilhite, 2000). The drought definitions developed by the American Meteorological Society (AMS) in 1997 have been widely used (Heim, 2002; A. K. Mishra & Singh, 2010; Zargar et al., 2011). The AMS divides the drought definitions into four categories: meteorological drought, agricultural drought, hydrological drought, and socioeconomic drought (American Meteorological Society, 1997). Meteorological drought is caused by precipitation deficiency (Palmer, 1965). It can develop quickly and end abruptly. The subsequent soil water depletion can cause an agricultural drought (William M Alley, 1985; Heim, 2002). Agricultural drought occurs during the crop growing season and has impacts on crop yield. Prolonged precipitation deficits that cause reductions in streamflow, groundwater, reservoir, and lake levels will result in hydrological drought (William M Alley, 1985; Dracup, Lee, & Paulson, 1980). Finally, the impacts of meteorological, agricultural, and hydrological drought can also affect people and economic activities, this is defined as

socioeconomic drought (American Meteorological Society, 2004; Heim, 2002; Zargar et al., 2011).

Drought indices are widely used for drought quantification. However, because of the complexity of drought characteristics and definitions, it is difficult to have a single index to adequately capture the intensity and severity of drought and its potential impacts (Vicente-Serrano et al., 2012). Many studies have developed drought indices and, at present, there are more than 150 drought indices (Zargar et al., 2011). These indices are used to measure different types of drought and are developed for a variety of applications. Some of the indices can describe the meteorological drought, such as the Rainfall Anomaly Index (Van Rooy, 1965), Drought Severity Index (Bryant, Arnell, & Law, 1992), and National Rainfall Index (Gommes & Petrassi, 1996). Some drought indices are used to quantify the impacts on agriculture and hydrology, such as Crop Moisture Index (Palmer, 1968), Crop Specific Drought Index (Meyer, Hubbard, & Wilhite, 1993) and Palmer Hydrological Drought Index (Palmer, 1965; Zargar et al., 2011).

Among these indices, the Palmer Drought Severity Index (PDSI), Standardized Precipitation Index (SPI) and Standardized Precipitation Evapotranspiration Index (SPEI) are three of the most widely used drought indices. PDSI is a popular drought index for meteorological and agricultural drought analyses. It is based on a water balance model. Precipitation, temperature, evapotranspiration, and soil moisture are all considered in this index. It is more comprehensive than precipitation-only indices.

However, the calculation is more complicated and the index is less transparent than the SPI (Vicente-Serrano, Begueria, & Lopez-Moreno, 2010; Zargar et al., 2011).

The SPI was developed after the PDSI and it is only based on precipitation. It overcomes some of the limitations of PDSI. For example, it can be used for the analysis of drought at variable time scales. It can be used to monitor meteorological, agricultural and hydrological drought, depending on the timescale of the SPI. One limitation of SPI is that it only uses precipitation data, so it cannot reflect actual water demand (PET) (S. M. Vicente-Serrano et al., 2010; Zargar et al., 2011).

The SPEI was developed by Vicente-Serrano et al. (2010) and it combines the advantages of PDSI and SPI. It is based on precipitation and temperature and can be calculated at different time scales. S. M. Vicente-Serrano et al. (2010) indicated that temperature and evapotranspiration can play an important role in drought. Therefore, it is important to use a drought index that captures this influence. SPEI is calculated in a similar way to the SPI. The difference is that SPI only uses precipitation as input, while the SPEI uses the difference between precipitation and potential evapotranspiration (PET). One of the limitations of SPEI is that it is sensitive to the method of calculating PET. In addition, the SPEI is based on probability distribution function. The calculation of SPEI is complicate.

In this chapter, a new drought index will be developed. It is simpler than the SPEI and it can be applied for meteorological, agricultural, and hydrological drought. The new drought index, called the Precipitation Evapotranspiration Difference Condition Index (PEDCI), is based on the difference between precipitation and evapotranspiration.

The PEDCI is calculated using PET based on the Penman scheme. One advantage of the PEDCI is that it uses a normalization method that does not require any empirical parameters.

2.2 Data and Methods

2.2.1 PRISM Precipitation

Precipitation data from the Parameter elevation Regression on Independent Slopes Model (PRISM) is used for the study. PRISM is a set of monthly gridded climatic data product for the United States developed by the Spatial Climate Analysis Service at Oregon State University. The dataset includes precipitation, mean temperature, maximum/minimum temperature and dewpoint temperature. In-situ station data are ingested into the PRISM statistical mapping system. PRISM products use a weighted regression scheme for the complex climate regimes associated with orography, rain shadows, temperature inversions, slope aspect, coastal proximity, and other factors. The number of stations used in the analysis is nearly 13000 (Daly et al., 2008). Normals are available at 30-arcsec (800 meters) and monthly data are available at 2.5 arcmin (4 km) resolution. The monthly precipitation data can be downloaded at http://prism.oregonstate.edu/. Monthly precipitation data from 1981to 2014 were used in this study.

2.2.2 NLDAS Potential Evapotranspiration

Monthly PET from North American Land Data Assimilation System (NLDAS) from 1981 to 2014 were used in this study. NLDAS is available in near-real time and has a spatial resolution of 0.125 * 0.125 degrees. The dataset is available from 1979 to the present at hourly and monthly resolution. The potential evaporation data in the NLDAS-2 primary forcing dataset was computed using the modified Penman scheme of Mahrt and Ek (1984) (Ek et al., 2011). Figure 2.1 shows the NLDAS PET in January, 2000.

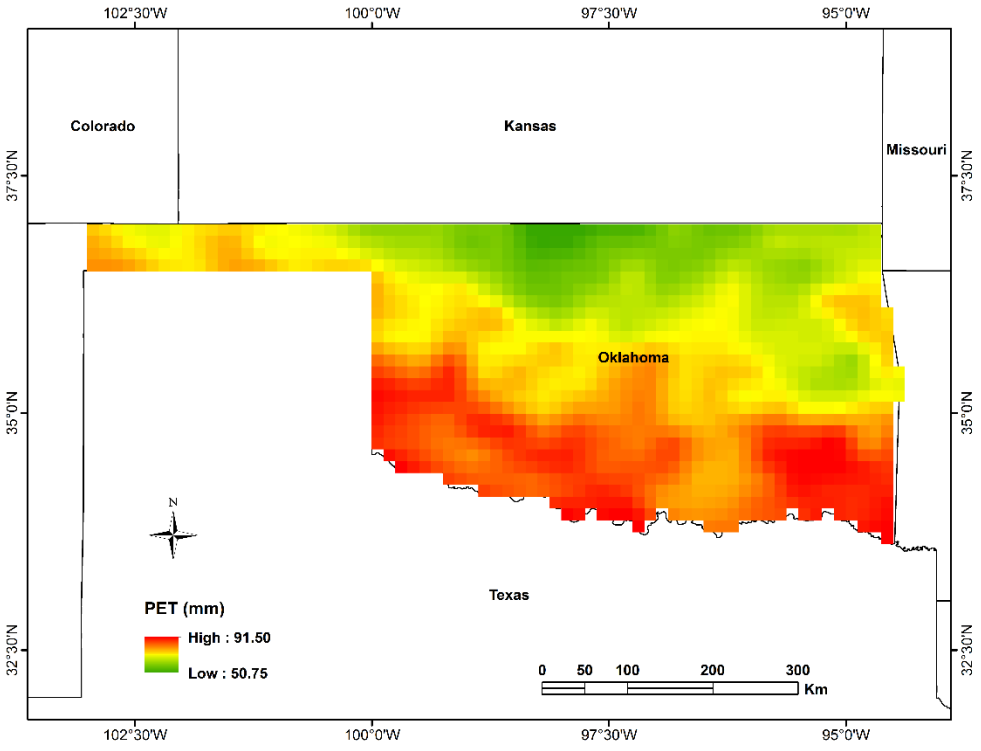

Figure 2.1 Monthly Potential Evapotranspiration (mm) derived from NLDAS-2 in Oklahoma in January, 2000.

2.2.3 Soil Moisture Data

Soil moisture data are used to evaluate the performance of the new drought index. This study uses in situ soil moisture measurements from 90 Oklahoma Mesonet stations (http://www.mesonet.org/) (Figure 1.1). Soil moisture measurements from Oklahoma Mesonet is volumetric water content of the soil which is estimated using the thermal matric potential that is measured by Campbell 229-L heat dissipation sensors at 5 cm, 25 cm and 60 cm. Daily volumetric water content were converted to monthly soil moisture percentiles. Soil moisture percentiles at 5 cm and 60 cm depth were used to evaluate the performance of the new drought index PEDCI. Figure 2.2 shows the monthly soil moisture percentile at 5cm from 2000 to 2014 at the station ACME, which is located in Grady, Oklahoma.

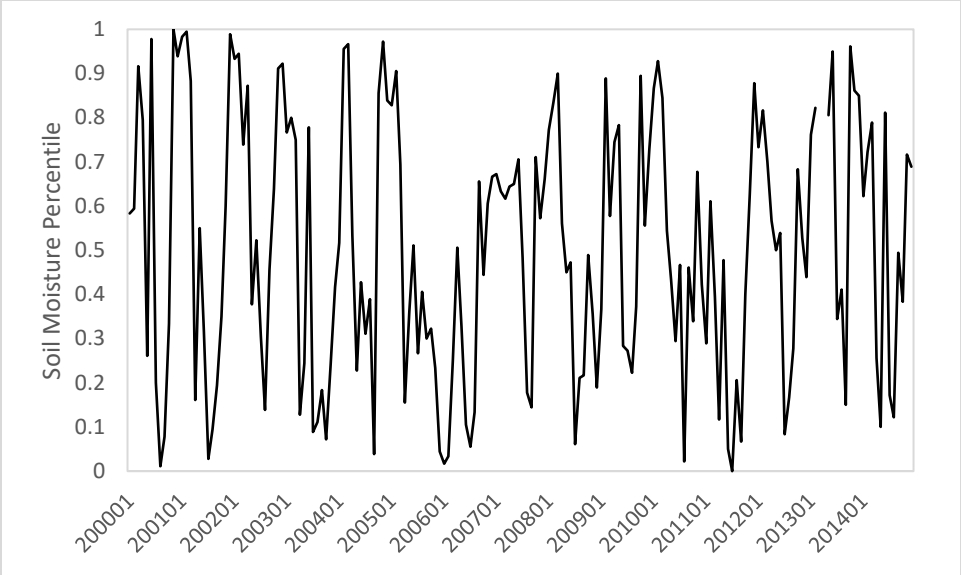

Figure 2.2 Mean monthly soil moisture (5 cm) from 2000 to 2014 in Acme, Oklahoma. Soil moisture data have been converted to percentiles based on the period of record.

2.2.4 PEDCI Calculation

The PEDCI is calculated using a location-based normalization method that is similar to that of the Vegetation Condition Index (Kogan, 1995). There are two steps to calculate PEDCI. The first step is to calculate the difference (D_i) between the precipitation *P* and PET for month *i* is calculated using:

$$D_i = P_i - PET_i \qquad \text{(Equation 2.1)}$$

This provides a simple measure of moisture supply (P) versus atmospheric water demand (PET) for the month.

The second step is to calculate the PEDCI for the month *i* using:

$$PEDCI_i = 100 * (D_i - D_{imin})/(D_{imax} - D_{imin}) \quad \text{(Equation 2.2)}$$

Where D_i, D_{imax}, and D_{imin} are the monthly difference between precipitation and PET for month *i*, its multi-year absolute maximum and minimum values for that month. The PEDCI varies from 0 to 100. PEDCI equals to 0 when D_i equals to D_{imin}, which corresponds to the driest conditions ever experienced. PEDCI equals to100 when D_i equals to D_{imax}, which corresponds to the wettest month ever experienced at that location in that month. The D_i values are positive when precipitation is larger than PET. The D_i values are negative when precipitation is less than PET. No matter whether the D_i values are positive or negative, the closer of the D_i values to D_{imax} values, the higher of PEDCI, which corresponds to the wetter conditions. The closer of the D_i values to D_{imin} values, the lower of PEDCI, which corresponds to the drier conditions.

2.3 Results

2.3.1 Regional Results

The PEDCI will first be compared to the SPEI from the global SPEI database (http://spei.csic.es/database.html) and the U.S. Drought Monitor (http://droughtmonitor.unl.edu/) for a single year so that the similarities and differences between these different drought indices can be visualized. This will be followed by a quantitative comparison of the PEDCI to soil moisture and SPEI in section 2.3.2 and 2.3.3. The SPEI and U.S. Drought Monitor were chosen for this comparison because they are both commonly used for drought monitoring. In addition, PEDCI uses similar

input data to the SPEI (P and PET) and therefore it is useful to directly compare these two indices. They have similar input data, but different calculation methods. The USDM is developed through an expert analysis a complex drought monitoring tool which incorporated with lots of drought information such as the measurements of climatic, hydrologic and soil moisture as well as reported drought impacts and observations.

In order to visually compare the PEDCI to the SPEI and USDM, the PEDCI and SPEI have been classified into five categories based on the USDM drought classification percentiles that are shown in Table 2.1.

Table 2-1 USDM Drought Classification

Level	Drought classes	Percentile
0	Abnormally dry	20% to 30%
1	Moderate drought	10% to 20%
2	Severe drought	5% to 10%
3	Extreme drought	2% to 5%
4	Exceptional drought	Less than 2%

The year of 2000 was subjectively chosen for this analysis because the available soil moisture data are from 2000 to 2014. The spatial patterns of drought conditions in 2000 based on PEDCI (Figure 2.3). Moisture conditions vary significantly from month to month. The year starts with no evidence of drought in Oklahoma. In February, there is

evidence of some scattered locations in western and southeastern Oklahoma where drought conditions are evident. However, these events are short-lived and by March, there is no evidence of drought in the state. The relatively moist conditions continue until August, when suddenly the majority of the state is in D3 and D4 conditions, except for a small region in northeastern Oklahoma. These drought conditions continue into September, although the severity and spatial extent of drought conditions, as represented by the PEDCI, has decreased by then. In October, conditions return to normal as a result of increased rainfall and there is no evidence of drought through the end of the year.

Figure 2.4 shows the spatial patterns of drought conditions in 2000 based on the SPEI. The SPEI is based the CRU precipitation and potential evapotranspiration dataset, which has a 0.5 * 0.5 degree spatial resolution. The spatial patterns of drought conditions based on the SPEI are similar to the spatial patterns of PEDCI in February, April, August and September. Since both of SPEI and PEDCI are based on the difference between precipitation and potential evapotranspiration, this makes sense. However, the PEDCI is available at a much higher spatial resolution (0.125 degrees). Therefore, it provides some finer-scale detail with regards to the spatial variability of drought conditions that is not available from the SPEI. It is also helpful to note that both the PEDCI and SPEI are in agreement that drought conditions are not present in March, June, October, November and December.

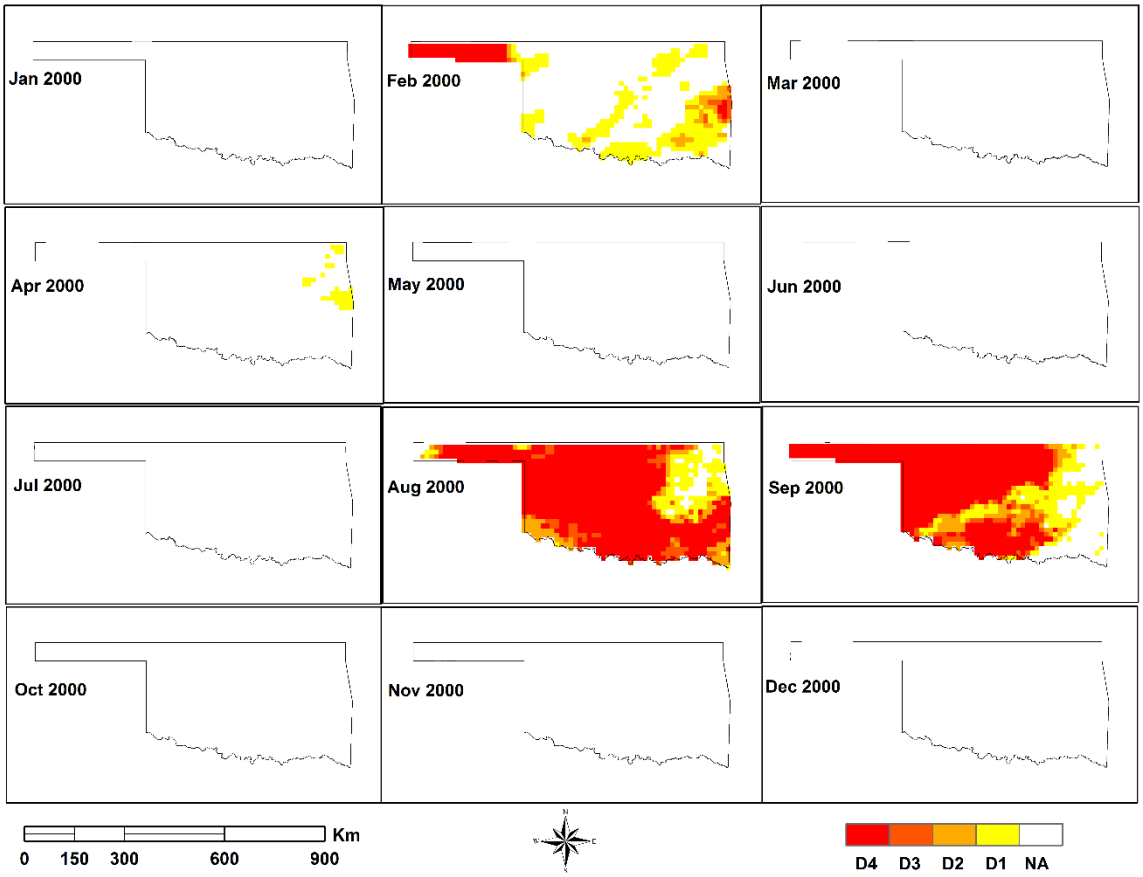

Figure 2.3 Monthly PEDCI values in 2000. PEDCI has been converted to USDM percentiles based on Table 2.1.

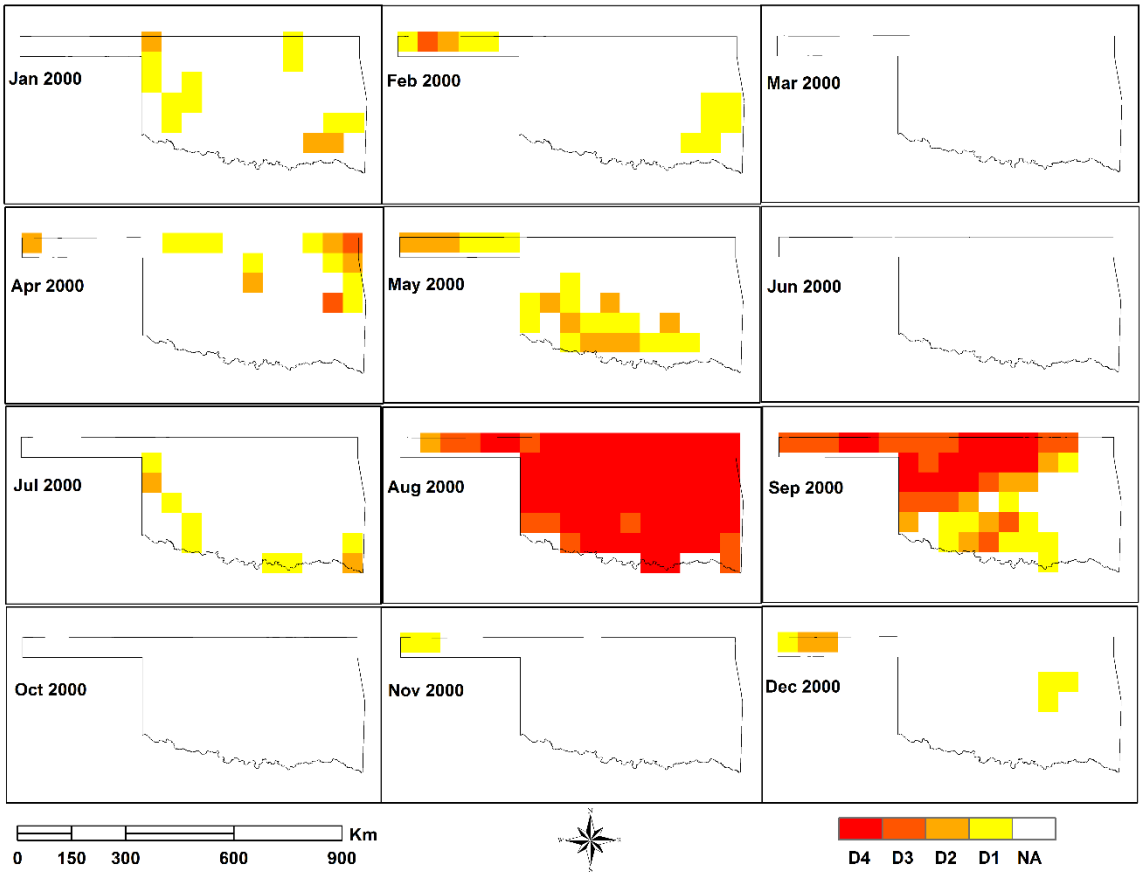

Figure 2.4 Monthly SPEI (1-month SPEI) in Oklahoma (January to December 2000).

However, there are a few months when differences between the SPEI and PEDCI are observed. The SPEI shows some D1 and D2 drought conditions scattered across Oklahoma in January, while the PEDCI does not indicate any drought conditions. Similarly, in April and May the SPEI indicates more widespread and severe drought conditions than depicted by the PEDCI. It is not surprising to observe that there are differences between these two drought indices because they have different spatial scales, different sources of input data and different calculation methods.

Figure 2.5 shows the drought patterns based on the USDM (Staff National Drought Mitigation Center, 2000). One challenge in comparing the PEDCI to the USDM is that it has a different spatial and temporal resolution. The USDM is relatively coarse spatially, but provides a weekly map of conditions. In addition, the USDM is a hybrid drought monitoring product. The USDM is developed using expert analysis of many types of information including precipitation, streamflow, soil moisture and drought impacts and observations, including the SPEI. It is updated on a weekly basis and the spatially resolution is roughly at the county level. Qualitatively, the spatial and temporal drought patterns depicted by the USDM are consistent with the PEDCI. For example, the presence and location of drought conditions depicted by the USDM on February 29, 2000 is consistent with the February PEDCI. There also is agreement between the USDM and PEDCI on the general lack of drought conditions in April through July. Beginning in August, the USDM depicts the onset of drought conditions across much of Oklahoma and that by the end of September the drought has peaked and covers most of the state. The USDM also depicts that recovery occurs relatively quickly and that by November, Oklahoma is drought free. The primary disagreement between the USDM and PEDCI is in regards to the severity and timing of drought onset and recovery. During September, the USDM depicts the drought severity as D1 and D2 (moderate and severe drought), while the PEDCI and SPEI depict drought conditions as D3 and D4 (extreme and exceptional drought). In general, the PEDCI depicts that drought conditions are substantially more severe than the USDM. This is in part because the USDM represents all types of drought, not just meteorological or agricultural. Therefore,

during short-term drought events, like August and September 2000, it will tend to under-predict the severity of meteorological drought because it is likely that long-term hydrological drought indicators like lake and reservoir levels have not responded. There is also a difference in the timing of drought onset and demise. The USDM tends to show that drought onset and demise occurs later than operational drought monitoring products. This is, in part, due to the fact that the USDM is an impacts-based drought monitoring product and so there is a lag between precipitation deficits and drought impacts.

Generally, it appears that the PEDCI can represent the spatial and temporal patterns of drought in Oklahoma.

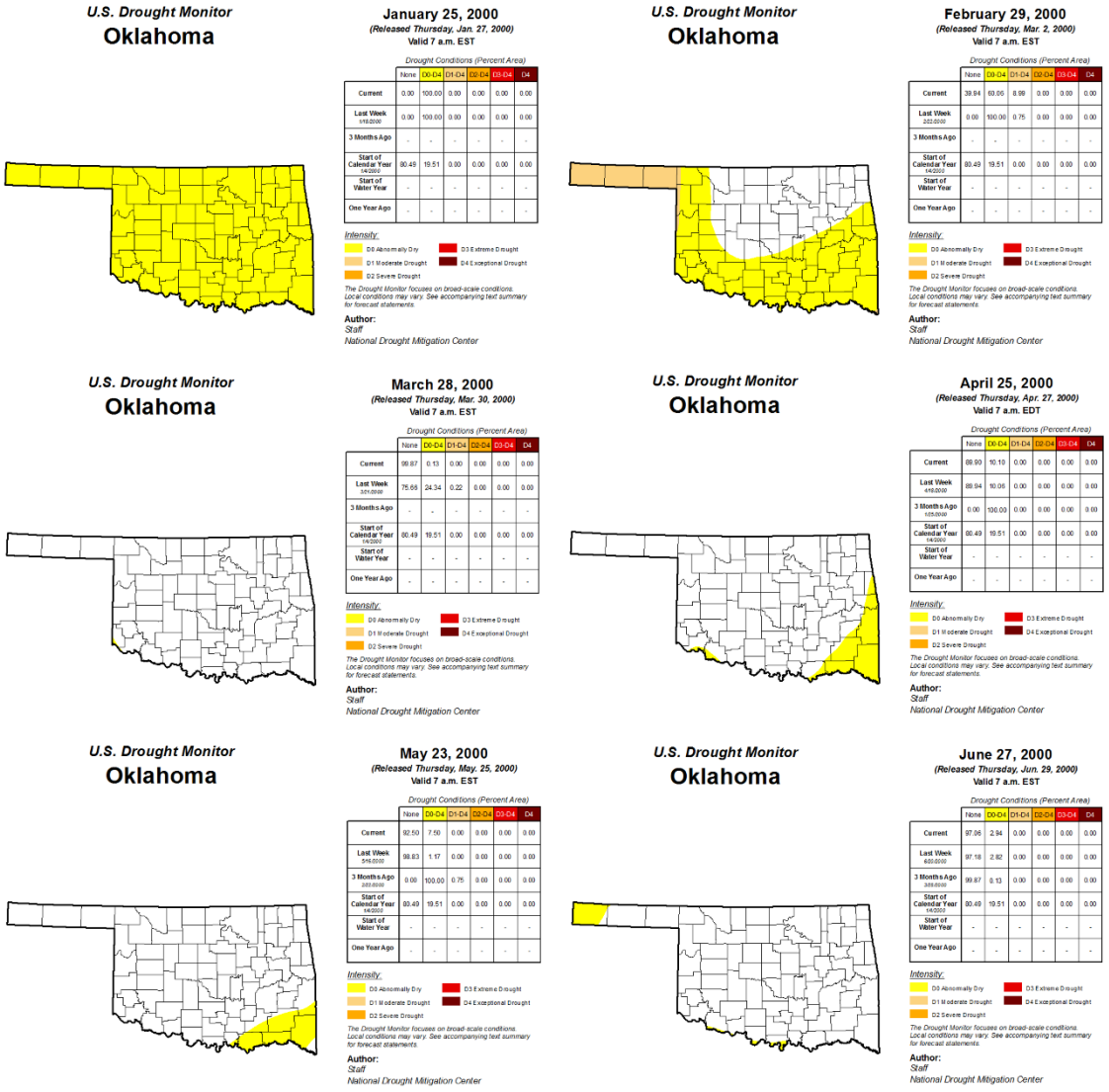

Figure 2.5 United States Drought Monitor maps for Oklahoma. A single weekly map is selected for each month to represent the evolution of drought conditions in Oklahoma during 2000 (Staff National Drought Mitigation Center, 2000).

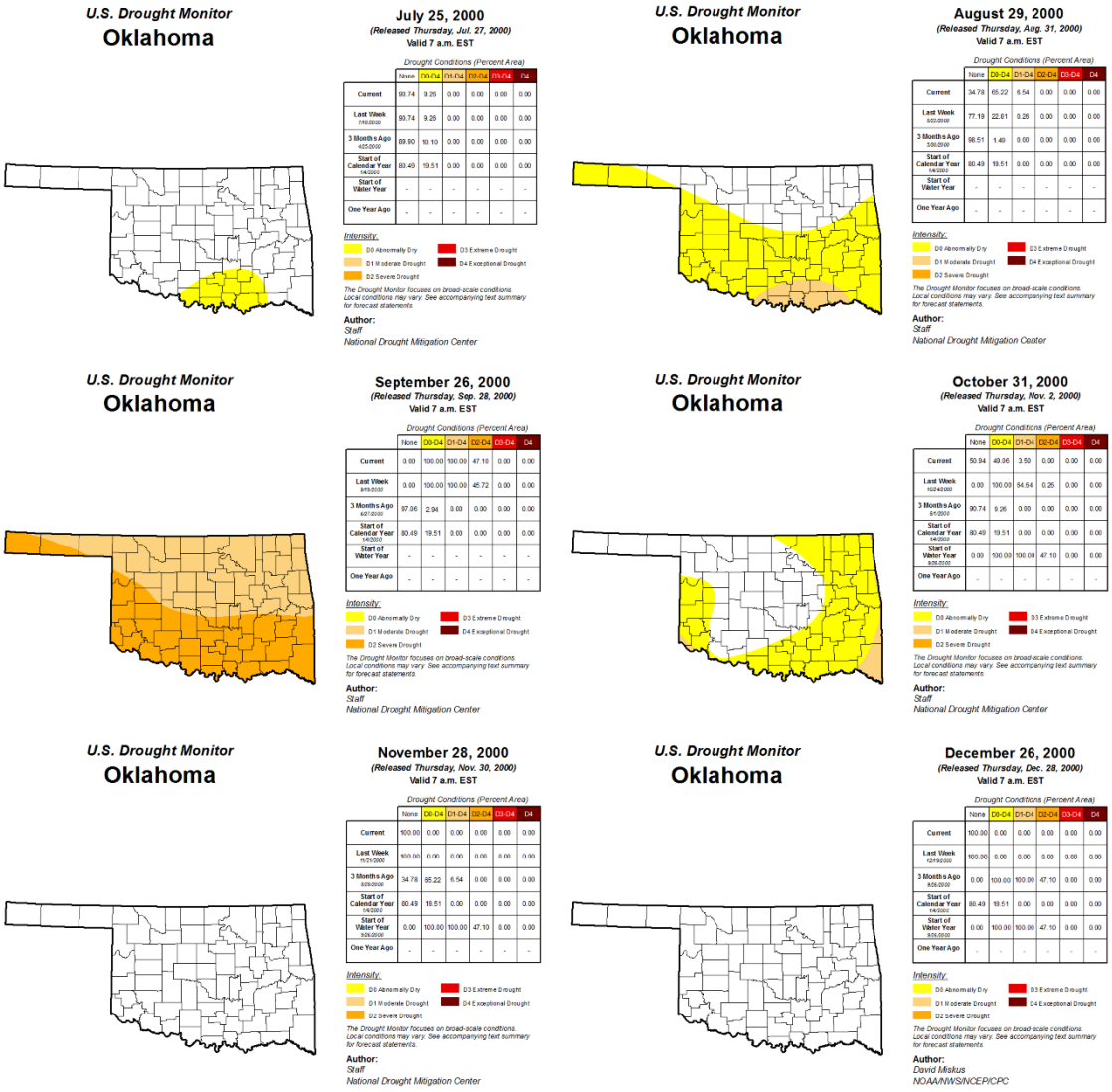

Figure 2.5 Continued

2.3.2 PEDCI Comparison with SPEI

Both PEDCI and SPEI are based on the difference between precipitation and potential evapotranspiration. In this section, the PEDCI is compared with the 1-month, 3-month, 6-month and 12-month SPEI. Figure 2.6 compares the time series of PEDCI

and SPEI at these four timescales. The PEDCI and SPEI values that are shown represent the mean for the state of Oklahoma. It is evident that both the PEDCI and SPEI can capture the fluctuations in moisture conditions. The timing of drought onset and the drought severity appear to be similar. For example, when the SPEI is negative, the PEDCI approaches 0. Not surprisingly, the variability in these two indices tends to decrease at longer time scales. Given that the SPEI has been shown as an effective tool for drought monitoring at different timescales (Vicente-Serrano, Begueria, Lopez-Moreno, Angulo, & El Kenawy, 2010), the consistency between the PEDCI and SPEI suggests that the PEDCI can also be an effective tool for drought monitoring.

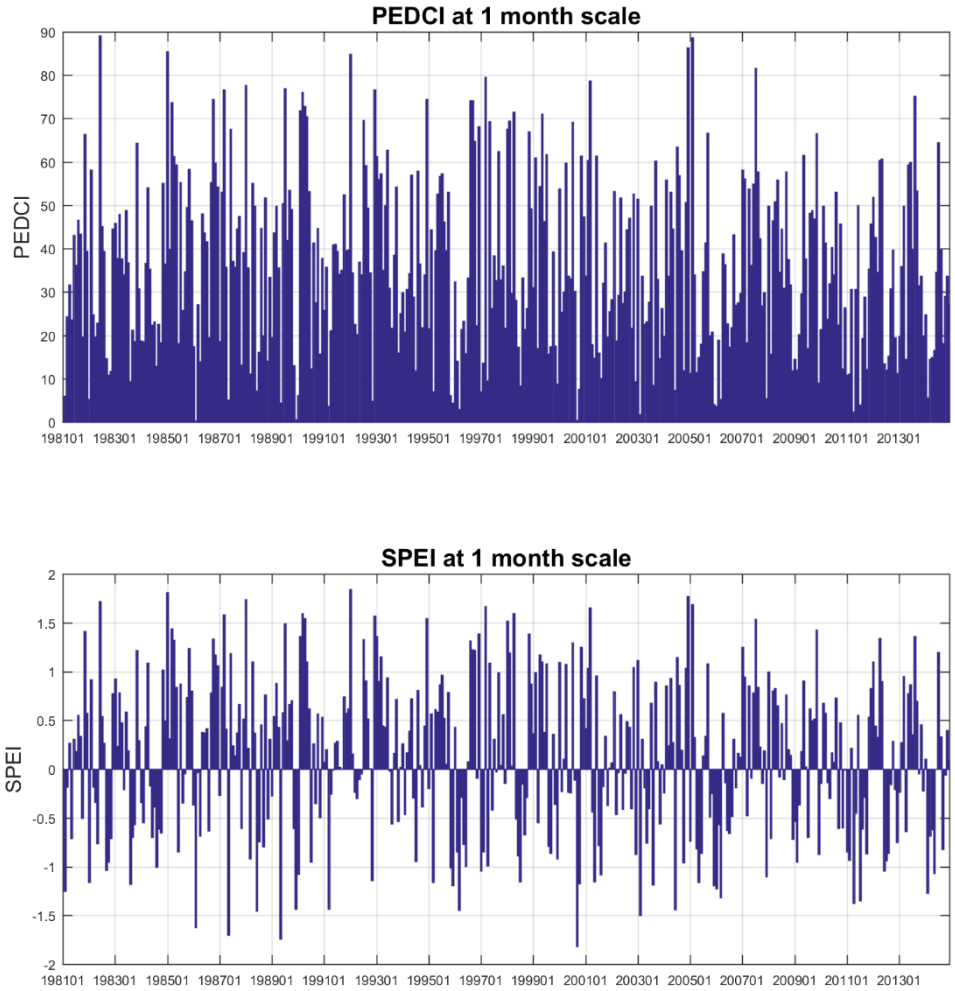

Figure 2.6 Mean state-wide PEDCI and SPEI in Oklahoma (1981-2014) at different timescales: (a) 1-month, (b) 3-month, (c) 6-month, and (d) 12-month.

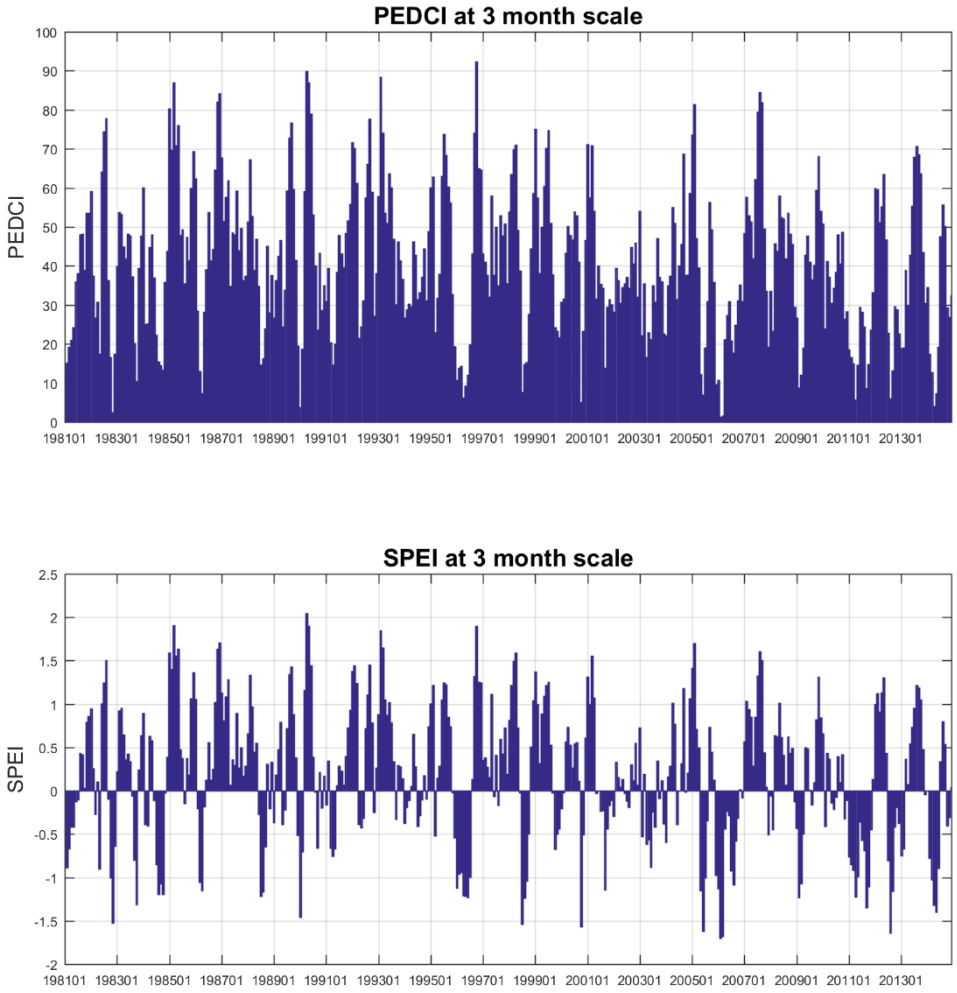

Figure 2.6 Continued

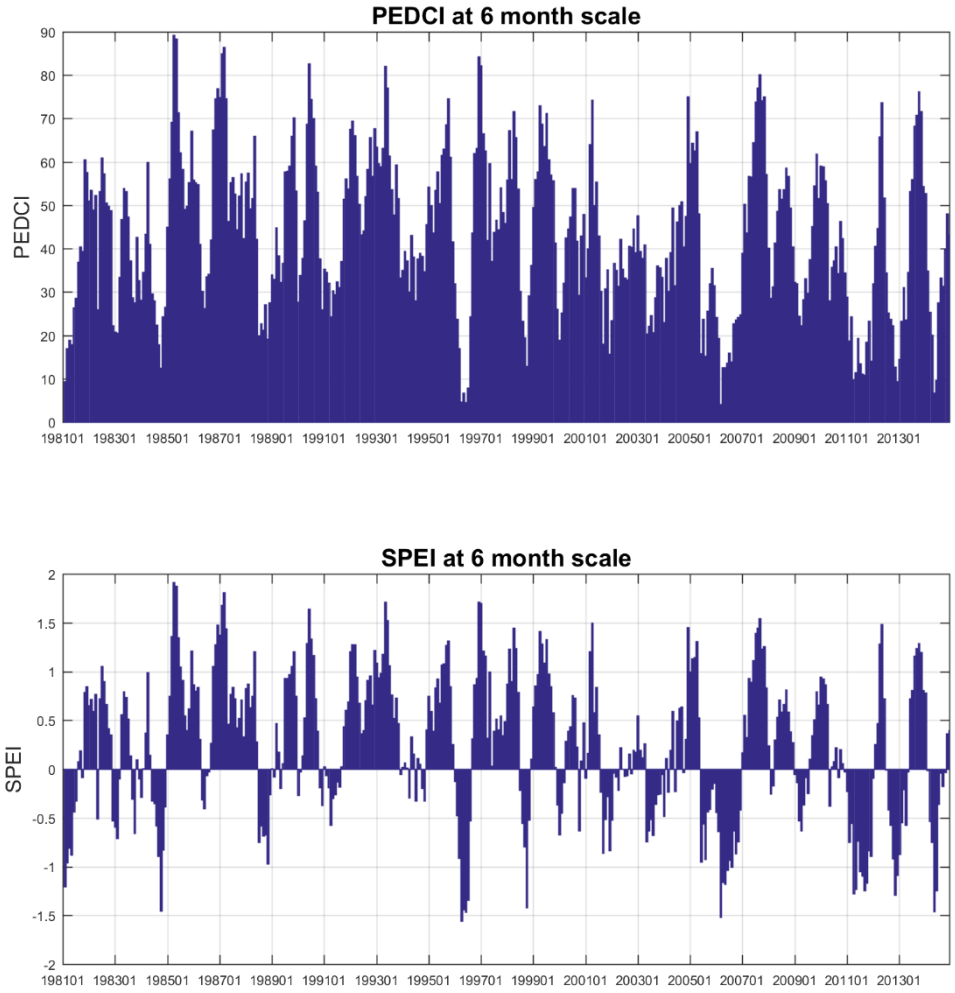

Figure 2.6 Continued

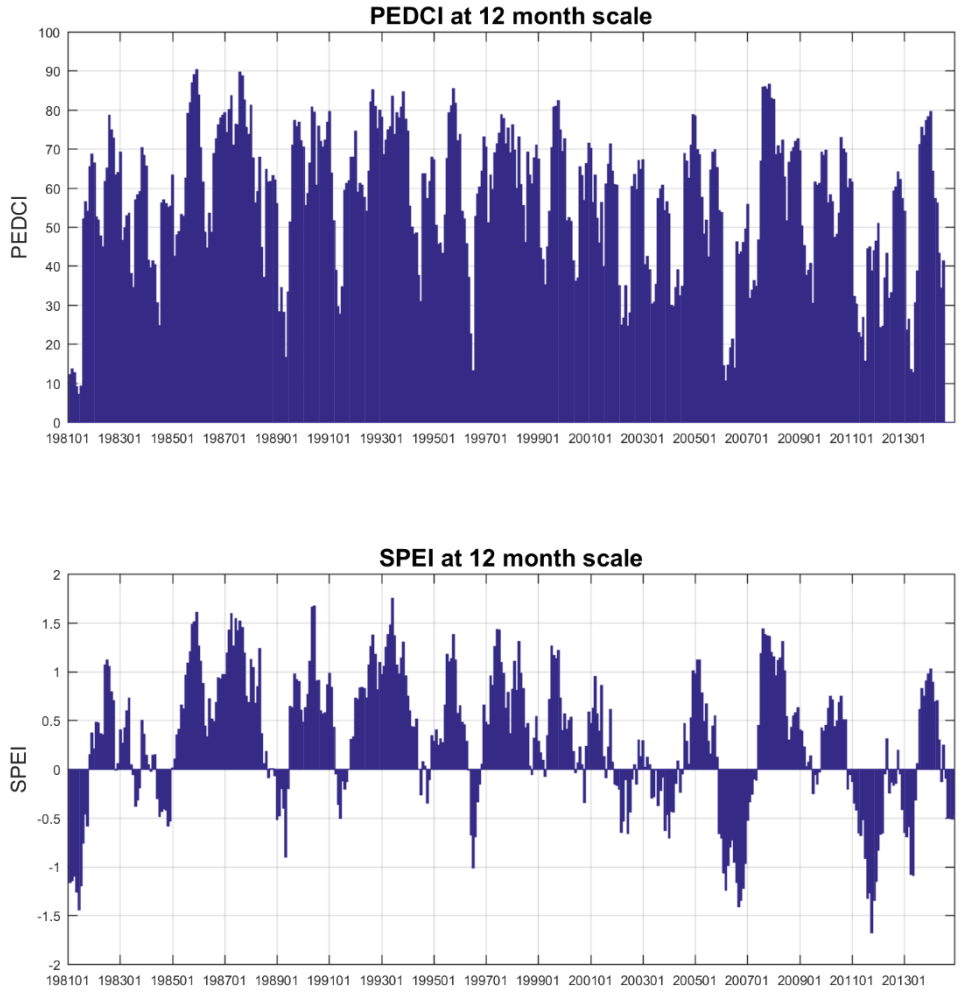

Figure 2.6 Continued

Figure 2.7 shows scatter plots of PEDCI and SPEI at different timescales. PEDCI is highly correlated with SPEI at all timescales. Correlations between the PEDCI and SPEI at 1-month to 6-month timescales are approximately 0.94. This suggests that these two drought indices share a lot of common variance (~88%) and that there is strong

agreement between these two indices in terms of their month-to-month evolution. Correlations between 12-month PEDCI and 12-month SPEI are lower than the correlations at other timescales. The correlation at the 12-month scale is 0.81, which is significant at the 95% significance level. It appears that the weaker correlations between the PEDCI and SPEI are because the PEDCI is more variable than the SPEI. For example, when looking at major drought events in 2007 and 2011, the SPEI stays persistently negative for a much longer period of time that the PEDCI. The 12-month SPEI tends to vary more slowly and smoothly than the PEDCI. This is a direct result of how each of these indices is calculated. The 12-month SPEI is based on precipitation over the last 12 months and therefore it integrates the long-term conditions and once a drought event begins, it takes a while for the SPEI to return to normal. The 12-month PEDCI is based on an average of the 12 monthly PEDCI values. Therefore, one high PEDCI value (of 90 or 100) can have a large influence on the mean PEDCI. The PEDCI tends to show a quicker drought recovery than the SPEI. This difference between the SPEI and PEDCI becomes more pronounced at longer timescales.

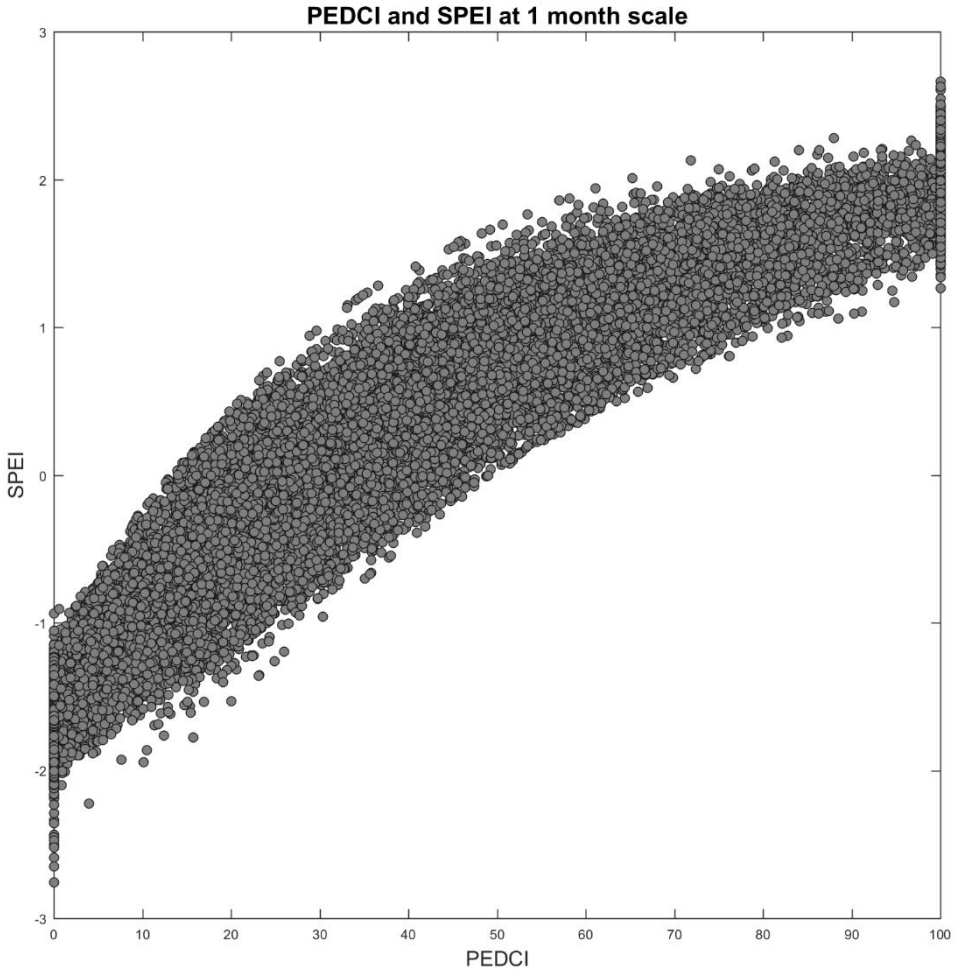

Figure 2.7 Scatter plots of PEDCI and SPEI at different scales.

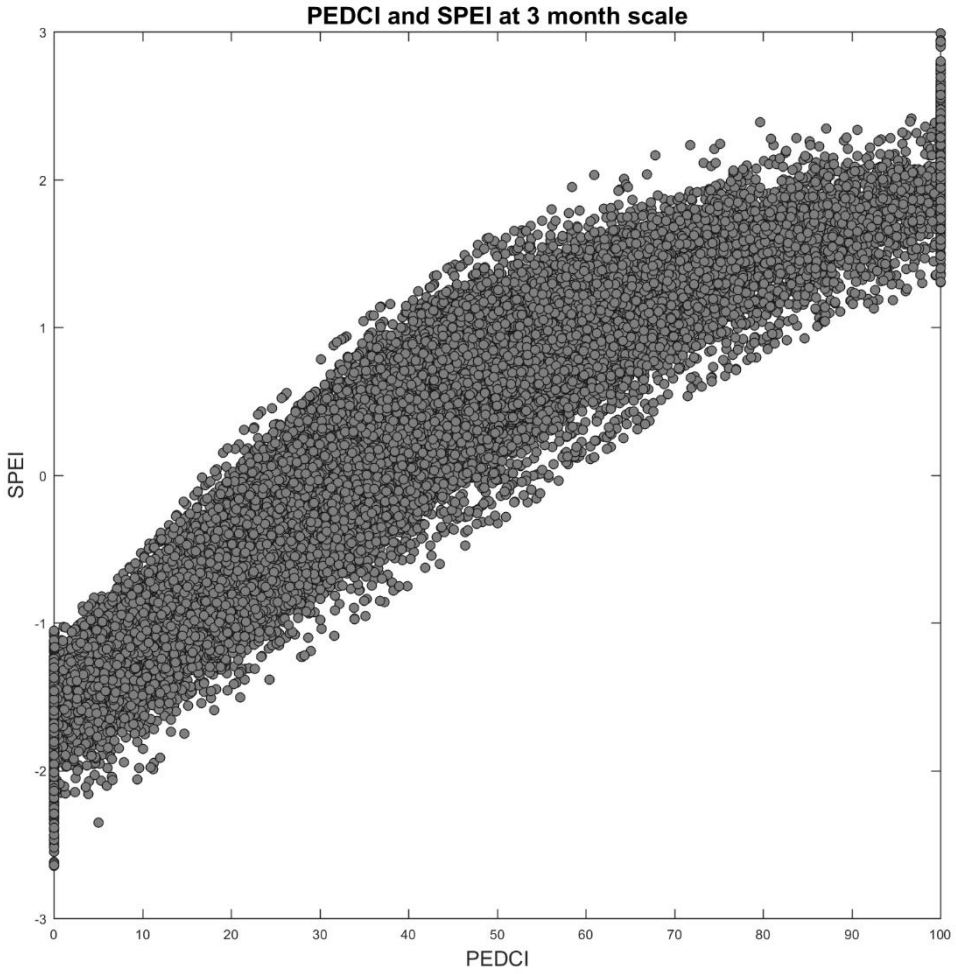

Figure 2.7 Continued

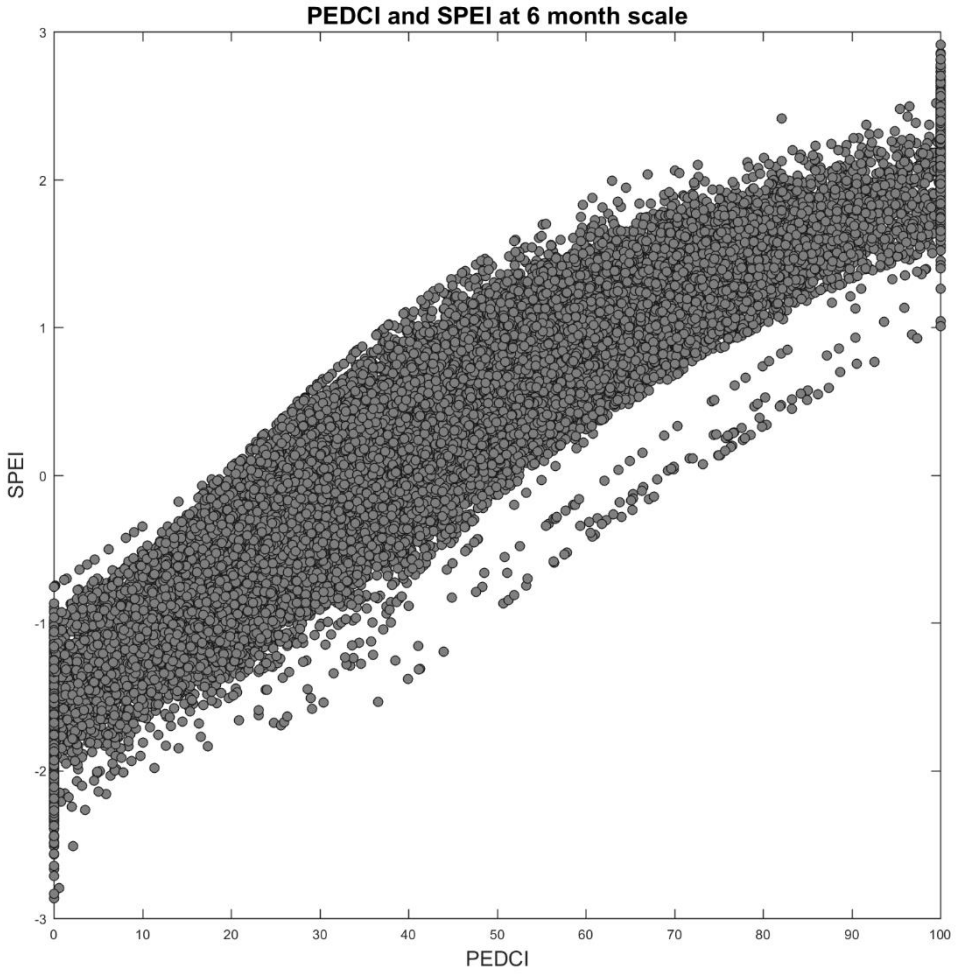

Figure 2.7 Continued

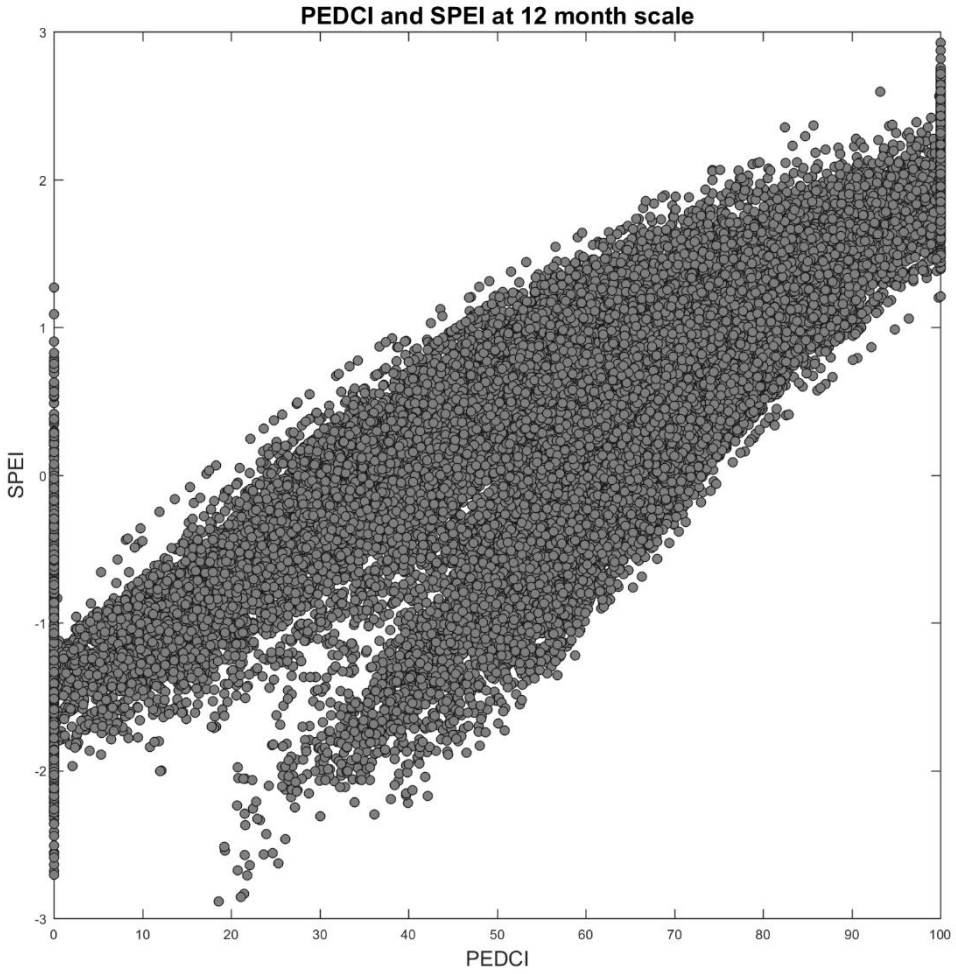

Figure 2.7 Continued

2.3.3 PEDCI Comparison with Soil Moisture

Soil moisture is an important indicator of drought conditions. Oklahoma Mesonet provides soil moisture at four depths. Correlations between the 1-month PEDCI and soil

moisture percentiles at the 5 cm are used to evaluate how well the PEDCI captures variations in near-surface soil moisture (Figure 2.8). The correlations between the PEDCI and the station-based soil moisture measurements varies significantly across Oklahoma. The minimum correlation between PEDCI and soil moisture is 0.26, while the maximum correlation is 0.74. There is a strong west to east gradient in the strength of the correlations. They tend to be higher in western Oklahoma than in eastern Oklahoma. There are a variety of reasons for these spatial variations in the strength of the correlations. Differences in climate, soil characteristics and land cover all likely play a role in these patterns. In addition, there is a spatial and temporal mismatch between these data. They PEDCI is calculated at a 0.125 degree grid cell, while soil moisture is measured at a point. Near-surface soil moisture varies substantially on a daily to weekly timescale. Therefore, comparing mean monthly soil moisture with the monthly PEDCI masks some of this high frequency variability. Nonetheless, it is evident that the PEDCI does capture some of the variance in soil moisture conditions in Oklahoma. Therefore, it may have some utility as an agricultural drought index.

Figure 2.9 shows the correlations between the 1-month PEDCI and soil moisture at 60 cm. The minimum correlation between PEDCI and soil moisture at 60 cm is 0.04, while the maximum correlation is 0.68. The west-east gradient in the strength of the correlations is less pronounced at 60 cm than at 5 cm. The decrease in the strength of the correlations is not surprising since near-surface soil moisture is more sensitive to environmental conditions. H. Wang, Rogers, and Munroe (2015) demonstrated that near-surface soil moisture is more effectively characterized by a drought index at shorter

timescales, while soil moisture deeper in the soil column is best characterized by a drought index at longer timescales. In this case, since the 1-month PEDCI was used for comparison with both the 5 cm and 60 cm soil moisture, it is not surprising that the correlations are weaker at 60 cm.

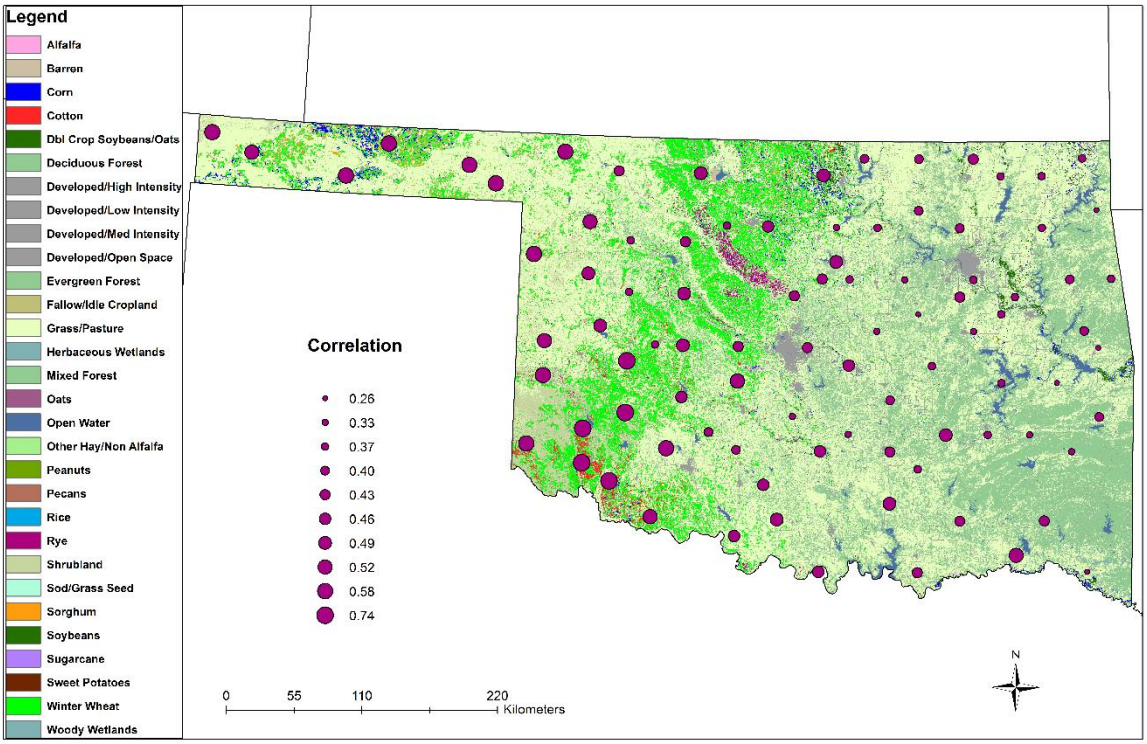

Figure 2.8 Correlations between the 1-month PEDCI and soil moisture at 5 cm (based on data from 2000 to 2014).

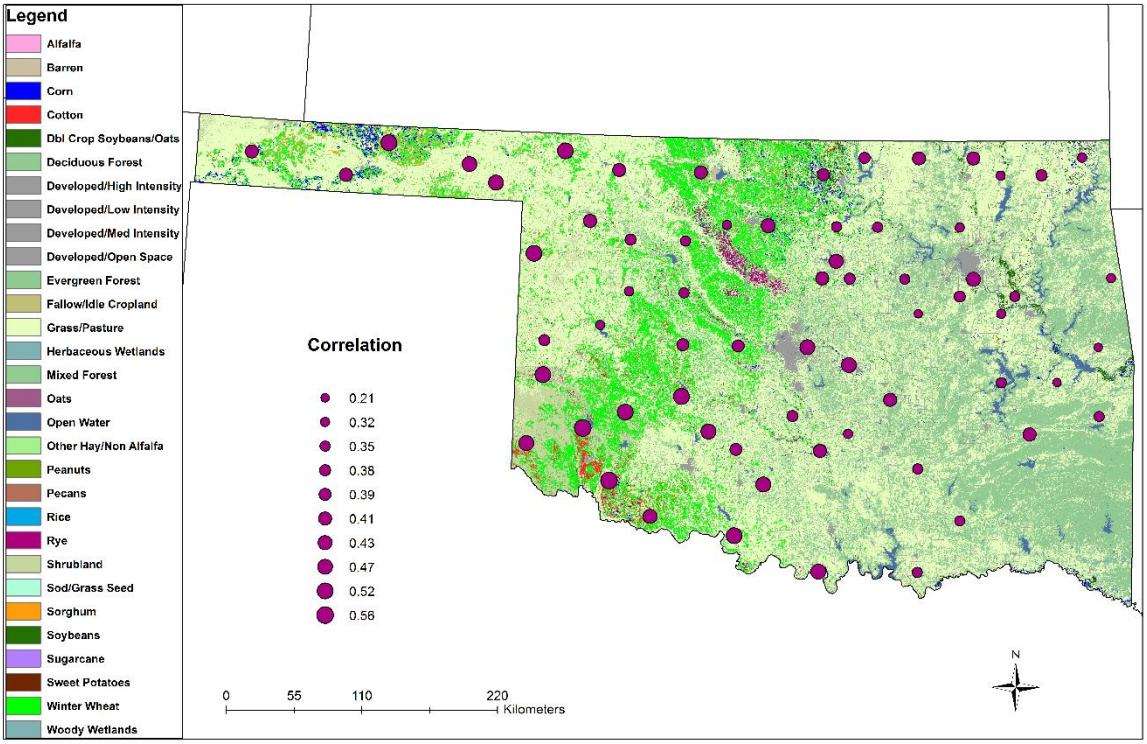

Figure 2.9 Correlations between PEDCI and soil moisture at 60 cm (based on data from 2000 to 2014).

2.4 Discussion and Conclusion

In this chapter, a new drought index Precipitation Evapotranspiration Difference Condition Index (PEDCI) was established based on the difference between precipitation and PET. This index combines the advantages of SPEI and VCI. The differences between water supply (precipitation) and atmospheric water demand (PET) can provide a simple water balance (S. M. Vicente-Serrano et al., 2010). By adopting the normalization method that is used by VCI, the PEDCI can compare the water balance at a given location and time period with the normal conditions. As a result, the PEDCI

provides a normalized value that removes the climatic and seasonal variations in water supply/demand.

There is strong agreement between the PEDCI, SPEI and USDM in terms of the spatial-temporal patterns in moisture conditions. In addition, there is strong agreement between the PEDCI and SPEI in terms of drought severity and month-to-month variations in drought conditions at timescales ranging from 1 to 6 months. There is less agreement between these two indices at the 12-month timescale due to differences in how these two indices are calculated. The primary differences between the PEDCI and the USDM are related to drought severity, and to a lesser extent, drought timing. The PEDCI and the SPEI both tend to show that drought conditions are more severe than the USDM. These differences are due to the fact that the USDM represents meteorological (short-term), agricultural and hydrological drought (long-term). While the PEDCI is most representative of short-term drought conditions. The USDM also incorporates drought impact information, so it is not solely based on climatic conditions.

Correlations between the PEDCI and SPEI at different timescales demonstrate that the PEDCI can capture fluctuations in drought conditions as effectively as SPEI. The direct correlations between PEDCI and soil moisture indicate that the PEDCI has utility for monitoring agricultural drought conditions. However, the correlations between the PEDCI and soil moisture are much higher in western Oklahoma than in eastern Oklahoma. This suggests that differences in soil characteristics and land cover have an influence on the strength of the relationships.

Robustness, tractability, transparency, sophistication, extendibility, and dimensionality are six criteria that can be used for evaluating drought indices (Steven M Quiring, 2009). Robustness refers to the spatial and temporal comparability of an index. Tractability refers to the practical ability of calculating the drought index. Transparency means the ability of an index to be understood. Sophistication is related to the conceptual merit of the index. Extendibility means the ability of an index to be extended back in time. Dimensionality refers to the connections between the drought index and the physical world. The relative importance of these six criteria are 30%, 25%, 15%, 10%, 10% and 10% (Keyantash & Dracup, 2002; Steven M Quiring, 2009). Both of PEDCI and SPEI can measure drought over a wide range of conditions, and they can be calculated for any interested time periods. SPEI is a standardized index, therefore, it is comparable spatially and temporally. PEDCI is based on normalization method, thus, its ability for the spatial and temporal comparison is not as good as SPEI. Based on the scoring method from Steven M Quiring (2009), SPEI is given 5 out of 5 for robustness, while PEDCI is given 4 out of 5 for robustness. In terms of tractability, since PEDCI is easier to calculate, PEDCI is given 5 out of 5, while, SPEI is given 4 out of 5. About the transparency, PEDCI also has advantage over the SPEI. The method to calculate SPEI is more complicate than the method to calculate PEDCI. Therefore, PEDCI receives 5 out 5 in terms of transparency while SPEI receives 4 out of 5. The complicate calculation of SPEI gives advantage to the sophistication of SPEI. Both of PEDCI and SPEI can be extended back in time for the locations that have long record of precipitation and PET. In addition, the units of SPEI and PEDCI can be easily related to the simple water

balance model. Therefore, they receive 5 out 5 for these two criteria. Table 2.2 shows the scores of SPEI and PEDCI based on these six criteria. Overall, PEDCI is comparable to SPEI.

Table 2-2 Qualitative evaluation of PEDCI and SPEI

	PEDCI	SPEI
Robustness	4	5
Tractability	5	4
Transparency	5	4
Sophistication	4	5
Extendibility	5	5
Dimensionality	5	5
Weighted Total	4.6	4.6

In this study, PEDCI were converted to a drought severity classification (D0 to D4) using the USDM percentiles. The classification was based on using the mean PEDCI values for Oklahoma. In the future, the PEDCI should be categorized based on the PEDCI values in each pixel. In addition, the PEDCI should be compared with more drought indices such as PDSI, Z-index and SPI for a further evaluation the performance of the PEDCI.

CHAPTER III

COMPARISON OF SEVERAL WIDELY USED DROUGHT INDICES FOR AGRICULTURAL DROUGHT MONITORING IN OKLAHOMA[1]

3.1 Introduction

3.1.1 Drought Indices

Drought indices are used to quantitatively measure drought conditions. More than 150 drought indices have been development for different types of drought and different places (Niemeyer, 2008). A number of studies have reviewed the development of drought indices and concluded their advantages and disadvantages (Heim, 2002; A. K. Mishra & Singh, 2010). For example, Kempes, Myers, Breshears, and Ebersole (2008) evaluated several different drought indices including PDSI and SPI in response to the tree-ring growth in the southwestern United States. The results indicated PDSI was best indicator of the tree ring width. Steven M Quiring (2009) compared the Palmer Drought Severity Index (PDSI), Palmer's Z-Index, Standardized Precipitation Index (SPI), Effective Drought Index (EDI), Vegetation Condition Index (VCI), percent normal, and percentiles for meteorological drought monitoring in the United States. Both of the literature and the drought index evaluation suggest that the SPI and percentiles are most suitable for monitoring meteorological drought. Lorenzo-Lacruz et al. (2010) compared

[1] A portion of this chapter is a part of paper that will be submitted to Agricultural and Forest Meteorology. Tian, L., Yuan, S. and S. M. Quiring, "Evaluation of six drought indices for agricultural drought monitoring in South Central United States".

the performance of SPEI and SPI to identify the impacts of droughts and water management on various hydrological systems in central Spain. They found that SPEI better reflects the influence of precipitation and temperature on the temporal variability of river discharge and reservoir storage. Vicente-Serrano et al. (2012) compared the PDSI, SPI and Standardized Precipitation Evapotranspiration Index (SPEI) for agricultural, hydrological, and ecological drought monitoring at global scale. Their results demonstrated that SPEI is the best drought index to capture the impacts of drought on those above agricultural, hydrological, and ecological variables. Drobyshev, Niklasson, and Linderholm (2012) compared the performance of six drought indices for fire frequency analysis in Sweden. They found that the calibrated PDSI is a better proxy of fire activity for the southern region, while, the ratio between actual and equilibrium evapotranspiration is better for the northern region. The aforementioned studies show that the performance of drought indices varies based on the region and intended application.

3.1.2 Agricultural Drought Monitoring

S. M. Quiring and Papakryiakou (2003) evaluated PDSI, Z-index, SPI and NOAA drought index by comparing the yield models predictions based on these drought indices. The result indicated that the Z-index is the most appropriate index for agricultural drought monitoring in Canadian prairies. H. Wang et al. (2015) compared PDSI, scPDSI, Z-index, SPEI and SPI based on the correlations with soil moisture in China. Their results showed SPEI has a higher correlation with soil moisture than SPI,

PDSI, and Z-index. Also, they found that the Z-index has a higher correlation with soil moisture in the top 5 cm of the soil column than the PDSI. However, the PDSI has a higher correlation with soil moisture at 90-100 cm. Correlations between soil moisture and four drought indices, including PDSI, Z-index, SPI, and SPEI, were compared at global scale and country level by Vicente-Serrano et al. (2012). Their results were similar with the results by H. Wang et al. (2015). Vicente-Serrano et al. (2012) also compared PDSI, Z-index, SPI and SPEI based on the correlations with wheat yield at global scale and country level. They calculated the correlation with de-trended wheat yields since yield changes over time not only depend on climate factors but also other factors such as new technologies and managements (Potopova, Boroneant, Boincean, & Soukup, 2016).

Potopova et al. (2016) investigated the impact of agricultural drought on main crop yields. The same method was used to de-trend yield. However, only low-yielding years were considered to show the variability in yield losses explained by drought. Even though a lot of research have been done about the comparison of drought indices, the results were not consistent. The performance of drought indices varies from regions since the specific physical environment varies from region to region. Comparison of drought indices for agricultural drought monitoring in one specific region is necessary for drought management and mitigation.

In this chapter, six commonly used drought indices: PDSI, Z-index, SPEI, SPI, precipitation percent normal, and precipitation percentiles, are compared for agricultural drought monitoring in Oklahoma. These indices were selected because past studies have

shown that they have utility for agricultural drought monitoring and they are used by stakeholders and ranchers. The newly developed PEDCI is also compared with these six drought indices to determine whether it outperforms existing drought indices. The goals of this chapter are to: (1) determine which drought index is the most representative of soil moisture conditions in Oklahoma, (2) identify which drought index is the best for the primary crop in Oklahoma, (3) evaluate the performance of drought indices in abnormal yielding year and investigate the variability in yield losses explained by drought.

3.2 Data and Methods

3.2.1 PRISM Precipitation

Monthly Parameter Elevation Regression on Independent Slope Model (PRISM) precipitation data (http://www.prism.oregonstate.edu) at 4 km resolution are used to calculate drought indices in this study. Long-term records from 1895 to the present at 800 meters and 4 kilometer resolution are available. For the intended climate study, a long and consistent record is needed to reduce the potential of error (A. K. Mishra & Singh, 2010). Therefore, data used in this study cover a 34-year period from 1981 to 2014.

3.2.2 NLDAS Potential Evapotranspiration

The potential evapotranspiration (PET) data are needed to calculate PDSI, Z-index, SPEI, and PEDCI. We use the PET data from North American Land Data

Assimilation System (NLDAS)-2 forcing dataset (http://ldas.gsfc.nasa.gov/nldas/NLDAS2forcing.php).

3.2.3 Soil Moisture

Soil moisture is a good indicator of meteorological and agricultural drought conditions. Observed soil moisture data from the North American Soil Moisture Database (NASMD) (http://soilmoisture.tamu.edu/) are used to compare the performance of drought indices. The NASMD is a harmonized and quality-controlled soil moisture dataset (Steven M Quiring et al., 2016). It can be used to validate the accuracy of soil moisture simulations in global land-surface models and from satellite platforms and in climate-hydrological research. The NASMD contains daily soil moisture data from 30 soil moisture networks. This study only uses data from the Oklahoma Mesonet. Figure 1.1 shows the soil moisture stations used in this study. Data from the NASMD are daily quality controlled soil moisture data. The soil moisture data from different depths are averaged in the top 60 cm of the soil column since 70% to 85% of the total water uptake for winter wheat occurs in the top 60 cm of the soil column (FAO Land and Water division, 2015). Daily soil moisture data are averaged to monthly values. Data from 2000 to 2014 are used in this study since data are only available since 2000 for most stations. Since missing data exists in some stations and some months, only months with less than 5 missing days are considered in this study. Otherwise, the monthly soil moisture value is set to missing. Soil moisture is transformed into percentiles so that it can be directly compared over space and time.

3.2.4 Crop Yields

Winter wheat yield from United States Department of Agriculture (UDSA) (https://quickstats.nass.usda.gov/) during the period from 1981 to 2014 are also used in this study. According to the land cover map (Figure 1.1), winter wheat is the primary agricultural crop grown in Oklahoma.

Since crop yield is affect by many factors besides climate, such as technological advances in cropping system and new management practices, crop yields show a positive trend (Potopova et al., 2016; Vicente-Serrano et al., 2012). Therefore, crop yield timeseries are detrended to isolate the non-climatic factors following the method of Lobell, Schlenker, and Costa-Roberts (2011). Equation 3.1 is used to detrend the crop yield:

$$y_{iT} = y_i - y_{i\tau} \qquad \text{(Equation 3.1)}$$

Where y_{iT} is the detrended crop yield, y_i is the observed crop yield, and $y_{i\tau}$ is the mean dynamical value resulting from fitting a quadratic polynomial line (Potopova et al., 2016).

The detrended crop yields are then standardized using equation 3.2 to compare yield variability among the locations with different means and standard deviations:

$$SYRS = \frac{y_{iT} - \mu}{\sigma} \qquad \text{(Equation 3.2)}$$

Where $SYRS$ is standardized yield residuals series, y_{iT} is the detrended yield, μ is the mean of the detrended yield, and σ is the standard deviation of the detrended yield.

3.2.5 Drought Indices

PDSI and Z-index were developed in 1965 (Palmer, 1965). The PDSI and Z-index are calculated based on a water balance model using a time series of daily temperature and precipitation data, and information on the available water content (AWC) of the soil. PDSI calculates evapotranspiration, runoff, soil recharge, and moisture based on the water balance model (Zargar et al., 2011). Z-index is an intermediate term within the PDSI. It is monthly standardized anomaly of available moisture. The PDSI was the first comprehensive drought index developed in the U.S. and it is still a popular drought index.

The Standardized Precipitation Index (McKee, Doesken, & Kleist, 1993) is a meteorological drought index that is calculated only using precipitation data. The SPI is simple and versatile. It can be calculated for any timescale of interest. Different timescales can be used for monitoring different types of drought. A probability distribution function, such as gamma distribution, is applied to transform the distribution of precipitation data into a normal distribution. Since the precipitation is transformed into a normal distribution, the mean of precipitation is set to zero. Therefore, it is possible to compare precipitation departures in regions with different climates.

The percent of normal precipitation (Keyantash & Dracup, 2004) is a simple method to reflect precipitation deficits by comparing observed precipitation to normal precipitation for a particular location and period. Normal precipitation is the mean precipitation based on a 30 years of data. It can be calculated for any time scale of

interest (Steven M Quiring, 2009). The strength of percent normal is it only requires precipitation data, and it is easy to calculate.

Percentiles are another simple method for representing precipitation deficits (Gibbs, 1967). Percentiles can be determined empirically by arranging the data (monthly precipitation) from lowest to highest (Steven M Quiring, 2009). Similar to percent normal, percentile only require precipitation data and they are easy to calculate.

The SPEI is similar to SPI, but it is produced by standardizing the probability of the difference between water supply (P) and atmospheric water demand (PET) (S. M. Vicente-Serrano et al., 2010). The SPEI can provide a more complete representation of drought since potential evapotranspiration is a function of surface air temperature, wind speed, solar radiation and humidity (H. Wang et al., 2015). The advantage of SPEI is it combines advantages of the SPI, but also includes information about evapotranspiration.

3.2.6 Crop Mask

There is a spatial mismatch between the drought indices that are calculated at 0.125 degrees and the county-level crop yield data. This makes it difficult to directly compare these data. To address this issue, we developed a crop mask to identify the locations where winter wheat is grown (Figure 3.1). Then, the drought index values in these grid cells were averaged to calculate a mean drought index value for each county. The crop mask was generated based on the 2015 crop frequency layer from USDA National Agricultural Statistics Service (NASS) (https://www.nass.usda.gov/). The crop frequency layers provide the planting frequency of winter wheat between 2008 and

2015. The crop frequency layers are at 30 meter resolution. Only locations where winter wheat was grown more than 4 times during this 8 year period were retained to generate the crop mask.

We followed the method presented by Huang et al. (2015) to re-scale the crop masks from 30 meter resolution to 0.125 degrees. A 0.125 degree grid was overlaid on the 30 meter winter wheat mask to obtain a pixel purity map based on the percentage of winter wheat in each grid cell. Only grid cells with more than 20 percent purity were identified as a winter wheat grid cell (Figure 3.1).

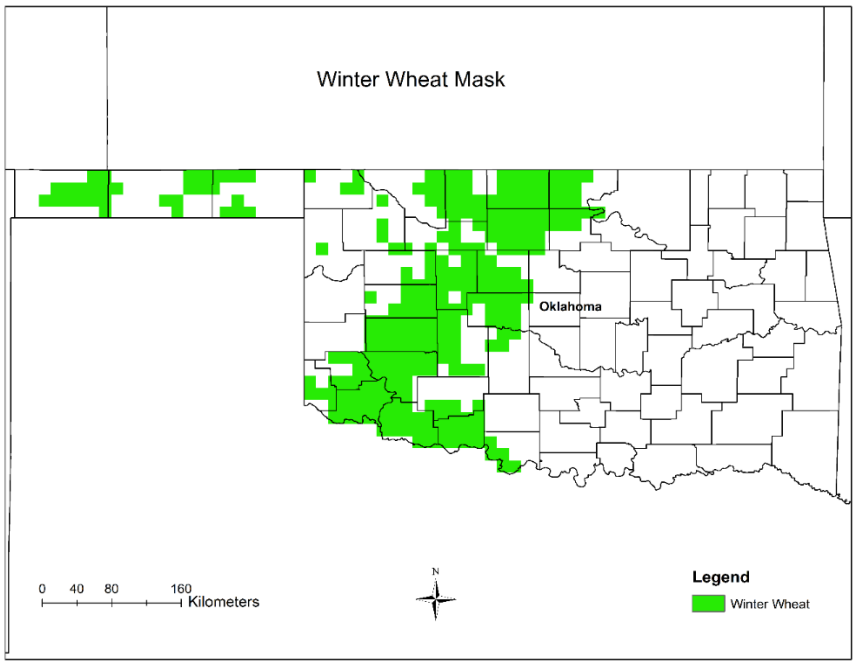

Figure 3.1 Winter wheat mask at 0.125 degree resolution. The pixels shown in green are locations where winter wheat was planted higher than 4 times during 2008 to 2015.

3.3 Results

Correlations between drought indices and soil moisture are reported at the station level, while correlations with crop yields were shown at the county level. Two different approaches were used to evaluate the relationship between the drought indices and crop yields. The first approach calculates correlations between crop yields and drought indices using the entire timeseries from 1981 to 2014. The second approach excludes the years with near-normal climate conditions (where near-normal is defined as the middle 40 percent of drought index distribution) and near-normal crop yield (where near-normal is defined as the middle 40 percent of SYRS). A second-order polynomial function was used to estimate the drought-yield relationship. In dry years, crop yields may be lower than normal due to the water stress. However, crop yields may be also lower than normal in wet seasons due to the factors associated with wet season, such as low global radiation, root anoxia, and higher infestation pressure of fungal diseases. A second-order polynomial function has been shown to provide a good approximation of the nature of crop yield-water relationships (Potopova et al., 2016).

3.3.1 Soil Moisture

Figure 3.2 shows the box plots of the correlations between different drought indices and soil moisture in the four seasons. The performance of the drought indices varies by season. All the drought indices have the highest correlations with soil moisture in JJA. The correlations between PDSI and soil moisture do not vary much from season to season ($\Delta r = 0.07$). This is primarily because the PDSI integrates moisture conditions

over the last 9 months. Therefore, it is influenced by moisture conditions over multiple seasons.

Generally, the correlation between soil moisture and SPEI is higher than the correlations with other indices, except in DJF. During the winter, the Z index outperforms the other indices. These differences are statistically significant. PDSI has the lowest correlation with soil moisture in all the seasons and it is insensitive to the seasons. As noted above, this is because it integrates weather conditions over a much longer period of time than the other drought indices. This means that the PDSI is not particularly useful for representing soil moisture conditions.

In most seasons, SPEI has the highest median correlation followed by PEDCI, Z-index, SPI, percent normal, percentiles, and PDSI. It is interesting to note that the best drought indices (SPEI, PEDCI and Z-index) all have a similar water budget formulation. They are based on the differences between P and PET at the monthly timescale. This suggests that the most appropriate drought indices for representing soil moisture conditions should account for both P and PET. However, each of these indices uses a different approach to standardize the monthly water balance (P-PET) values.

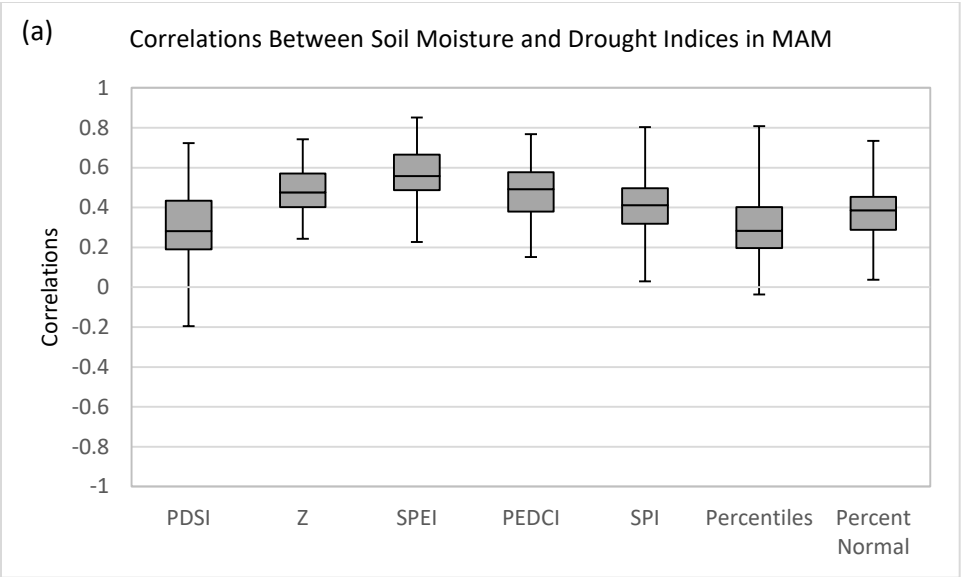

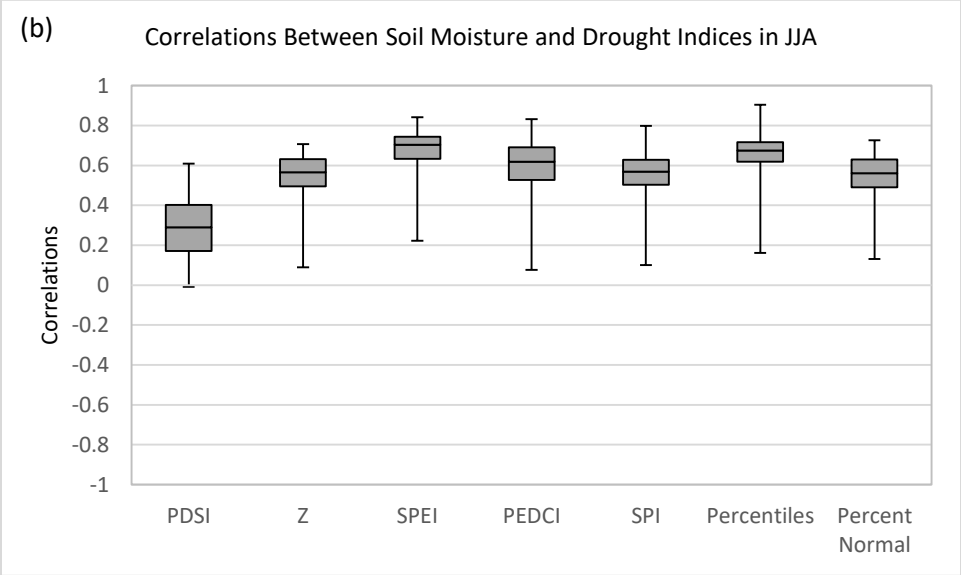

Figure 3.2 Boxplots of the correlations between drought indices and soil moisture (0 to 60 cm) (2000 to 2014) at 90 stations from the Oklahoma Mesonet. Results are reported separately for each season: (a) MAM, (b) JJA, (c) SON, and (d) DJF.

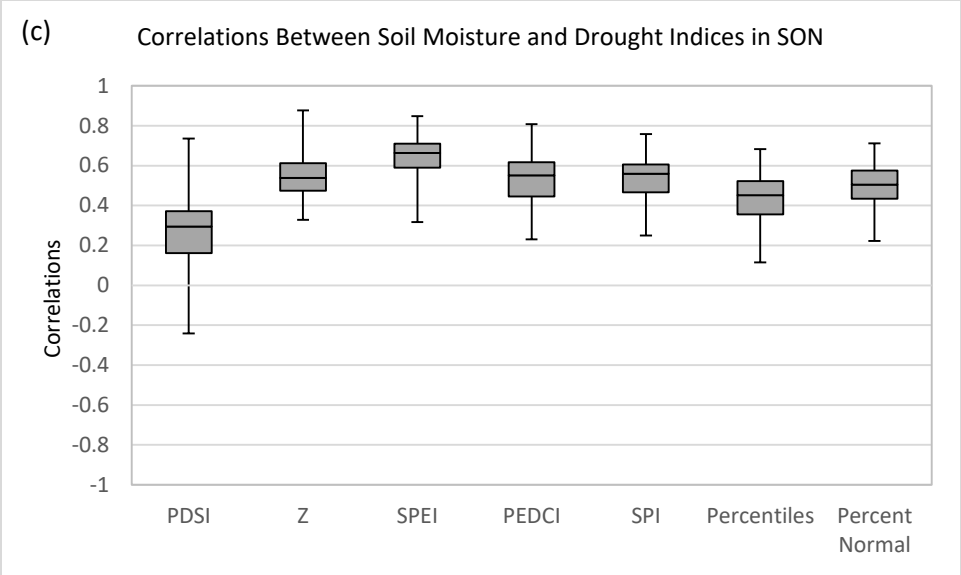

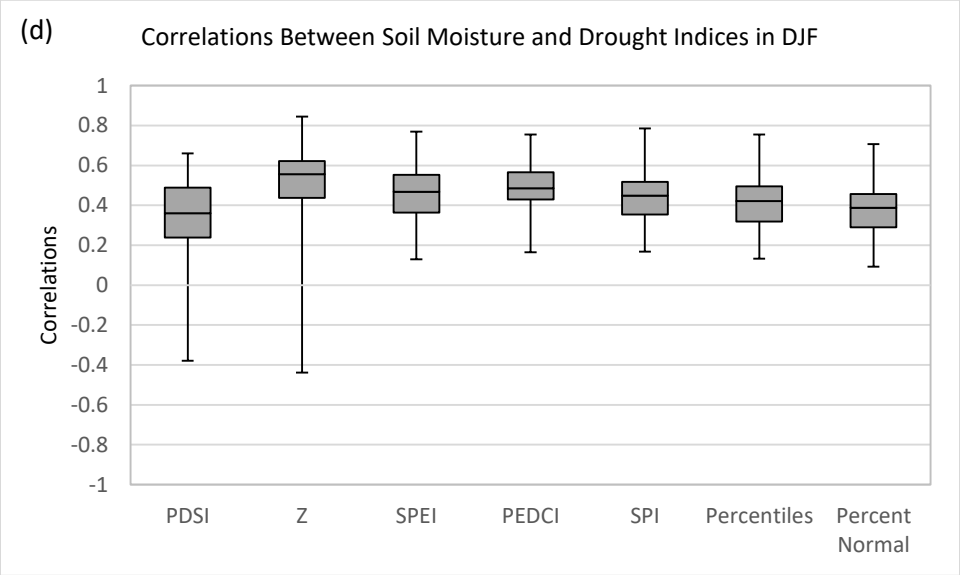

Figure 3.2 Continued

Figure 3.3 shows the percentage of stations with significant correlations (α=0.05). In general, the SPEI has the largest number of stations with statistically significant correlations and the PDSI has the smallest number of stations with

statistically significant correlations. All of the drought indices, except the PDSI, show substantial seasonal variation. The number of stations with statistically significant correlations percentage is greatest during the warm season and least during the cold season. Specifically, in MAM, the percentage of stations with statistically significant correlations varies substantially among the drought indices. The variation between drought indices is minimal in JJA. The percentage of stations with significant correlations in SON is lower than in JJA. In DJF, the Z-index has the highest number of stations with statistically significant correlations followed by PEDCI, SPEI, SPI, percentiles, percent normal, and PDSI.

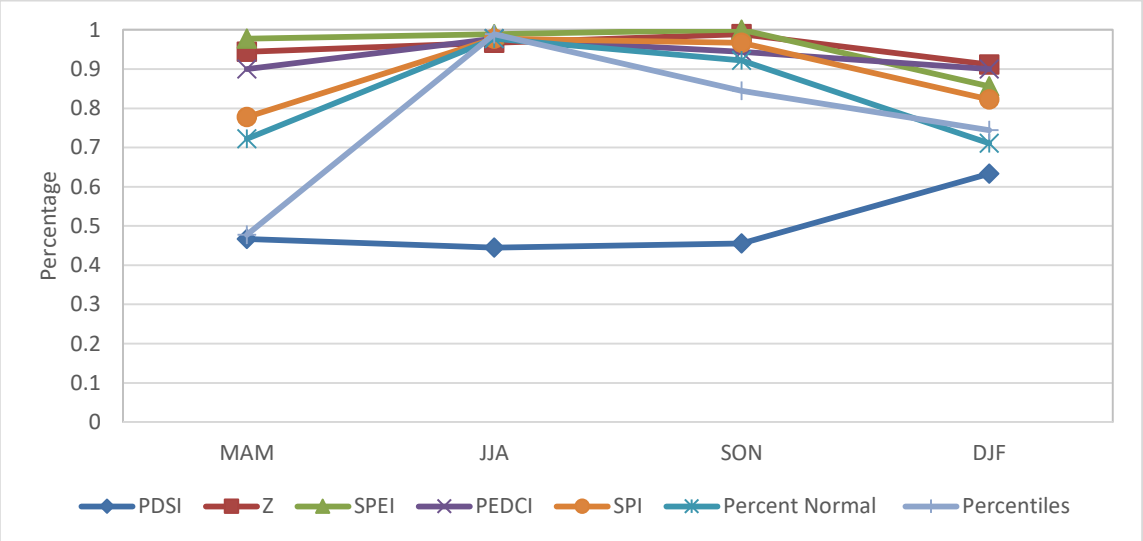

Figure 3.3 Percentage of stations with statistically significant correlations between the monthly drought indices and soil moisture (0 to 60 cm) (α=0.05). Based on data from 2000 to 2014.

Figure 3.4 shows the spatial pattern of the correlations between soil moisture and the seven drought indices. Generally, correlations in summer months are higher than the correlations in winter months. In JJA, the correlations with SPEI and percentiles are higher than the other drought indices. SPI and percent normal both have a distinct spatial pattern to the correlations, with higher correlations in western Oklahoma and lower correlations in eastern Oklahoma. Z-Index and PEDCI do not have a strong spatial pattern. This is particularly interesting since the results from Chapter 2 show that the PEDCI does have a strong spatial pattern in the strength of the correlations when it is compared to the 5 cm soil moisture. This suggests that much of the spatial pattern is driven by the near-surface variability. By integrating soil moisture conditions over the root zone (0 to 60 cm), this pattern no longer appears.

At most stations, correlations with PEDCI are higher than correlations with SPI, percentiles, Z-Index and PDSI. This demonstrates that the new drought index outperforms many of the traditional drought indices.

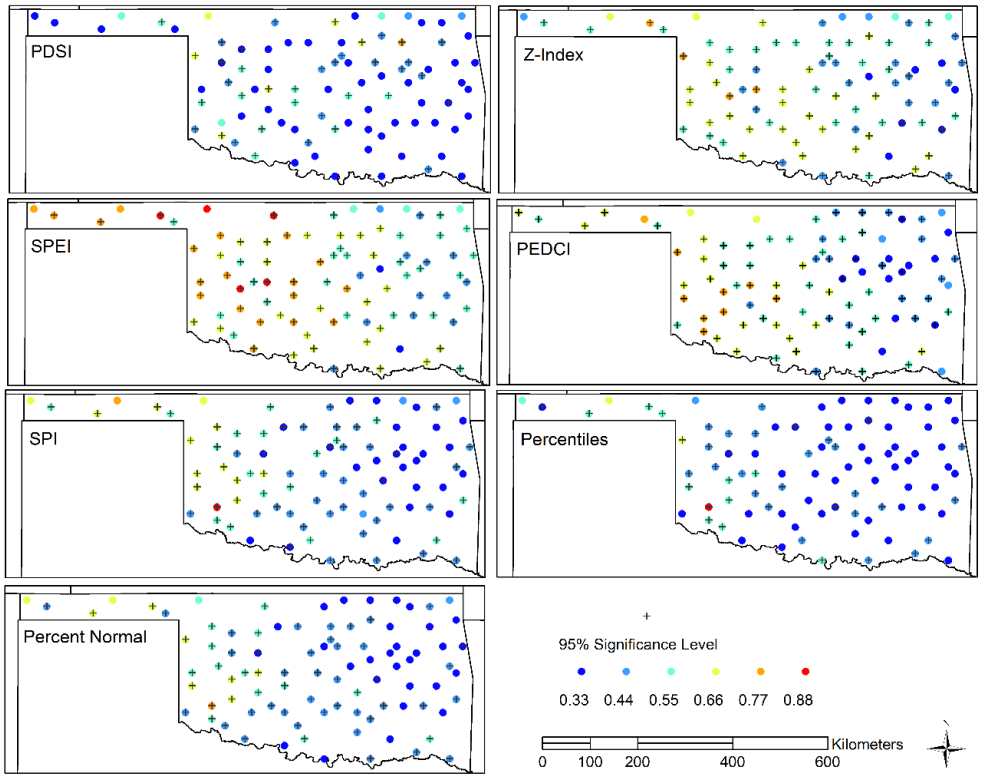

Figure 3.4 Spatial distribution of correlations between monthly drought indices and soil moisture (0 to 60 cm) (2000 to 2014) by season: (a) MAM, (b) JJA, (c) SON and (d) DJF.

Figure 3.4 Continued

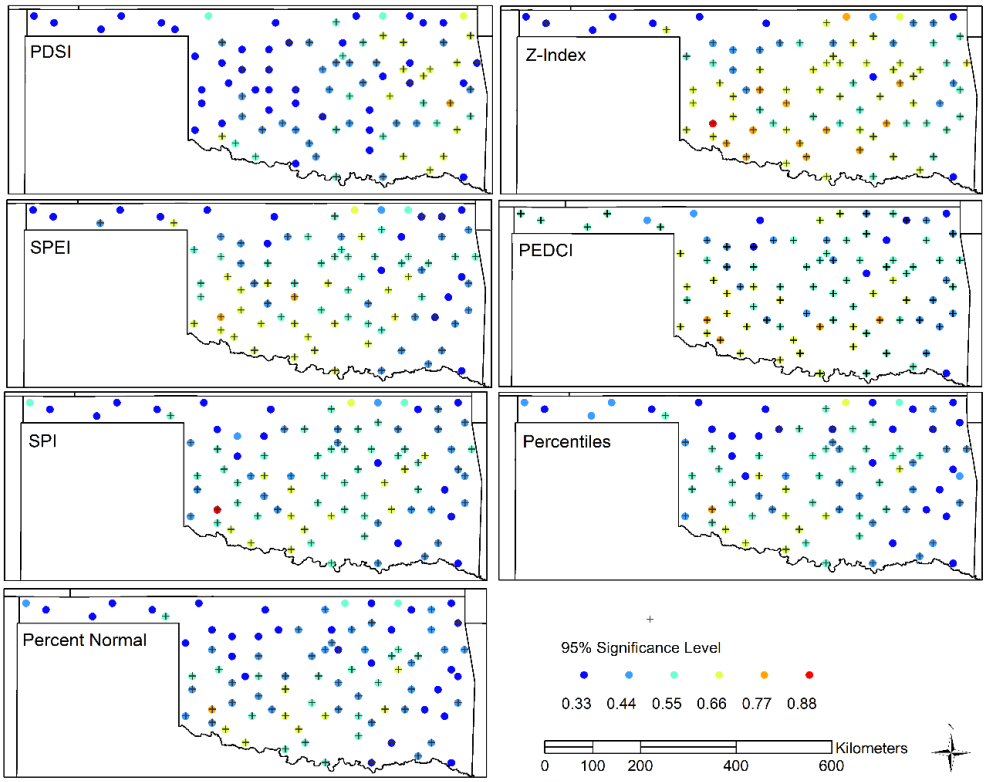

Figure 3.4 Continued

3.3.2 Winter Wheat Yield Results: All Years

Correlations between winter wheat yield and drought indices for each month during the planting period to harvesting period were calculated to evaluate the performance of drought indices based on the crop phenophase. NASS (2010) provides typical planting and harvest dates for major field crops. In Oklahoma, winter wheat is typically planted in October and harvested in June of the following year. Therefore, correlations between winter yield and drought indices for each month from October to June were calculated. There are 30 counties in Oklahoma where winter wheat is planted.

Figure 3.5 shows the percentage of counties with statistically significant correlations between drought indices and winter wheat yield. There are peaks in December and April, which is related to the sensitivity of winter wheat to water supply. There are two main phases when winter wheat is sensitive to water supply (FAO Land and Water division, 2015). The first occurs about 40 to 130 days after seeding when the plants complete tillering and start elongation. The total number of heads and the number of seed per head are determined during this period. The second occurs around 130 to 180 days after seeding, when the flowering period begins. The number of seeds per head is greatly influenced by the water deficits during this period. In December, PEDCI is the drought index that has a statistically significant correlation with winter wheat yield in the greatest number of counties. While in April, SPEI is the drought index that has a statistically significant correlation with winter wheat yield in the greatest number of counties. Overall, the Z-index has the most consistently strong relationship with winter wheat yield between November and April. It has a statistically significant correlation with winter wheat yield in about 80% of the counties during this time period. Conversely, the PDSI consistently has the weakest relationship with winter wheat yield, except in May. This is because the timescale of the PDSI is not appropriate for monitoring weather conditions that influence yield.

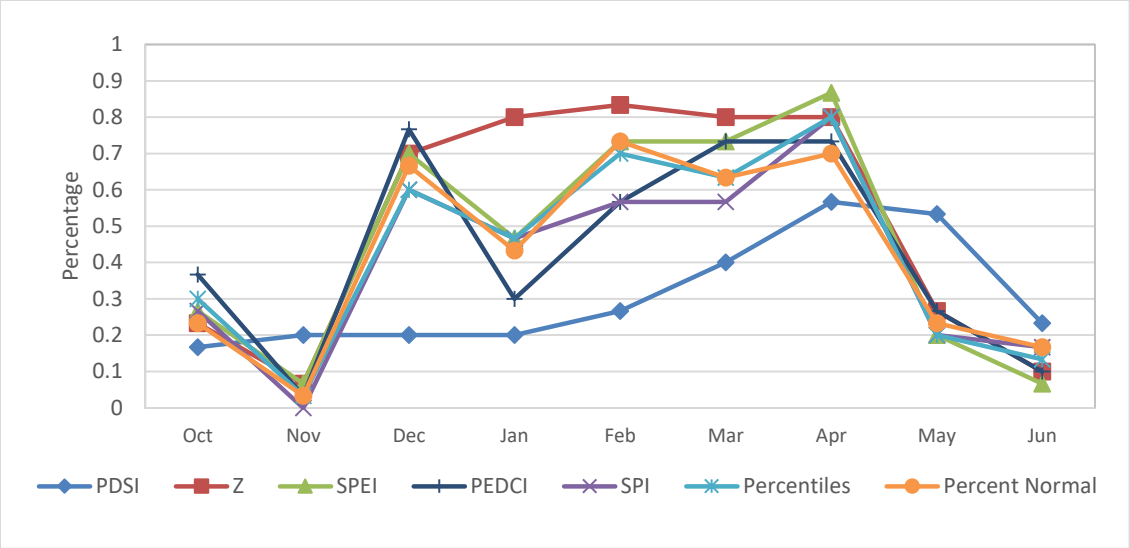

Figure 3.5 Percentage of the 30 counties in Oklahoma with statistically significant correlations between drought indices and winter wheat yield, based on data from 1981 to 2014.

Figure 3.6 shows boxplots of the correlations between the drought indices and winter wheat yield in December and April. The median correlations in December are all around 0.4, except for PDSI. Percent normal appears to be the best drought index to use in December because it has the highest median correlation and the least variability in the county correlations. This suggests that it is not necessary to use a drought index that accounts for PET during the winter. Z-index, SPEI, and PEDCI also have relatively high median correlations, but they show greater variability from county to county.

In April, the median correlations are higher than in December (> 0.45) and the SPEI is the drought index with the highest median correlation. A number of the other drought indices have similar performance to the SPEI, including the PEDCI and Z-index. It appears that the drought indices that incorporate PET are more important during

the warmer months. However, it should be noted that there is substantial county-to-county variability in the strength of the correlations between winter wheat yield and the drought indices. For example, the correlations for the SPEI vary between about 0.1 and 0.6. The PDSI has even greater inter-county variations in the correlations, minimum correlations are 0.05 and maximum correlations are nearly 0.7. This suggests that these results should be interpreted with caution and that there are factors other than moisture conditions that have an important influence on yield.

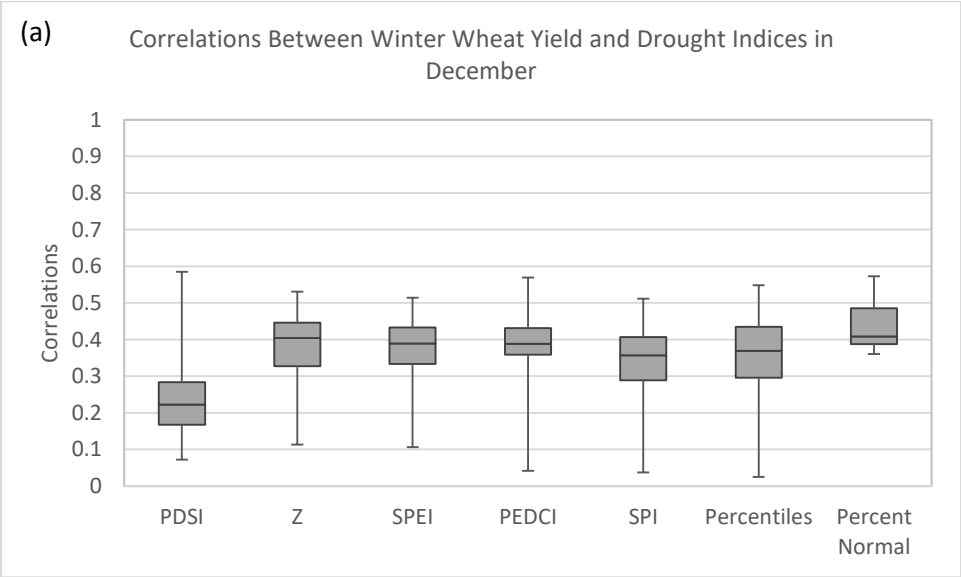

Figure 3.6 Correlations between the seven drought indices and winter wheat yield for 30 counties in Oklahoma (1981 to 2014): (a) December and (b) April.

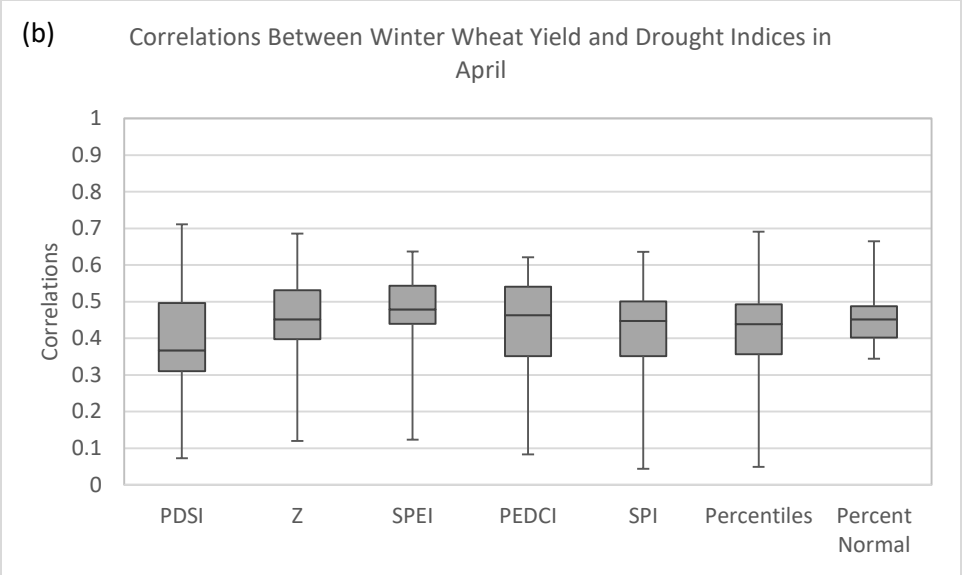

Figure 3.6 Continued

The spatial distribution of the correlations between the winter wheat yield and the seven drought indices can also be used to evaluate the performance of the drought indices (Figure 3.7). The performance of drought indices varies from the counties. In December, Z-index and PEDCI have high and significant correlations with winter wheat yield in more counties than other drought indices. In April, correlations between drought indices and winter wheat yield are higher than in December in many of the counties. SPEI has a statistically significant correlation with winter wheat yield in more counties than other indices.

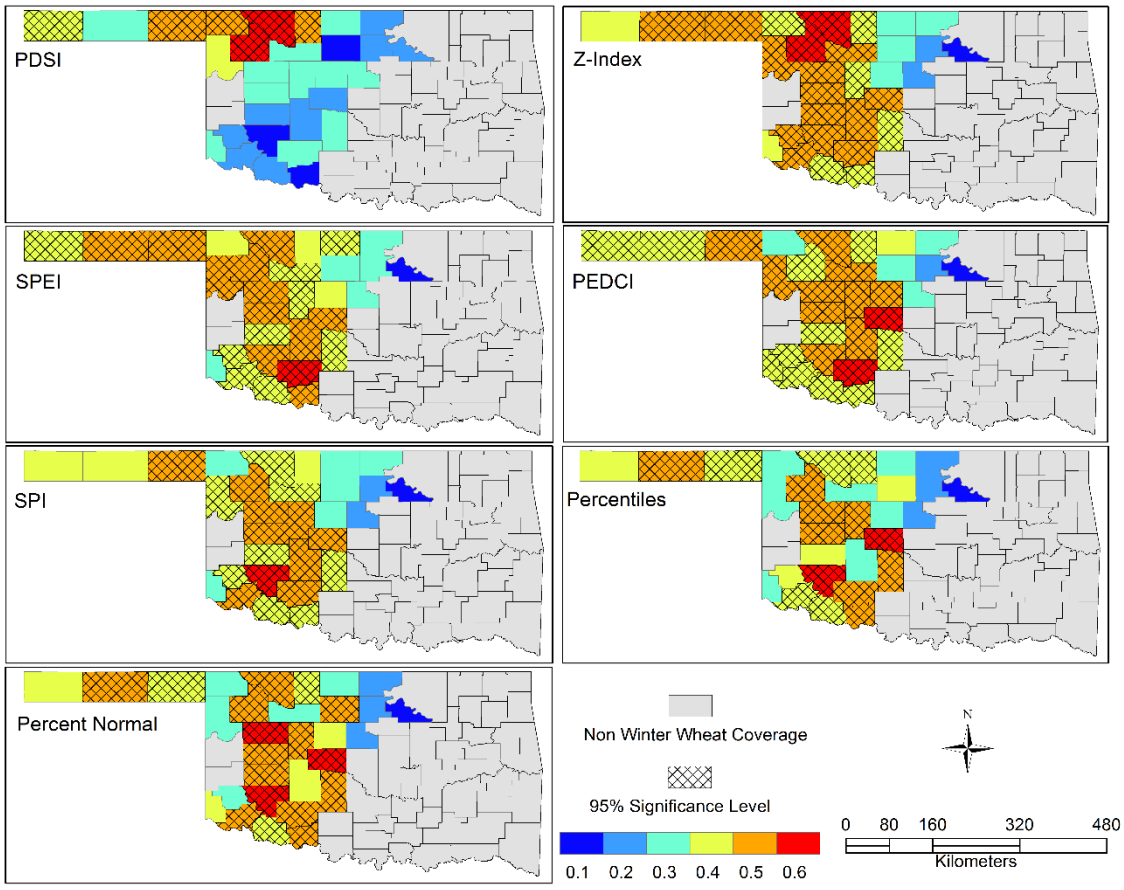

Figure 3.7 Spatial distribution of correlations between drought indices and winter wheat yield based on data from 1981 to 2014 in: (a) December and (b) April.

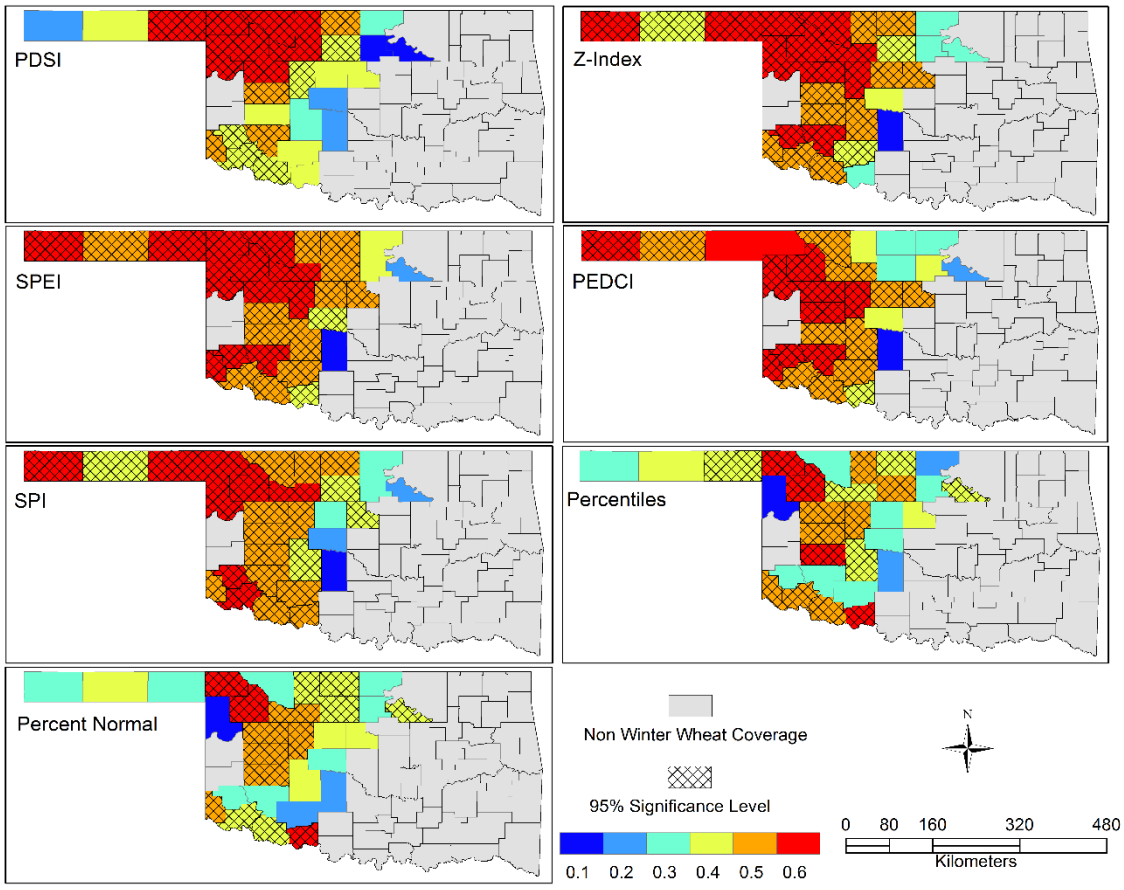

Figure 3.7 Continued

3.3.3 Winter Wheat Yield Results: Abnormal Years

Correlations between winter wheat yield and drought indices were also calculated using only years when moisture conditions and yield were well above or below normal. There are 34 years of crop yield and drought index data (1981 to 2014). Since years with near-normal yield and moisture conditions were excluded from this analysis, correlations are only calculated and reported when there are at least 10 years of data.

Figure 3.8 shows the percentage of counties with significant correlations with winter wheat yield during extreme conditions (years when neither yield or moisture conditions are near-normal). Peaks in the percentage of counties with statistically significant correlations occur in December and March/April. In December, SPI is the drought index that has the highest percentage of counties with statistically significant correlations with winter wheat yield. In March and April, Z-index has the highest percentage of counties with statistically significant correlations with winter wheat yield. However, it is evident that other indices such as PEDCI and percent normal also are among the best performing indices in most months.

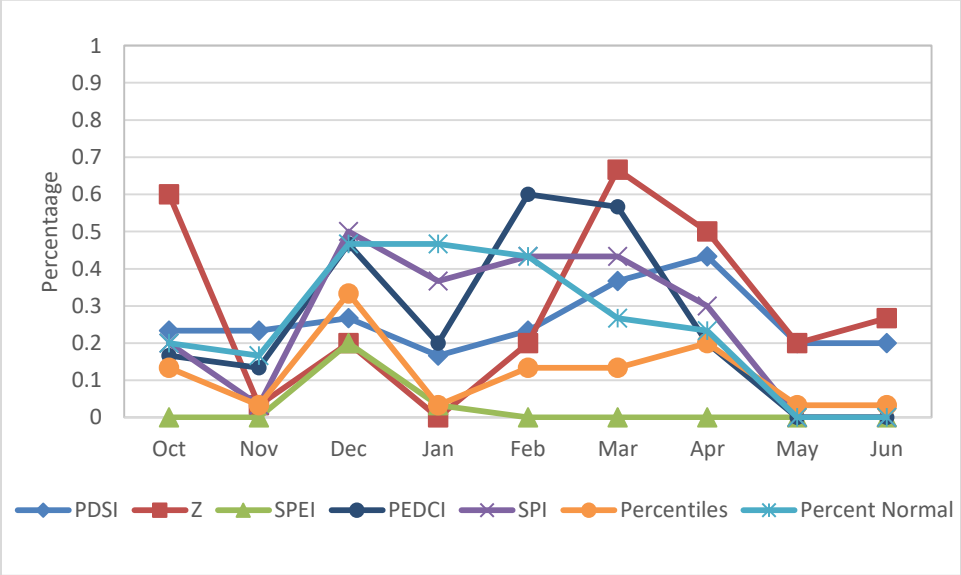

Figure 3.8 Percentage of the 30 counties in Oklahoma that have statistically significant correlations between drought indices and winter wheat yield during years with extreme moisture and yield conditions.

Figure 3.9 shows the correlations between the drought indices and winter wheat yield for December and April. In December, Z-index have the highest median correlation with yield. However, it is obvious that all of the drought indices, except for the SPEI, have a similarly strong relationship with winter wheat yield. The influence of only considering the years when moisture and yield conditions are extreme can be seen by comparing this figure to Figure 3.6. The median correlations have increased from ~0.4 (all years) to ~0.9 during extreme years for most of the drought indices, except SPEI. This suggests that drought indices are most useful for determining winter wheat yield during years that are abnormally wet or dry. It is unclear why the performance of the SPEI is relatively poor as compared to the other drought indices.

In April, the median correlations are similar for each drought index, except SPEI. Since none of the 30 counties has more than 10 years of time series of SPEI and winter wheat yield after exclude the normal yielding and climate years, no correlations are calculated for the SPEI in April. Interestingly, even the PDSI has strong correlations with winter wheat yield when only extreme years are considered.

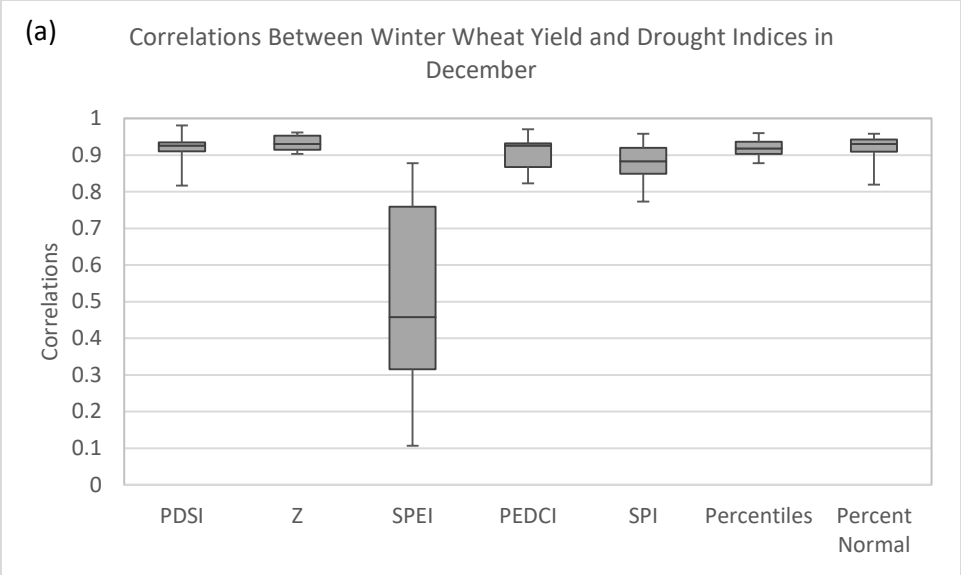

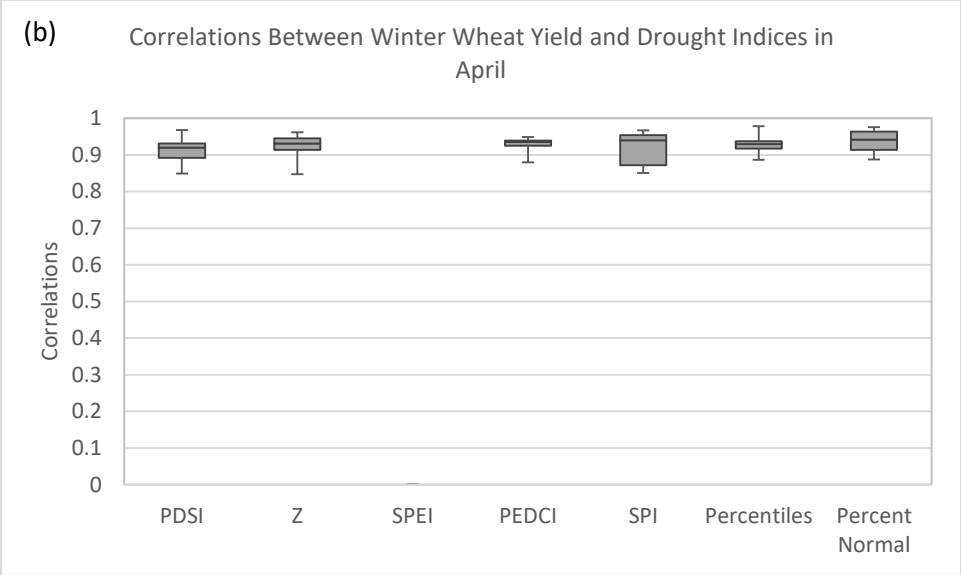

Figure 3.9 Correlations between the drought indices and winter wheat yield years with extreme moisture and yield conditions in: (a) December and (b) April.

Figure 3.10 shows the spatial distribution of correlations between drought indices and winter wheat yield in December and April. The correlations between drought indices and winter wheat yield during extreme years differ from the correlation maps using all

years. Generally, the correlations during extreme years are quite high in most counties. However, the SPEI correlations have decreased substantially. In December, percent normal performs somewhat better than the other drought indices. In April, Z-index has higher correlations and statistically significant correlations in more counties than other indices.

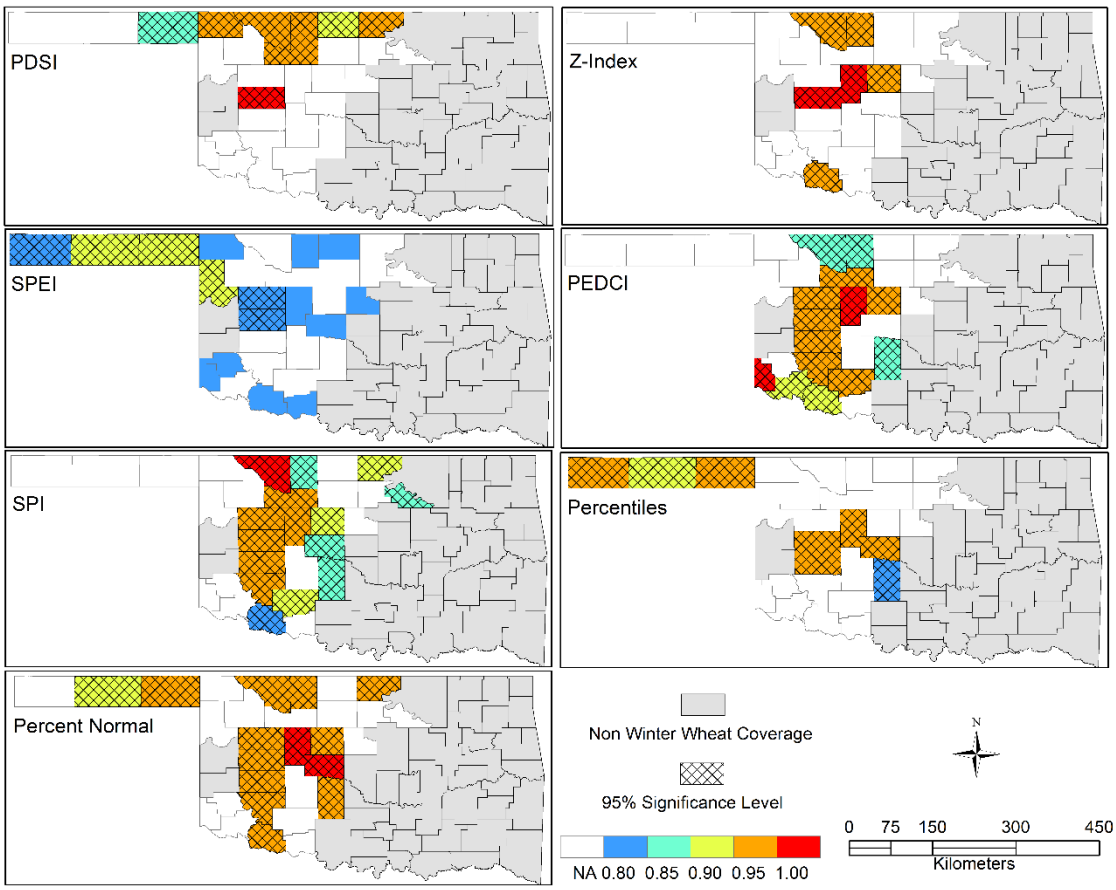

Figure 3.10 Spatial distribution of correlations between drought indices and winter wheat yield during years with extreme moisture and yield conditions: (a) December and (b) April.

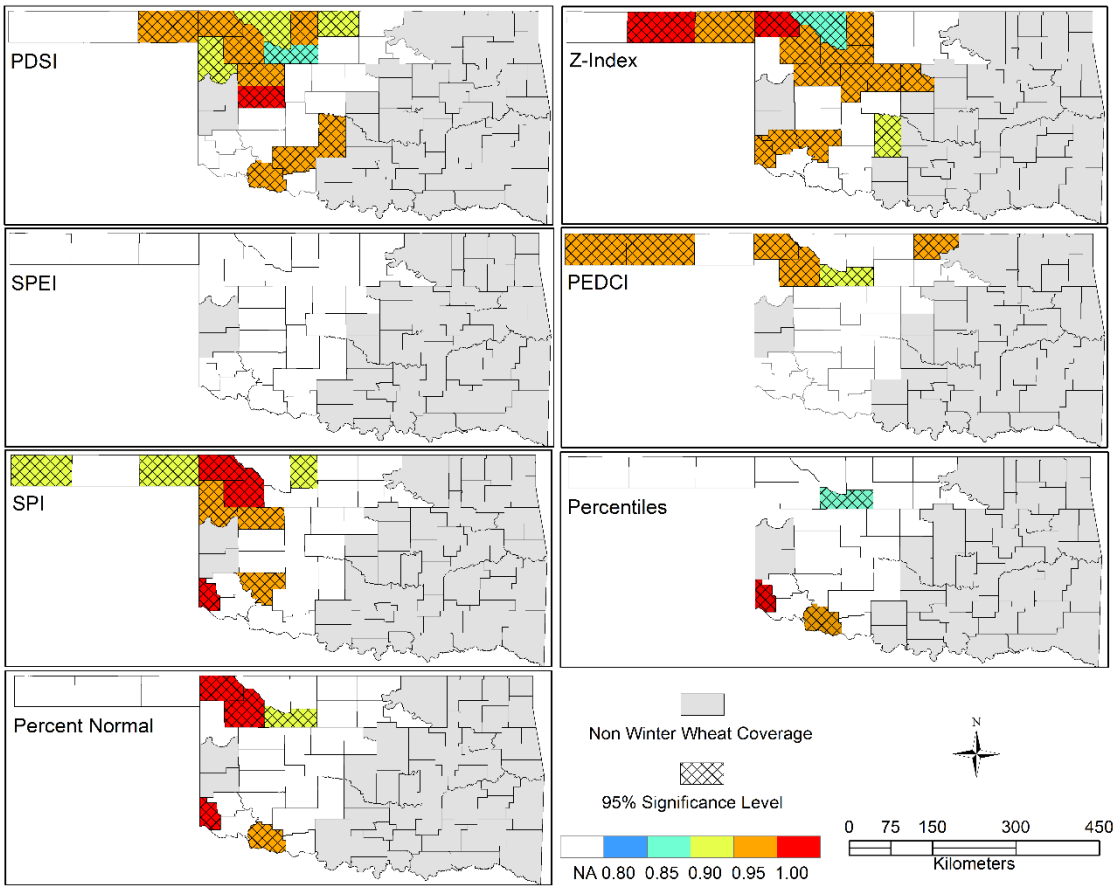

Figure 3.10 Continued

3.4 Conclusions and Limitation

3.4.1 Discussions and Conclusions

The performance of the seven drought indices was evaluated using soil moisture and winter wheat yield data to identify the most appropriate drought index for agricultural drought monitoring in Oklahoma. Correlations between soil moisture and drought indices are higher in JJA than in DJF. This result is consistent with Vicente-Serrano et al. (2012). Specifically, in JJA, correlations between soil moisture and

drought indices shows SPEI and percentile have higher correlations with soil moisture. In MAM and SON, SPEI has higher and more significant correlations with soil moisture. In DJF, Z-index has higher and more significant correlations with soil moisture, but the correlations are lower than correlations in warm months. One reason for the low correlations during winter months is that soil moisture recharge typically occurs during this period. Figure 3.11 shows the mean monthly soil moisture and precipitation percentiles in Oklahoma. Soil moisture is determined by inputs from precipitation and outputs from evapotranspiration (Belmans, Wesseling, & Feddes, 1983; Denmead & Shaw, 1962; Rushton, Eilers, & Carter, 2006). In summer, the soil dries out because evapotranspiration increases and these increases are not offset by the increases in precipitation. In winter, there is less precipitation than in summer, but there is also much less evapotranspiration. Therefore, soil moisture recharge occurs during this time (Hamlet, Mote, Clark, & Lettenmaier, 2007; Scott, Shuttleworth, Keefer, & Warrick, 2000; Vicente-Serrano et al., 2012). Due to the recharge factor in cold months, the performance of drought indices were evaluated based on correlations in warm months. Therefore, SPEI is more representative of soil moisture conditions in Oklahoma.

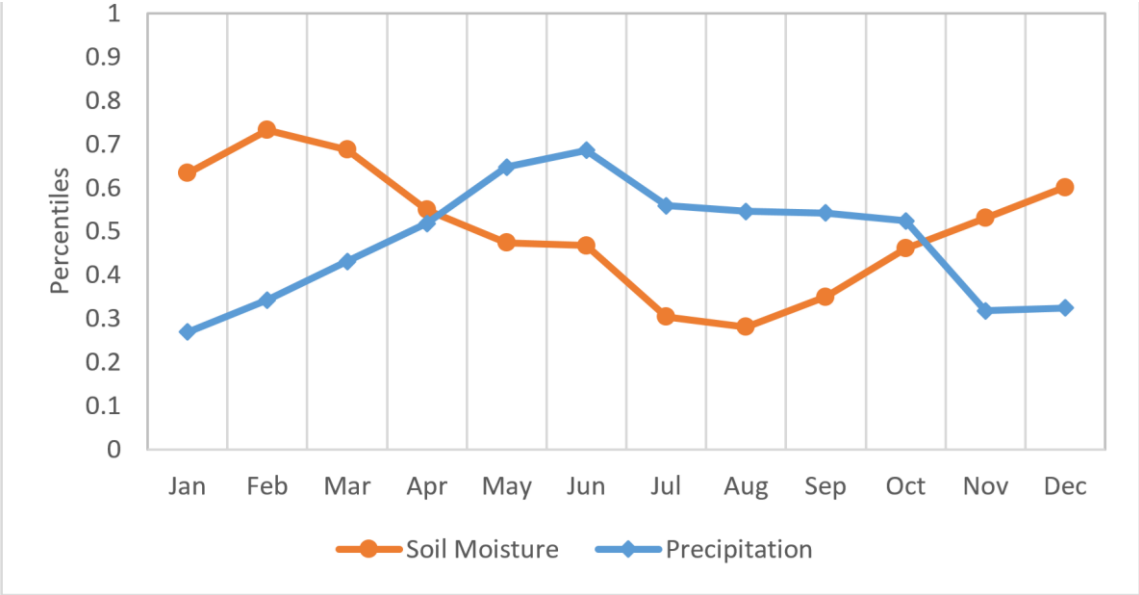

Figure 3.11 Mean monthly soil moisture and precipitation percentiles in Oklahoma (2000 to 2014).

The correlation results with winter wheat yield indicate that the performance of the drought indices varies by month during the planting period. Winter wheat yield is most strongly influenced by water deficit during two phases. In December, the Z-index is the best index to use because it has higher correlations with winter wheat yield in more counties than other indices. In April, SPEI is the best index to use because it has higher correlations with winter wheat yield in more counties than other indices. The Z-index also has similar performance to the SPEI.

S. M. Quiring and Papakryiakou (2003) also compared several drought indices for agricultural drought monitoring in Canada. They used drought indices in June and July, when the spring wheat is during the heading and soft dough stages, to develop a series of crop yield models. Their results are in agreement with the findings presented

here since they also found that the Z-index is best for predicting wheat yield when there is significant moisture stress. The S. M. Quiring and Papakryiakou (2003) was done prior to the development of the SPEI and so it was not included in their analysis. Vicente-Serrano et al. (2012) evaluated six drought indices for agricultural drought monitoring based on correlations between annual wheat yields and the drought indices. The maximum correlation between annual wheat yield and the drought indices of the month of the year in which the highest correlation was found shows SPEI and SPI have a stronger correlations with wheat yield.

Potopova et al. (2015) argue that years with near-normal yield should be excluded from these type of drought index evaluations because moisture conditions may not be an important determinant of yield during these years. Therefore, this study also evaluated the performance of the drought indices using only years with above- and below-normal moisture and yield conditions. The results differ from those based on all years of yield data. In December, percent normal is the best drought index because it has higher correlations with winter wheat yield than other drought indices, while Z-index is better than other drought indices in April.

Few of the drought index comparisons have focused on the relationship with yield during above- and below-normal conditions. The results of this study demonstrate that the relationship between drought indices and crop yield can be substantially different if only anomalous years are considered. The results of this study also demonstrate that even though the PEDCI is not the best index for monitoring agricultural drought in Oklahoma, it can provide useful information for monitoring agricultural

drought conditions (e.g., soil moisture and crop yield). The correlations between soil moisture and the SPEI and PEDCI are very similar. While for winter wheat, the PEDCI is more strongly correlated with winter wheat yield than the SPEI.

3.4.2 Limitations

One of the limitations of the correlation method used in this study is that it is sensitive to the sample size. Specifically, when the near normal 40% data were excluded, the sample size decreases. Since we only have data from 1981 to 2014, the sample size can get quite small. Therefore, we only calculated correlations if the sample size was larger than 10. This means that individual years can have a substantial influence on the correlation and the results are quite variable from county-to-county. Therefore, we reported the results from using all years of yield data as well as the anomalous years. Using just the 'extreme' years is, theoretically, the best approach for identifying which drought index to select for monitoring agricultural drought conditions. However, it requires a longer period of record to generate statistically robust results.

Another limitation of this study is that crop yield is used as one measure of agricultural drought impacts. Crop yield is influenced by more than just moisture conditions. Therefore, below-normal yield is not necessarily indicative of drier than normal conditions. Other factors such as disease, pests, fertility, and crop management practices also influence yield. In addition, the crop yield used in this study do not account for the influence of irrigation. Although USDA provides non-irrigated crop yields at the county level, the period of record is shorter than the regular (irrigated +

non-irrigated) crop yield record. The regular winter wheat yield data for Oklahoma are available through 2015, while the non-irrigated winter wheat yield data for Oklahoma are only available through 2009. An ANOVA analysis showed that there is not a statistically significant difference between the mean of the regular yield and non-irrigated winter wheat yield in Oklahoma. However, it obviously would be better to only consider non-irrigated yield. In future, more comparison should be done to investigate the impact of irrigation on the performance of drought indices.

We focused on winter wheat in this study because it is the primary crop type in Oklahoma. However, some counties in Oklahoma also plant significant amounts of corn and cotton. The relationship between drought indices and yield for other crops does not always match the results for winter wheat (results not shown). For example, correlations between the drought indices and corn yield in June showed that the SPEI has the highest correlation. Correlations between the drought indices and cotton yield in June showed that precipitation percentiles are the best index, but in August the SPEI has a higher correlations with cotton yield than other drought indices. Generally, the results demonstrate that there is no one 'best' drought index for monitoring agricultural drought in Oklahoma. The best index varies by crop and by month. A number of the drought indices have similar correlations with crop yield. For convenience, future chapters will use the SPEI and/or Z-index because they are two of the best drought indices for monitoring agricultural drought conditions. In addition, it has been widely used in the literature and its strengths and weaknesses are well known.

CHAPTER IV

SPATIAL TEMPORAL PATTERNS OF DROUGHT IN OKLAHOMA

4.1 Introduction

Drought is a normal and recurrent climate feature for all regions of the globe, but the character of drought varies spatially and temporally, reflecting the unique climatic, meteorological, hydrological, and socioeconomic characteristics (Ge, Apurv, & Cai, 2016; Wilhite, 1996). A better understanding of the spatial-temporal patterns of drought is essential for the evaluation of drought risk and drought mitigation in future. Lack of proper information of the spatial-temporal characteristics of droughts may lead to poor decisions and additional costs and damages (Saadat, Khalili, Kamgar-Haghighi, & Zand-Parsa, 2013).

The spatial-temporal patterns of droughts tend to be complex. As indicated by Field (2012), extreme weather and climate events, such as droughts, are influenced by the changing climate. Climate change can lead to the changes in the frequency, duration, intensity, spatial extent and duration of extreme weather and climate events. Analysis of the spatial and temporal patterns of drought can be helpful for improving understanding of drought behavior in a region.

Many previous studies have analyzed the spatial-temporal patterns of drought in different regions. Aiguo Dai (2011) analyzed the spatial-temporal variations in drought on a global scale from 1900 to 2008 using the PDSI. The results indicated that the global percentage of drought-affected area has increased since 1950, and more severe drying

will occur in the coming decades. A special report of the Intergovernmental Panel on Climate Change (IPCC) also suggests that regions such as southern Europe and West Africa have experienced more intense and longer droughts since 1950 (Field, 2012). However, Field (2012) also found decreasing drought trends in some regions of the world. There is also evidence that the increases in the number extreme droughts found by Aiguo Dai (2011) may be overestimated due to their use of the PDSI (Sheffield, Wood, and Roderick (2012)). The PDSI uses a simplified method for calculating potential evapotranspiration that only considers the impact of temperature. The IPCC AR5 report concludes that there is low confidence in the observed trends in global drought patterns due to the lack of direct observations (Hartmann, Tank, & Rusticucci, 2013).

On a regional scale, the IPCC AR5 report shows that drought frequency and intensity has increased in the Mediterranean and West Africa since 1950. While in central North America and northwest Australia, drought frequency and intensity has likely decreased since 1950 (Hartmann et al., 2013). However, there is a lack of consensus about this. Ge et al. (2016) investigated the spatial and temporal patterns of drought in the U.S. during the past century. They found that the duration, severity, and intensity of droughts had increased in most of the western and eastern U.S. and the Great Plains. In addition, the duration, severity, and intensity of more frequent and less severe drought events differed from the less frequent and more severe droughts. Obviously, the differences in drought trends between extreme and mild droughts complicate the analysis and makes comparing the results of different studies more difficult.

Ford and Labosier (2014) analyzed the spatial patterns of drought persistence in the southeastern U.S. Their results showed that some areas in the southeastern U.S., such as north-central Alabama, are more prone to drought than others. In addition, areas in the western portion of their study region, such as Texas and Oklahoma have greater summer-to-fall drought persistence.

In China, Xu et al. (2015) found large magnitude droughts were usually centered in the region from North China Plain to the downstream of Yangtze River. The western part of North China Plain had a significant drying trend due to the significant decrease of precipitation. Tan, Yang, and Li (2015) also found the same trends in Ningxia Hui Autonomous Region, which is located in the northwest China.

A review of spatial-temporal patterns of drought on the African continent by Masih, Maskey, Mussa, and Trambauer (2014) shows that droughts have become more frequent, intense and widespread during the last 50 years. The Sahel and equatorial eastern Africa are more prone to the most prolonged and intense droughts.

Vicente-Serrano (2006) investigated the spatial and temporal patterns of drought in Iberian Peninsula, Spain. The main drought period and the spatial distribution of drought episodes were identified. Their results highlighted the usefulness of drought regionalization in the context of drought management schemes.

The studies that are summarized above demonstrate that, even though the IPCC AR5 provides regional summaries of drought trends, it is still important to analyze drought characteristics because the results are sensitive to the data and methods that are used. For example, some studies indicate that drought frequency and intensity is

decreasing in central North America (Hartmann et al. (2013). While others suggest that the duration, severity, and intensity of droughts in this region has increased (Ge et al., 2016).

The main objective of this chapter is to investigate the spatial and temporal patterns of drought in Oklahoma. SPEI and Z-index will be used to analyze the spatial-temporal patterns of drought because these two indices are two of the best indices for agricultural drought monitoring in Oklahoma.

4.2 Data and Methods

4.2.1 CRU Precipitation and Evapotranspiration

The precipitation and potential evapotranspiration from the Climatic Research Unit Time-Series (CRU TS) 3.24 dataset, which is produced by the Climatic Research Unit at the University of East Anglia, are used for the calculation of SPEI and Z-Index in this study. Long-term drought indices are needed for the spatial and temporal drought analysis. The CRU TS 3.24 dataset contains monthly time series of climatic variables covering Earth's land area over a long period from 1901 to 2015. The climate variables include cloud cover, PET, precipitation, diurnal temperature range, daily mean temperature, monthly average daily minimum temperature, monthly average daily maximum temperature, vapor pressure, wet day frequency, and frost day frequency. The spatial resolution of CRU dataset is 0.5 * 0.5 degree. The principal sources used for the CRU datasets include the climatic data from the World Meteorological Organization (WMO), monthly climatic data for the world (MCDW) provided by National Climatic

Data Center (NCDC), and World Weather Records (WWR) decadal data publications. Many of the input records have been homogenized, but the dataset itself is not homogeneous. However, it is pointed out that the dataset can be used for climate trend analysis (Harris, Jones, Osborn, & Lister, 2014). According to Schneider et al. (2014), the full database has data for more than 10,000 stations around 1970. Even though the number of stations used in the CRU dataset changes over time, the CRU dataset uses a correlation decay distances (CDD) method in the interpolation procedure. Data for each grid cell is interpolated using stations that are outside the cell, but lie within the CDD range (Harris et al., 2014). This method produces gridded values that are relatively robust to changes in the station density over time.

The PET dataset is calculated based on the Penman-Monteith method, which has been shown to be better than the temperature-only based Thornthwaite method (Yuan & Quiring, 2014). The CRU PET data incorporates the values of daily mean temperature, minimum temperature, maximum temperature, vapor pressure, cloud cover, and a fixed monthly climatology for wind speed (Harris et al., 2014). The Penman-Monteith method is a physical-based method which considers both of the earth's surface energy balance and atmospheric water demand (Westerhoff, 2015). The Food and Agricultural Organization (FAO) defines PET as equation 3.1

$$PET = \frac{0.408\Delta(R_n - G) + \gamma \frac{900}{T+273.16} U_2 (e_a - e_d)}{\Delta + \gamma(1 + 0.34U_2)} \qquad \text{(Equation 4.1)}$$

Where

$$U_2 = U_{10} \frac{\ln(128)}{\ln(661.3)} \qquad \text{(Equation 4.2)}$$

Δ is slope of the vapour pressure curve; R_n is net radiation at crop surface; G is soil heat flux; γ is psychrometric constant; T is average temperature at 2 m height; U_2 is wind speed at 2 m height; U_{10} is wind speed at 10 m speed; $(e_a - e_d)$ is vapour pressure deficit at 2 m height (Harris et al., 2014).

The Z-Index and SPEI from 1901 to 2014 were use for the spatial and temporal analysis of drought patterns in Oklahoma. Drought indices at 1-month, 3-month and 6-month timescales were selected for this analysis because these timescales are most appropriate for agricultural drought monitoring (Vicente-Serrano et al., 2013). Shorter or longer time scale may be too sensitive to extreme conditions and may miss relevant drought events (Spinoni, Naumann, Carrao, Barbosa, & Vogt, 2014).

4.2.2 Principal Component Analysis

Principal Component Analysis (PCA) is used to define regions in Oklahoma that have similar drought characteristics. PCA is commonly used for spatial regionalization because it can effectively reduce dimensionality and extract patterns (Hannachi, Jolliffe, & Stephenson, 2007; Lorenz, 1956; Navarra & Simoncini, 2010). The main procedure of PCA technique is linearly transforming the original set of variables to a new substantial smaller set of uncorrelated variables, called principal components (PCs). The goal of PCA analysis is to explain the maximum amount of variance with the fewest number of PCs. The first PC is the linear combination of x-variables that has the largest variance among all linear combinations. The *i*th PC is the linear combination that has as much of the remaining variation as possible, and it is not correlated with the other PCs. The first

several PCs can explain the major variance of the original variables. Therefore, they can identify the major spatial patterns of the original high-dimensional dataset (Song et al., 2014; Xie, Ringler, Zhu, & Waqas, 2013). The first step of PCA analysis is to calculate the covariance matrix among all variables. PCA can be performed using either a covariance matrix or a correlation matrix. When the input data have same units and scales for all variables, covariance matrix is better than the correlation matrix method (Kwitt & Hofmann, 2006). Before calculating the covariance matrix, the input dataset was centered by removing the mean values from the dataset.

A VARIMAX (orthogonal) rotation method was applied because it simplifies the structure of the resultant patterns by forcing the value of the loading coefficients towards zero or ± 1 (Hannachi et al., 2007). The VARIMAX rotation technique is a popular method used in climate regionalization studies because the rotation tends to produce more spatially coherent regions [*White et al.,* 1991]. An unrotated PCA is primarily used for data reduction and it is not appropriate for climate regionalization (Yarnal, 1993). After rotation, each grid cell was assigned to the factor on which they had the highest loadings.

4.2.3 Mann-Kendall Test

Mann-Kendall test is a nonparametric trend test technique. It is widely used to detect the significant increasing or decreasing trend in hydro-meteorological time series (Tan et al., 2015). Comparing to other trend test methods such as simple linear

regression and Student-t test, Mann-Kendall test is less sensitive to outliers and the sample distributions (M. N. Kumar, Murthy, Sai, & Roy, 2012).

The first step of Mann-Kendall organizing the data in rank order. The differences between any two data in rank order are used to determine the number of positive differences and the number of negative difference. Then, the Mann-Kendall test statistics can be calculated. A positive value of the statistics means the increasing trend in the data, while, a negative value of the statistics indicates a decreasing trend over time. The significance of the trend can be checked at the 95% significance level to reject the null hypothesis that there is no trend in the time series. More details about the Mann-Kendall test can be found in S. Kumar, Merwade, Kam, and Thurner (2009) and Song et al. (2014)

Many studies have indicated the autocorrelations of the time series may affect the results of Mann-Kendall test (Bayazit & Onoz, 2007; Tan et al., 2015; Von Storch, 1999; Yue & Wang, 2002). Therefore, prewhitening was applied to the autocorrelated time series before the Mann-Kendall test to reduce the effects of the autocorrelation on the trend detection.

4.2.4 Drought Characteristics

Yevjevich (1967) proposed a running theory to define a drought event. A drought starts when the drought indicator first falls below a certain threshold and it ends when the drought indicator is greater than the threshold (McKee et al., 1993). Drought duration is the number of months or days during the drought event. Drought severity is

the maximum absolute value of the drought index values during the event. Spatial extent of a drought event is the percentage of the study region that has a drought index value less than the threshold for each month during the drought event and then averaging them over the entire drought duration (Steven M Quiring & Goodrich, 2008). Drought frequency is the ratio of the number of drought events to the total number of years of the study period (Tan et al., 2015).

Table 4.1 and 4.2 shows the drought severity classification for the SPEI (McKee et al., 1993; A. Mishra & Desai, 2005) and Z-Index (W. M. Alley, 1984).

Table 4-1 Drought classification based on the SPEI (A. Mishra & Desai, 2005)

Drought class	SPEI values
Mild drought	$-1.0 < SPEI < 0$
Moderate drought	$-1.5 < SPEI \leq -1.0$
Severe drought	$-2.0 < SPEI \leq -1.5$
Extreme drought	$SPEI \leq -2.0$

Table 4-2 Drought classification based on the Z-Index (W. M. Alley, 1984)

Drought class	Z-Index values
Mild drought	$-2.0 < Z\text{-Index} \leq -1.0$
Moderate drought	$-3.0 < Z\text{-Index} \leq -2.0$
Severe drought	$-4.0 < Z\text{-Index} \leq -3.0$
Extreme drought	$Z\text{-Index} \leq -4.0$

These drought classifications are derived subjectively. However, S. M. Quiring (2009) indicated objective method should be used to define the drought thresholds for specific locations. Figure 4.1 shows the probability density function (PDF) of the SPEI for locations in west and east Oklahoma. The distributions in eastern and western Oklahoma are different. This suggests that the SPEI is not a spatially invariant (i.e., SPEI values from one climate region cannot directly be compared to another climate region because the probability of occurrence for a given index value is not the same in both locations). Therefore, it is necessary to define drought severity using objective thresholds.

S. M. Quiring (2009) developed objective operational drought definitions based on the PDFs of several drought indices. Normal, gamma, lognormal, and exponential PDFs were compared, and one of these functions was selected to determine the operational drought thresholds for each drought index. The drought categories criteria is based on the drought classes employed by the United States Drought Monitor (USDM), as shown in Table 4.3 (Svoboda et al., 2002). According to S. M. Quiring (2009), the normal PDF is more appropriate for the objective operational drought thresholds for SPEI and Z-Index. Therefore, the normal PDF is used in this study.

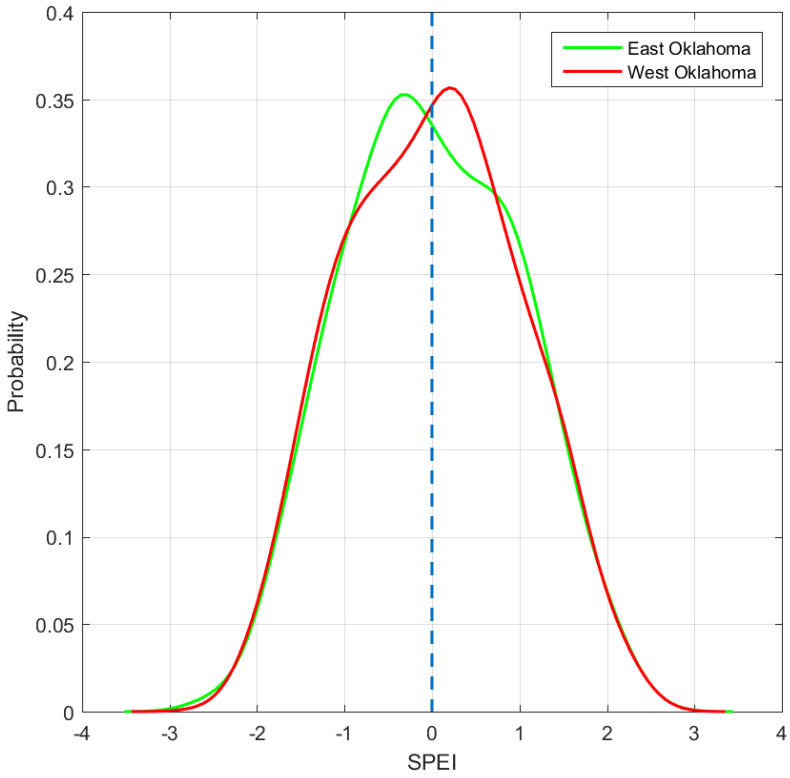

Figure 4.1 Probability density function of SPEI for east and west Oklahoma (1901 to 2014).

Table 4-3 USDM drought definitions

Category	Drought classes	Percentile
D0	Abnormally dry	20% to 30%
D1	Moderate drought	10% to 20%
D2	Severe drought	5% to 10%
D3	Extreme drought	2% to 5%
D4	Exceptional drought	Less than 2%

4.3 Results

4.3.1 Spatial Patterns of Drought

Since the results of SPEI and Z-Index are similar, we have chosen to only show the results for the SPEI in this section. The regionalization results are similar for the SPEI at different scales. Here, we display the PCA results for the 6-month SPEI (SPEI6). PCA of the SPEI6 field demonstrates that four regions should be retained for spatiotemporal analysis of drought patterns in Oklahoma. Figure 4.2 shows the explained variance of SPEI6 by PCA. The first four PCs account for 83.8% of the variance.

Figure 4.3 shows the loadings of the first four PCs. The loadings are the correlation coefficients between the PC scores and the original variables. The first PC has the highest loadings in southeastern Oklahoma. The second PC has the highest loadings in southwestern Oklahoma. The third PC has the highest loadings in northeastern Oklahoma. The fourth PC has the highest loadings in northwestern Oklahoma. Based on the PC loadings, drought regions in Oklahoma are generated as shown in Figure 4.4.

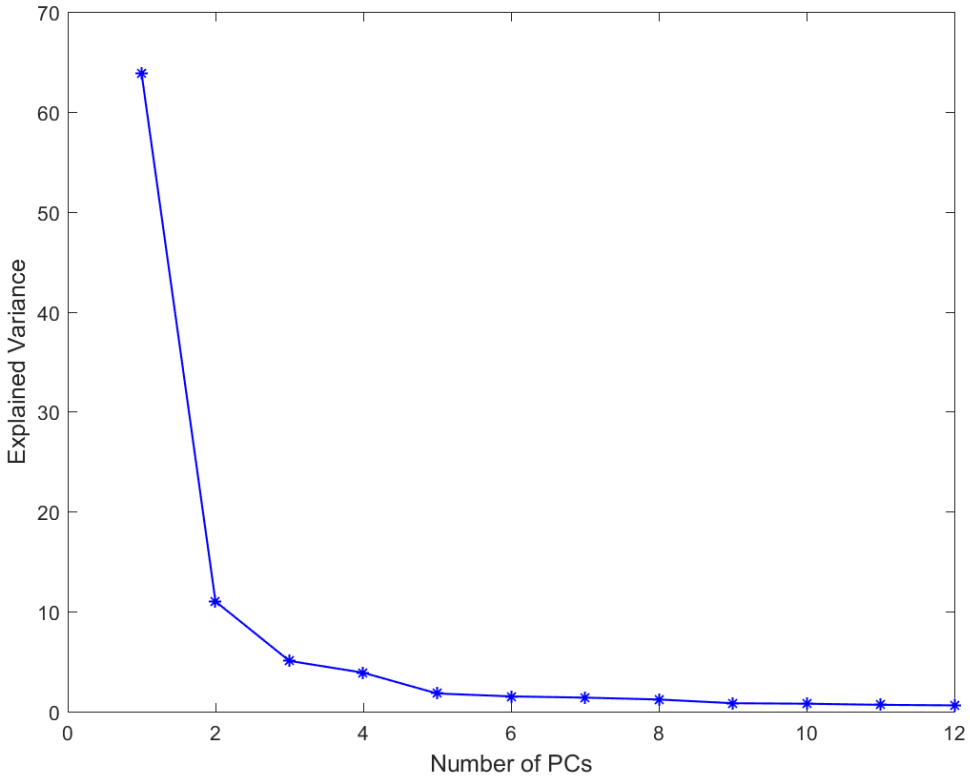

Figure 4.2 Explained variance of SPEI.

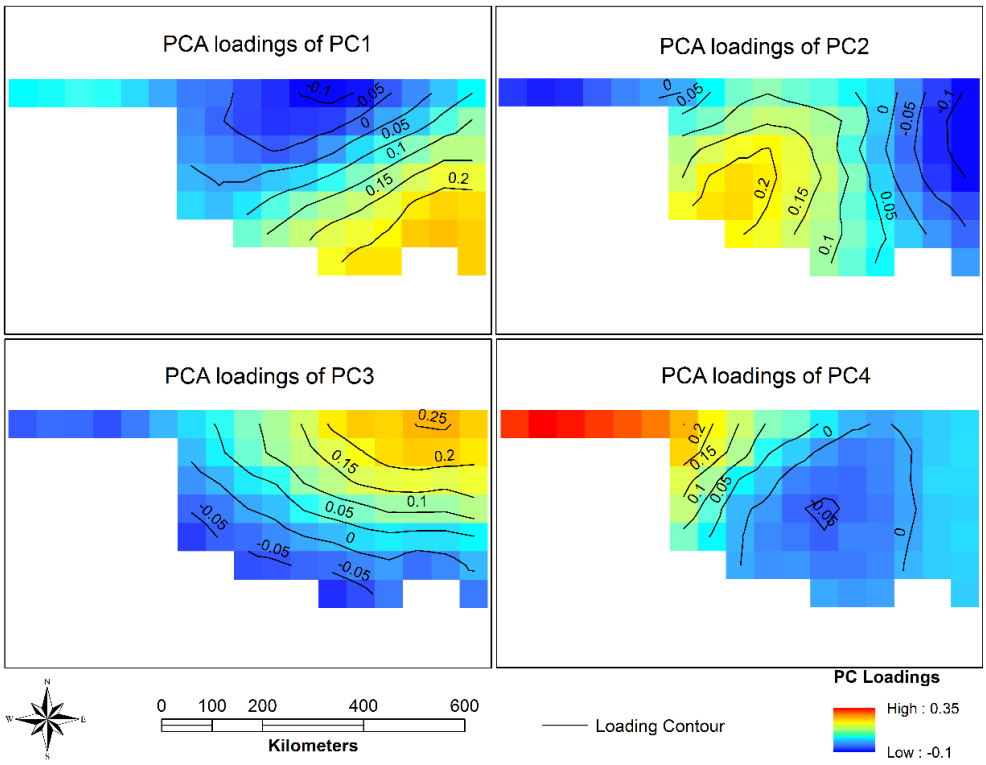

Figure 4.3 Loadings for the first four PCs.

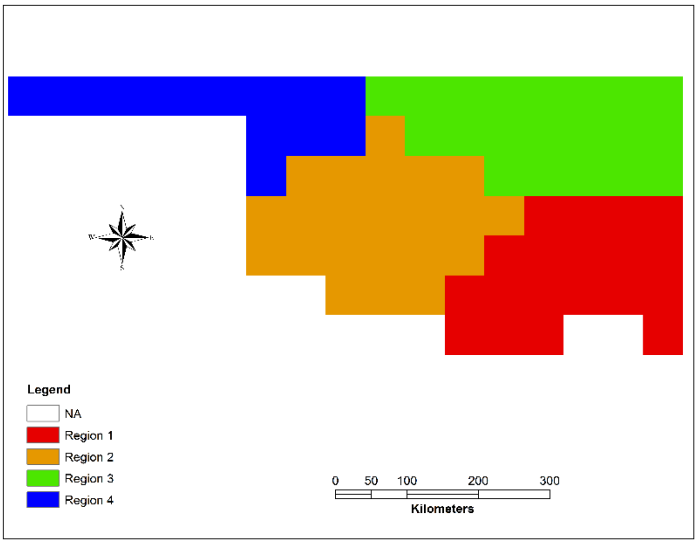

Figure 4.4 Drought regions based on PCA.

Based on the PCA results, drought indices for each region are calculated by averaging all the grid cells in each region. Figure 4.5 shows the SPEI6 in the four regions in Oklahoma. The data have been smoothed by applying a 120-month moving average. For example, the SPEI6 in 1910 is the based on the mean SPEI6 from 1901 to 1910. Similarly, SPEI6 in year_X is the mean SPEI6 from year_{X-9} to year_X. The SPEI6 indicates that there are decadal-scale cycles in Oklahoma. Prolonged periods of drier than normal conditions occurred in the 1910s, 1930s, 1950s, 1970s, and 1980s. Conditions from the 1980s to the 2000s were wetter than normal. Recently, the SPEI6 has decreased in Oklahoma, which suggests that the state may be at the beginning of another dry cycle. These findings are consistent with the report from the Oklahoma Water Resources Board (Oklahoma Water Resources Board, Oklahoma Climatological Survey, & (U.S.), 2012).

Regionally, drought conditions during the 1930s were most severe in region 4. Drought conditions during the 1980s were most severe in region 1. During the wetter conditions from the 1980s to the 2000s, Region 4 remained drier than other regions.

The trends in the 3-month SPEI (SPEI3) and 1-month SPEI (SPEI1) are consistent with SPEI6. These figures are shown in Appendix A (Figure A.1 and A.2).

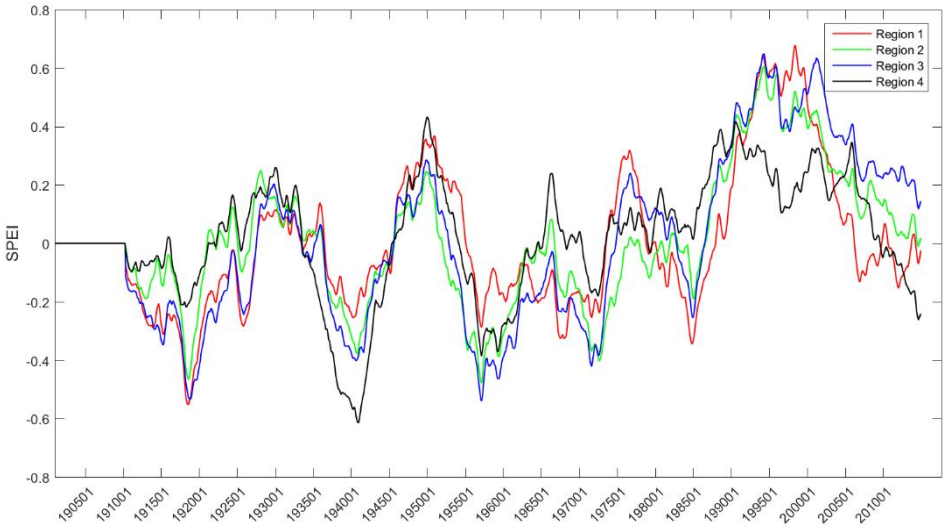

Figure 4.5 6-month SPEI (SPEI6) for each region in Oklahoma from 1901 to 2014. Data have been smoothed with a 120-month moving average.

4.3.2 Historical Drought Characteristics

Figure 4.6 shows the SPEI6 for each region in Oklahoma from 1901 to 2014. For Region 1, the objective drought threshold for the SPEI6 is -0.75. In Region 1 there were 42 drought events between 1901 and 2014. Six drought events lasted more than ten months. These drought events occurred in 1900s, 1920s, 1950s, and 2005. In Region 2 the objective SPEI drought threshold is -0.74. There were 47 drought events during the study period in this region. Three of these drought events lasted longer than 10 months. These drought events occurred in the 1900s and 1950s. In Region 3 the objective SPEI drought threshold is -0.73. There are 37 drought events during the study period and 6 of them lasted longer than 10 months. Four of these drought events occurred between 1952 and 1964. The objective SPEI drought threshold in Region 4 is -0.72. There are 40

drought events that occurred in this region and 5 of them lasted longer than 10 months. 3 of these events occurred in the 1950s.

The SPEI is much more variable at shorter timescales. Therefore, the number of drought events increases and the severity and duration decreases when using the SPEI1 and SPEI3 as shown in Appendix A (Figure A.3 and A.4).

The duration, severity, and spatial extent of each drought event in Region 1 are reported in Table 4.4. The top ranked drought (based on drought severity) began in March 1909 and ended in July 1911 (29 months). This was the most severe drought that occurred in this region. The rank of drought duration is similar to the rank of drought severity. The top 10 ranked droughts based on drought duration are also the top 10 ranked droughts based on drought severity. 7 of the 10 top ranked droughts occurred before 1960. The rank of spatial extent is different from the rank of drought duration and severity, which suggests that the spatial extent of drought events is not as strongly correlated as drought duration and severity. The drought climatology developed in this study using the SPEI was compared to the drought history developed by the South Central Climate Science Center (SC-CSC) (http://www.southcentralclimate.org/index.php/pages/resources/category/oklahoma_drought_histories). The SC-CSC drought history is based on temperature and precipitation records and PDSI for each climate division in Oklahoma as shown in Figure 4.7 (Oklahoma Climatological Survey, 2014). Region 1 in our study is similar to climate divisions 6, 8 and 9. Based on the drought history for climate divisions 6, 8 and 9, there were severe droughts in 1909 to 1918, 1930 to 1944, 1950 to 1956, 1962 to 1967, 1977

to 1981, 2002 to 2006, and 2010 to 2012. The top ten ranked drought events in region 1 from our study were also recorded in the SC-CSC, except the drought events in 1924 and 1901. These differences are likely due the spatial mismatch between the region and the climate divisions.

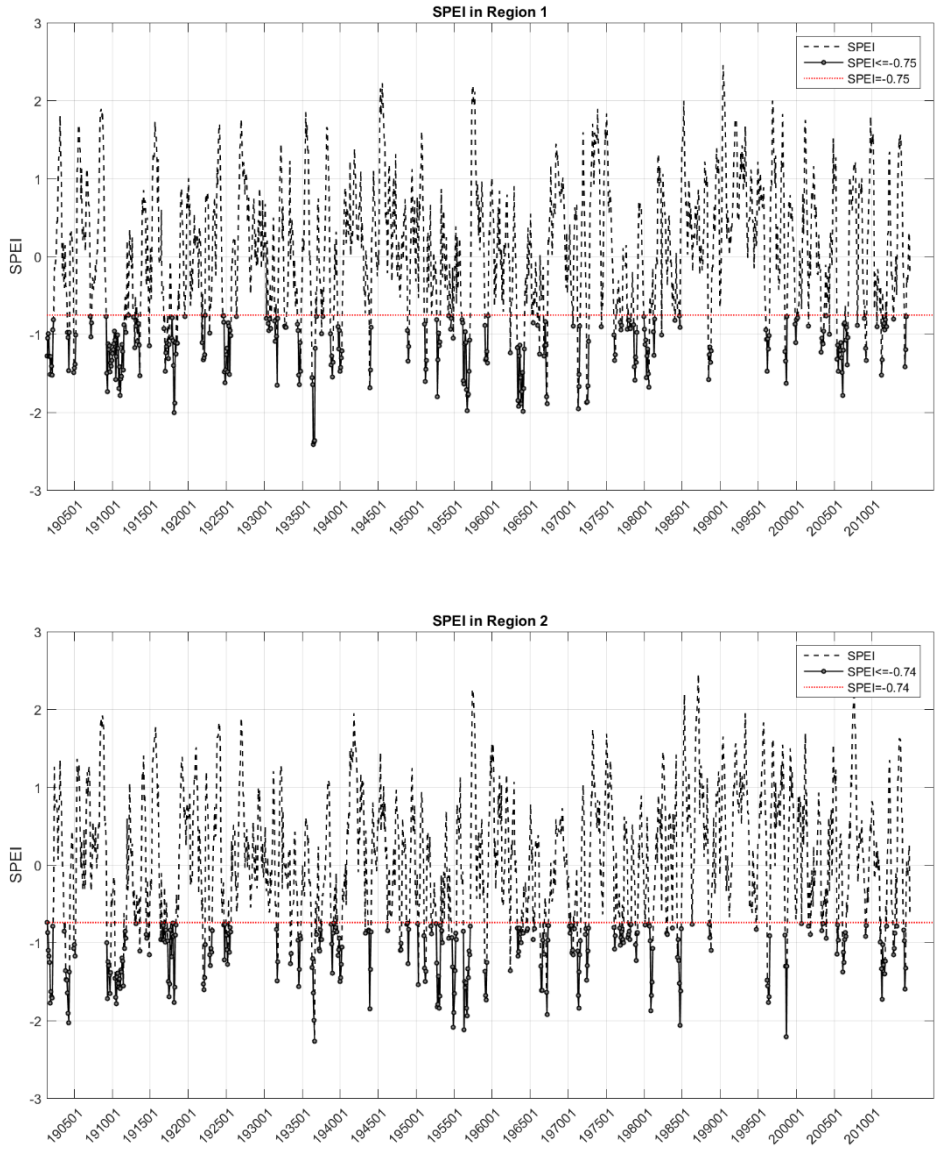

Figure 4.6 6-month SPEI for each region in Oklahoma from 1901 to 2014 (SPEI6).

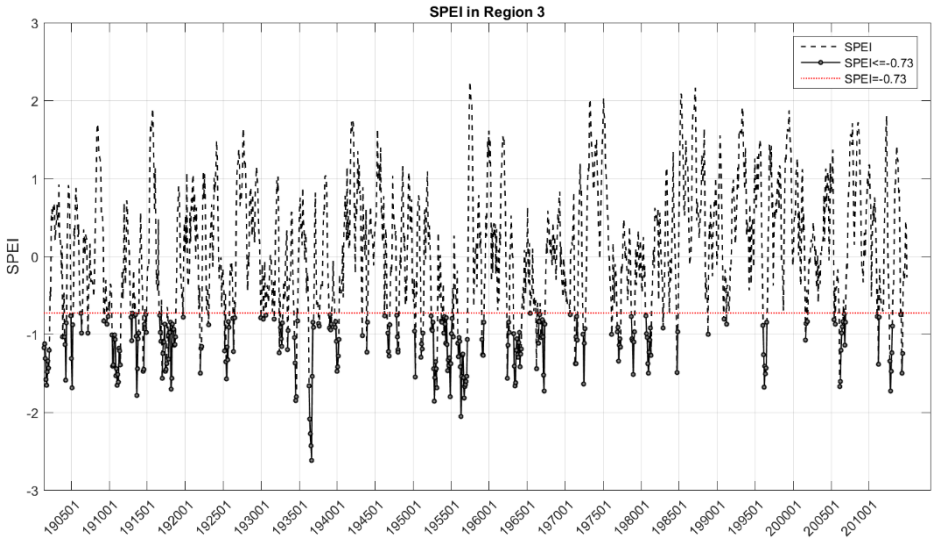

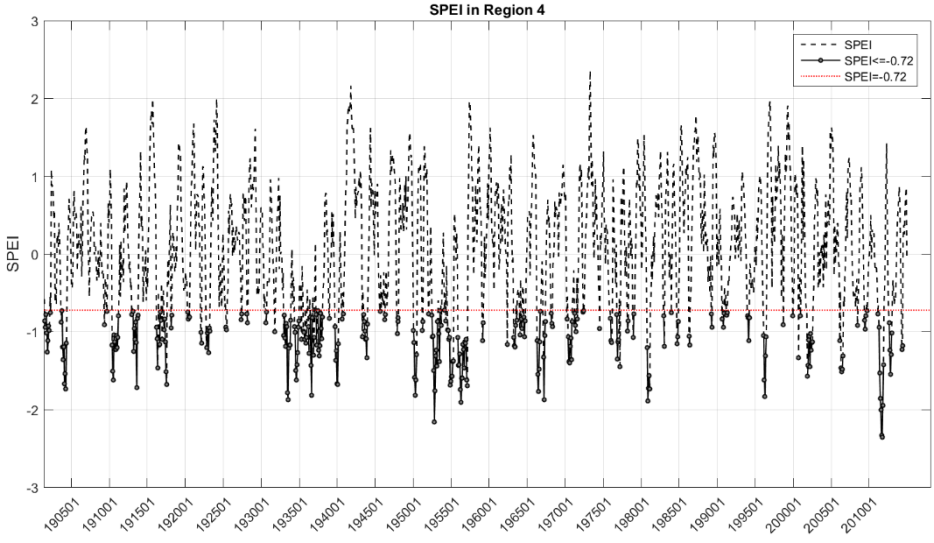

Figure 4.6 Continued

Table 4-4 Drought characteristics for each drought event from 1901 to 2014 in Region 1 (southeastern Oklahoma).

Start Month	End Month	Duration (month)	Duration Rank	Severity	Severity Rank	Spatial Extent (%)	Spatial Extent Rank
190903	191107	29	1	37.50	1	84.21	12
192407	192508	14	2	16.10	5	76.32	28
195601	195701	13	3	17.90	3	83.81	17
200505	200605	13	3	16.18	4	77.73	27
196304	196403	12	5	18.92	2	96.49	1
190106	190204	11	6	13.37	6	84.21	12
197912	198008	9	7	11.13	8	80.70	23
191710	191805	8	8	10.58	9	81.58	21
193909	194003	7	9	8.46	10	84.96	11
193604	193609	6	10	11.55	7	90.35	5
196610	196703	6	10	8.09	11	83.33	18
193405	193410	6	10	7.58	12	75.44	29
197808	197901	6	10	7.52	13	78.95	25
195209	195302	6	10	7.18	14	85.09	10
195901	195906	6	10	6.89	15	78.07	26
199601	199606	6	10	6.75	16	71.93	32
198806	198810	5	17	6.59	17	88.42	6
193809	193901	5	17	6.57	18	85.26	9
200304	200308	5	17	5.48	21	81.05	22
197206	197209	4	20	6.50	19	93.42	3
197104	197107	4	20	6.04	20	86.84	8
190412	190503	4	20	5.33	22	94.74	2
195102	195105	4	20	5.27	23	84.21	12
191612	191703	4	20	4.98	24	88.16	7
199807	199810	4	20	4.97	25	82.89	19
192112	192203	4	20	4.66	26	73.68	31
190402	190405	4	20	4.46	27	84.21	12
200607	200610	4	20	4.43	28	71.05	35
201106	201109	4	20	3.51	32	64.47	38
197712	197803	4	20	3.49	33	59.21	40
194311	194401	3	31	4.06	29	91.23	4
197601	197603	3	31	3.60	30	84.21	12
191306	191308	3	31	3.54	31	82.46	20
193108	193110	3	31	3.48	34	71.93	32
194811	194901	3	31	3.45	35	80.70	23
201404	201406	3	31	3.38	36	75.44	29
198103	198105	3	31	3.05	37	71.93	32

Table4-4 Continued

Start Month	End Month	Duration (month)	Duration Rank	Severity	Severity Rank	Spatial Extent (%)	Spatial Extent Rank
199911	200001	3	31	2.80	38	68.42	36
193209	193211	3	31	2.71	39	64.91	37
197611	197701	3	31	2.67	40	59.65	39
190702	190704	3	31	2.66	41	57.89	41
193007	193009	3	31	2.63	42	52.63	42

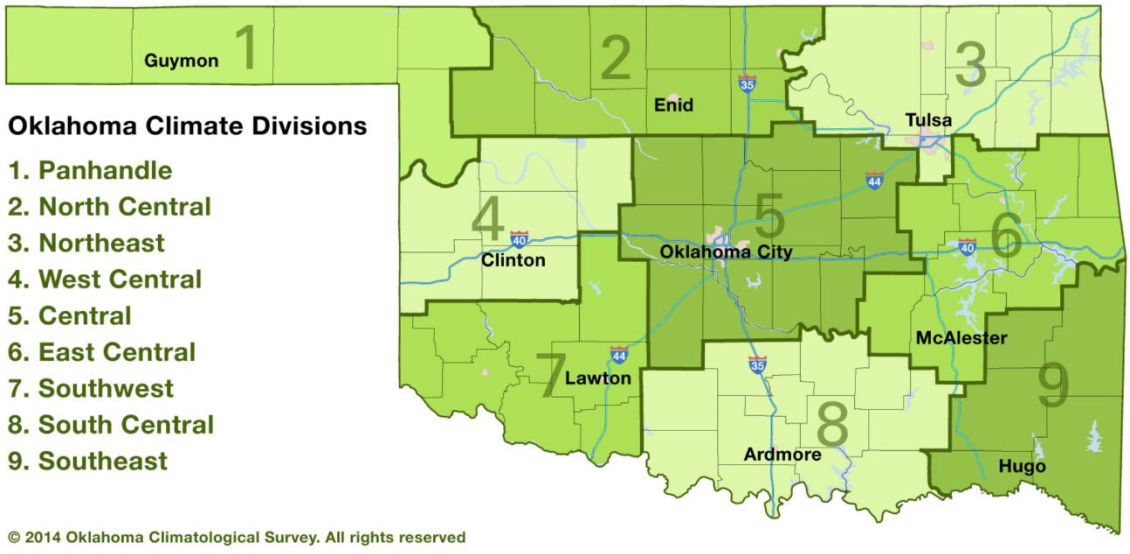

Figure 4.7 Climate divisions of Oklahoma from South Central Climate Science Center (Oklahoma Climatological Survey, 2014)

Table 4.5 shows the drought characteristics for Region 2. The most severe drought in this region began in May 1910 and ended in June 1911 (14 months). 94.81% of the region experienced drought during this drought event. It is ranked as the second largest drought area. Similar to region 1, the rank of drought duration is similar to the rank of drought severity but the rank of spatial extent is different from the rank of

drought duration and severity. Among the top 10 ranked droughts, 8 of them happened before 1960. Specifically, 3 of them happened in 1900s, 2 of them happened in 1910s, and 3 of them happened in 1950s. The drought durations and severities of droughts in region 2 is moderate than the drought conditions in region 1. Region 2 in our study based is similar to the climate divisions 4, 5 and 7. Based on the drought history for climate divisions 4, 5 and 7, there were severe droughts in 1909 to 1918, 1933 to 1940, 1950 to 1957, 1963 to 1972, 1976 to 1981, and 2003 to 2012. The top ten drought events in region 2 from our study were also recorded in the SC-CSC drought climatology, except the drought events in 1900s.

Table 4-5 Drought characteristics for each drought event from 1901 to 2014 in Region 2 (southwestern Oklahoma).

Start Month	End Month	Duration (month)	Duration Rank	Severity	Severity Rank	Spatial Extent (%)	Spatial Extent Rank
191005	191106	14	1	20.67	1	94.81	2
195603	195702	12	2	17.21	2	84.47	14
190106	190203	10	3	12.74	3	79.09	21
195208	195303	8	4	11.39	4	84.09	15
195409	195504	8	4	11.10	6	82.39	18
191710	191805	8	4	8.76	10	71.02	34
190311	190405	7	7	11.28	5	98.70	1
190904	190910	7	7	9.73	7	90.91	6
198405	198411	7	7	9.41	8	79.22	20
201103	201109	7	7	9.27	9	85.71	11
198008	198102	7	7	8.68	11	77.27	22
193909	194003	7	7	8.49	12	82.47	17
196304	196310	7	7	6.66	16	67.53	37
197103	197108	6	14	8.14	14	86.36	10
200602	200607	6	14	6.50	18	73.48	29
197204	197209	6	14	6.43	19	66.67	38

Table 4-5 Continued

Start Month	End Month	Duration (month)	Duration Rank	Severity	Severity Rank	Spatial Extent (%)	Spatial Extent Rank
197711	197804	6	14	5.18	28	51.52	47
193604	193608	5	18	8.44	13	92.73	4
199603	199607	5	18	7.42	15	89.09	7
191704	191708	5	18	6.54	17	84.55	13
194309	194401	5	18	5.76	21	71.82	32
193406	193410	5	18	5.74	22	68.18	35
192210	192302	5	18	5.51	25	75.45	27
193810	193902	5	18	4.80	30	65.45	39
195901	195904	4	25	6.04	20	93.18	3
199807	199810	4	25	5.73	23	80.68	19
192112	192203	4	25	5.61	24	92.05	5
196605	196608	4	25	5.50	26	88.64	8
196702	196705	4	25	5.31	27	77.27	22
195101	195104	4	25	5.11	29	88.64	8
201402	201405	4	25	4.74	31	84.09	15
197005	197008	4	25	4.17	32	68.18	35
197811	197902	4	25	4.02	33	72.73	30
192505	192508	4	25	3.67	34	63.64	40
197610	197701	4	25	3.64	35	61.36	43
194810	194901	4	25	3.60	36	59.09	44
191607	191610	4	25	3.48	38	53.41	46
193108	193110	3	38	3.57	37	75.76	25
190412	190502	3	38	3.27	39	84.85	12
192501	192503	3	38	3.27	40	75.76	25
194711	194801	3	38	3.19	41	71.21	33
201210	201212	3	38	3.11	42	77.27	22
193703	193705	3	38	3.02	43	74.24	28
200505	200507	3	38	2.89	44	72.73	30
191108	191110	3	38	2.87	45	62.12	42
197601	197603	3	38	2.80	46	63.64	40
192409	192411	3	38	2.75	47	56.06	45

Table 4.6 shows the drought characteristics for Region 3. The most severe drought in region 3 began in November 1955 and ended in February 1957 (16 months). 86.88% of the region experienced drought during this drought event. It is ranked as the third largest in terms of drought area. The rank of drought duration is also similar to the rank of drought severity in this region. The rank of spatial extent is different from the rank of drought duration and severity. Among the top 10 ranked droughts, 8 of them happened before 1960. Specifically, 3 of them happened in 1910s and another 3 of them happened in 1950s. Region 3 in our study is similar to the climate divisions 2, 3 and 5. Based on the drought history for climate divisions 2, 3 and 5, there were severe droughts in 1909 to 1926, 1930 to 1940, 1950 to 1958, 1962 to 1972, 1975 to 1982, 2003 to 2006, and 2010 to 2012. The top ten ranked drought events in region 3 were also recorded in the SC-CSC drought climatology, except the drought events in 1901.

Table 4-6 Drought characteristics for each drought event from 1901 to 2014 in Region 3 (northeastern Oklahoma).

Start Month	End Month	Duration (month)	Duration Rank	Severity	Severity Rank	Spatial Extent (%)	Spatial Extent Rank
195511	195702	16	1	22.98	1	86.88	3
191005	191106	14	2	18.51	2	82.14	11
195401	195502	14	2	16.13	4	71.79	26
196303	196403	13	4	16.46	3	78.08	17
191710	191809	12	5	13.43	6	71.25	27
195205	195302	10	6	12.84	7	84.00	7
190106	190202	9	7	12.30	8	85.56	5
198008	198104	9	7	10.17	9	80.00	14
193604	193611	8	9	14.37	5	90.00	2
191612	191707	8	9	10.17	10	82.50	10
199601	199607	7	11	9.03	11	80.00	14

Table 4-6 Continued

Start Month	End Month	Duration (month)	Duration Rank	Severity	Severity Rank	Spatial Extent (%)	Spatial Extent Rank
193909	194003	7	11	8.08	12	84.29	6
196610	196704	7	11	8.04	13	77.14	21
200602	200607	6	14	7.21	14	70.00	28
192505	192510	6	14	7.16	15	80.83	13
191306	191311	6	14	7.06	16	69.17	30
197611	197704	6	14	6.59	18	75.00	22
197809	197902	6	14	6.50	19	75.00	22
201209	201301	5	19	6.68	17	91.00	1
197104	197108	5	19	5.64	21	78.00	18
193405	193408	4	21	6.06	20	86.25	4
197205	197208	4	21	4.68	22	77.50	19
190412	190503	4	21	4.64	23	72.50	25
190402	190405	4	21	4.61	24	78.75	16
195101	195104	4	21	4.60	25	81.25	12
196205	196208	4	21	4.52	26	75.00	22
195901	195904	4	21	4.44	27	77.50	19
194608	194611	4	21	4.37	28	70.00	28
194710	194801	4	21	4.22	29	66.25	31
193207	193210	4	21	3.98	30	65.00	32
193812	193903	4	21	3.48	33	58.75	35
192112	192202	3	32	3.83	31	83.33	8
191406	191408	3	32	3.79	32	83.33	8
191608	191610	3	32	2.83	34	63.33	33
200609	200611	3	32	2.72	35	56.67	37
196606	196608	3	32	2.71	36	58.33	36
191211	191301	3	32	2.59	37	63.33	33

Table 4.7 shows the drought characteristics for Region 4. The most severe drought in region 4 began in November 1955 and ended in February 1957 (16 months). The drought severity is 22.62. 91.35% of the region experienced drought during this drought event and it is ranked as the fourth largest drought area. The rank of drought

severity is also similar to the rank of drought duration in this region. Among the top 10 ranked drought events, 8 of them happened before 1960s. Specifically, 3 of them happened in 1950s. Region 4 in our study is similar to the climate divisions 1 and 2. Based on the drought history for climate divisions 1 and 2, there were severe droughts in 1909 to 1926, 1932 to 1940, 1950 to 1957, 1962 to 1972, and 2010 to 2012. The top ten ranked drought events in region 4 were also recorded in the SC-CSC drought climatology, except the droughts in 1903 and 2001.

Region 1 tends to have the longest and most severe drought in history. Drought from March 1909 to July 1911 in region 1 lasted 29 months and was the most severe drought from 1901 to 2014 in Oklahoma. Drought from November 1903 to May 1904 in region 2 influenced the largest area in Oklahoma. 98.7% of region 2 experienced drought during this drought event.

Table 4-7 Drought characteristics for each drought event from 1901 to 2014 in Region 4 (northwestern Oklahoma).

Start Month	End Month	Duration (month)	Duration Rank	Severity	Severity Rank	Spatial Extent (%)	Spatial Extent Rank
195511	195702	16	1	22.62	1	91.35	4
193212	193311	12	2	14.02	3	73.72	24
191005	191103	11	3	13.07	6	74.83	21
195407	195504	10	4	13.39	4	77.69	20
195206	195303	10	4	13.19	5	80.00	14
190309	190405	9	6	11.47	7	83.76	10
200111	200207	9	6	11.16	8	79.49	16
191302	191310	9	6	9.41	10	70.09	29
201104	201111	8	9	14.41	2	95.19	2

Table 4-7 Continued

Start Month	End Month	Duration (month)	Duration Rank	Severity	Severity Rank	Spatial Extent (%)	Spatial Extent Rank
193405	193412	8	9	9.57	9	77.88	19
193706	193801	8	9	8.09	14	74.04	23
190107	190202	8	9	7.90	16	54.70	36
197005	197011	7	13	8.35	12	82.42	11
194306	194312	7	13	7.07	18	70.33	28
195001	195006	6	15	8.46	11	88.46	6
193909	194002	6	15	8.05	15	89.74	5
196604	196609	6	15	7.79	17	80.77	12
192210	192303	6	15	6.44	20	79.49	16
198010	198102	5	19	8.12	13	95.38	1
199602	199606	5	19	6.88	19	84.62	7
191703	191707	5	19	6.15	21	78.46	18
201208	201212	5	19	5.99	22	80.00	14
200604	200607	4	23	5.78	23	94.23	3
196702	196705	4	23	5.12	24	80.77	12
193606	193609	4	23	4.89	25	71.15	26
197610	197701	4	23	4.37	26	71.15	26
196303	196306	4	23	4.37	27	84.62	7
191607	191610	4	23	3.94	28	59.62	32
199312	199403	4	23	3.55	29	63.46	31
192004	192007	4	23	3.22	31	44.23	40
191603	191605	3	31	3.51	30	84.62	7
195305	195307	3	31	3.14	32	71.79	25
193507	193509	3	31	3.10	33	58.97	33
198409	198411	3	31	3.09	34	69.23	30
197512	197602	3	31	3.09	35	74.36	22
196407	196409	3	31	2.74	36	58.97	33
194711	194801	3	31	2.72	37	48.72	39
197103	197105	3	31	2.68	38	56.41	35
200905	200907	3	31	2.62	39	53.85	37
196802	196804	3	31	2.59	40	51.28	38

Figure 4.8 shows the drought frequency for each region in Oklahoma. There is not a large difference in the drought frequency between regions. Drought frequency in

Region 4 is highest, followed by Region 2, Region 1, and Region 3. Seasonally, droughts are more likely to occur in spring (MAM) season in all of the regions, except Region 2, as shown in Figure 4.9. In Region 2, summer has the highest drought frequency.

Figure 4.10 shows the seasonal frequency for different drought categories and each region in Oklahoma. The seasonality of drought frequency is most variable in Region 4. The frequency of each drought category varies among the seasons and regions. Generally, moderate drought is more frequent than severe drought and extreme drought for all regions and in all seasons. For severe and extreme drought, there is little difference between the drought frequency in spring and summer. However, in fall and winter, severe droughts are more frequent than extreme droughts.

In Region 1, moderate droughts are most frequent in summer, severe droughts are most frequent in winter, and extreme droughts are most frequent in spring. In Region 2, moderate droughts are most frequent in cold seasons (DJF and MAM), severe droughts are most frequent in warm seasons (JJA and SON), and extreme droughts are most frequent in spring and summer. In Region 3, moderate droughts are most frequent in fall, severe droughts are frequent in all seasons, except in fall, and extreme droughts are most frequent in spring and summer. In Region 4, moderate droughts are most frequent in spring and extreme droughts are most frequent in summer. Severe droughts do not show a seasonal preference.

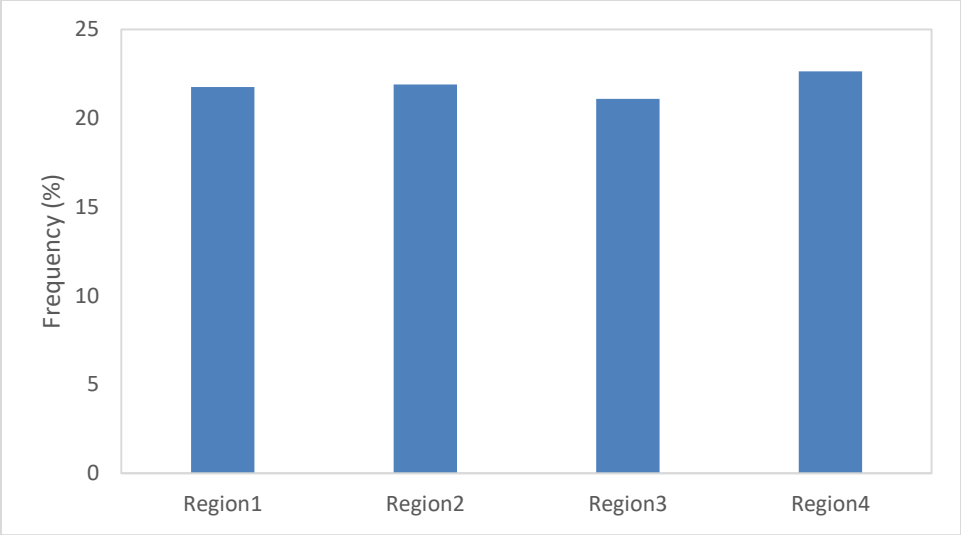

Figure 4.8 Drought frequency for each region in Oklahoma.

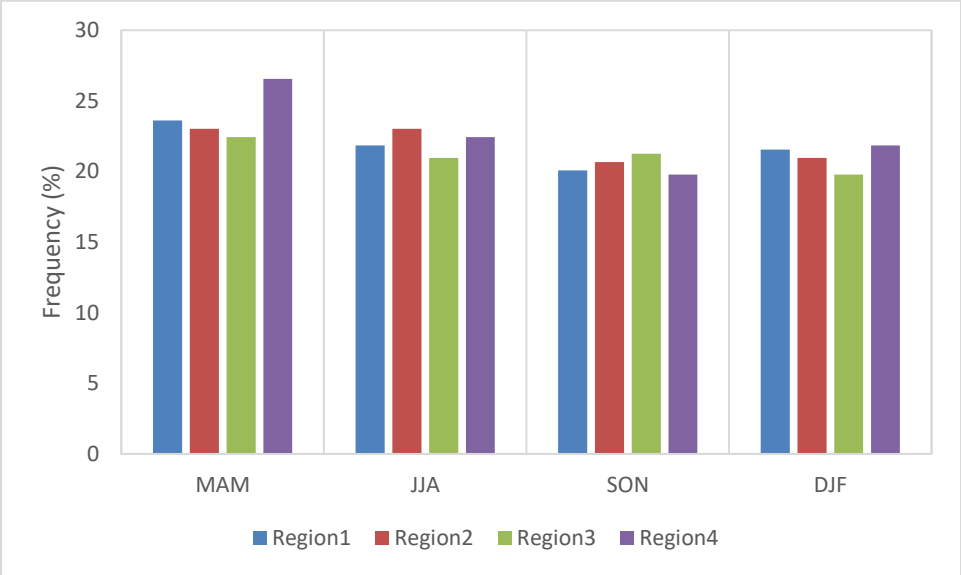

Figure 4.9 Seasonal drought frequency for each region in Oklahoma.

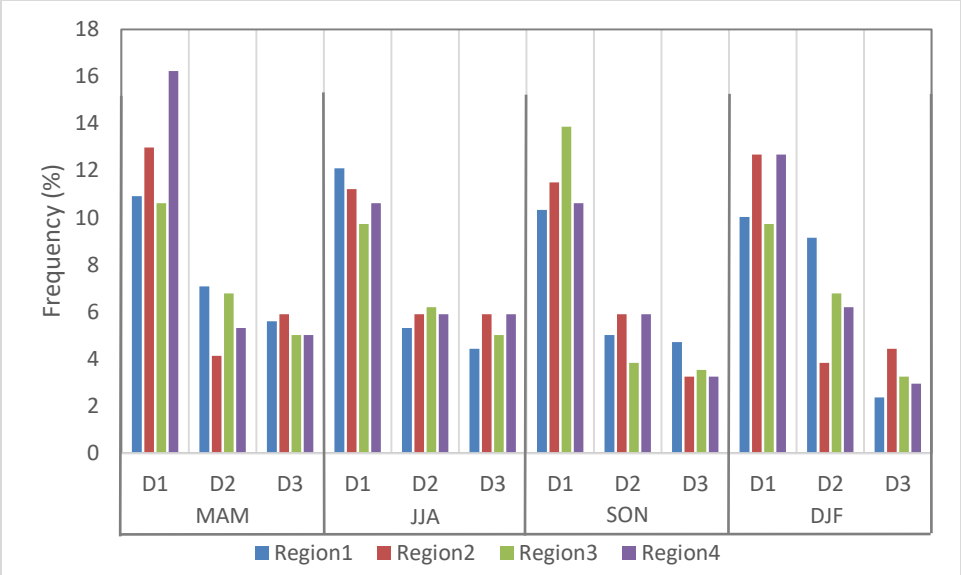

Figure 4.10 Seasonal drought frequency for each region in Oklahoma for different drought categories.

4.3.3 Mann-Kendall Trend Tests

The Mann-Kendall test was applied to all possible periods that are at least 10 years in length between 1901 to 2014 since trends can be sensitive to the beginning and ending date (McCabe & Wolock, 2002; Zhu & Quiring, 2013). Figure 4.11 shows the results of the SPEI6 trend test for each region in Oklahoma. Only trends that are statistically significant at the 95% significance level are shown.

At long timescales, like from 1901 to 2014, the SPEI has a significant increasing trend in all regions. However, at a shorter timescales, there are decadal-scale increasing and decreasing trends in the SPEI. There are about five periods that have statistically significant decreasing trends (i.e., trends toward drier conditions). The first significant occurs in the 1910s, and it is prominent in Region 3. The trends in Region 3 from 1901

to the late of 1910s are all negative. There is another period with decreasing trends in the SPEI from the 1920s to 1940s. The decreasing rate is especially prominent in Region 4. During the 1930s to 1970s, the SPEI also has a decreasing trend. However, the periods from the 1980s and 1990s to 2010s show decreasing trends, especially in Region 1. This is primarily due to the major drought events during 2011, 2012 and 2013.

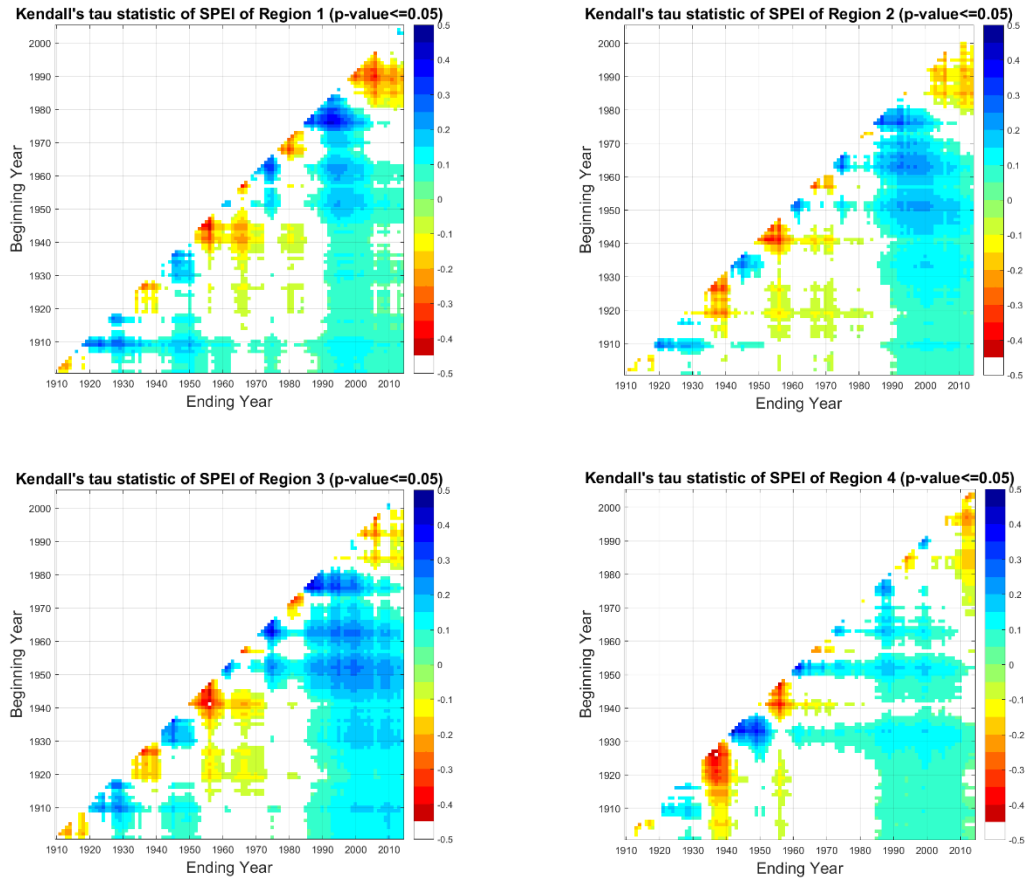

Figure 4.11 Kendall's tau statistic to test for trends in the 6-month SPEI for all time periods longer than 10 years. Blue colors indicate statistically significant increasing trends (wetter conditions) in the SPEI and red colors indicate statistically significant decreasing trends (drier conditions). Each region in Oklahoma is shown separately.

Trends in the SPEI can either be caused by trends in precipitation or trends in evapotranspiration, or both. Therefore, in this section the trends in precipitation and temperature are evaluated to determine which is the most important determinant of the drought conditions. Figure 4.12 shows the results of the Mann-Kendall test of precipitation trends for each region in Oklahoma. The precipitation trends are very similar to the SPEI trends. For example, for most time periods between the 1990s and 2010s, there are statistically significant increasing trends in both of precipitation and SPEI, especially in Region 3. The decreasing trends in the SPEI during the 1930s and 1950s in Region 4 and the decreasing trends in the SPEI between 1980s to 2010s in Region 1 are also coincident with decreasing precipitation trends.

The temperature trends are also evaluated using the Mann-Kendall test (Figure 4.13). All regions show that drought conditions from 1980s to 2010s are related to increases in temperature. With the increase of temperature, PET increases, therefore, the SPEI decreases. Especially in region 1, the significant decreases in the SPEI in recent years coincide with increases in temperature. However, there are many fewer statistically significant trends in temperature than in precipitation. This suggests that the precipitation trends are more important in determining drought trends than the temperature trends.

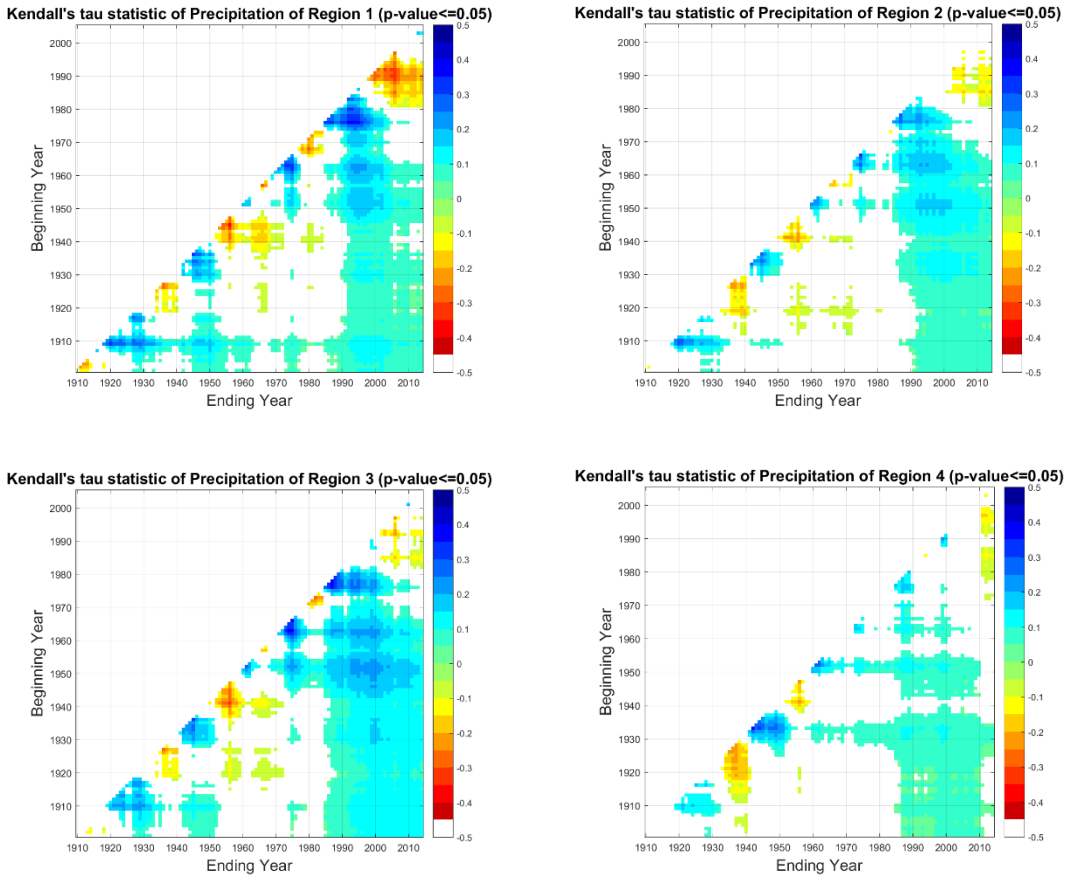

Figure 4.12 Kendall's tau statistic to test for trends in precipitation for all time periods longer than 10 years. Blue colors indicate statistically significant increasing trends (wetter conditions) in precipitation and red colors indicate statistically significant decreasing trends (drier conditions). Each region in Oklahoma is shown separately.

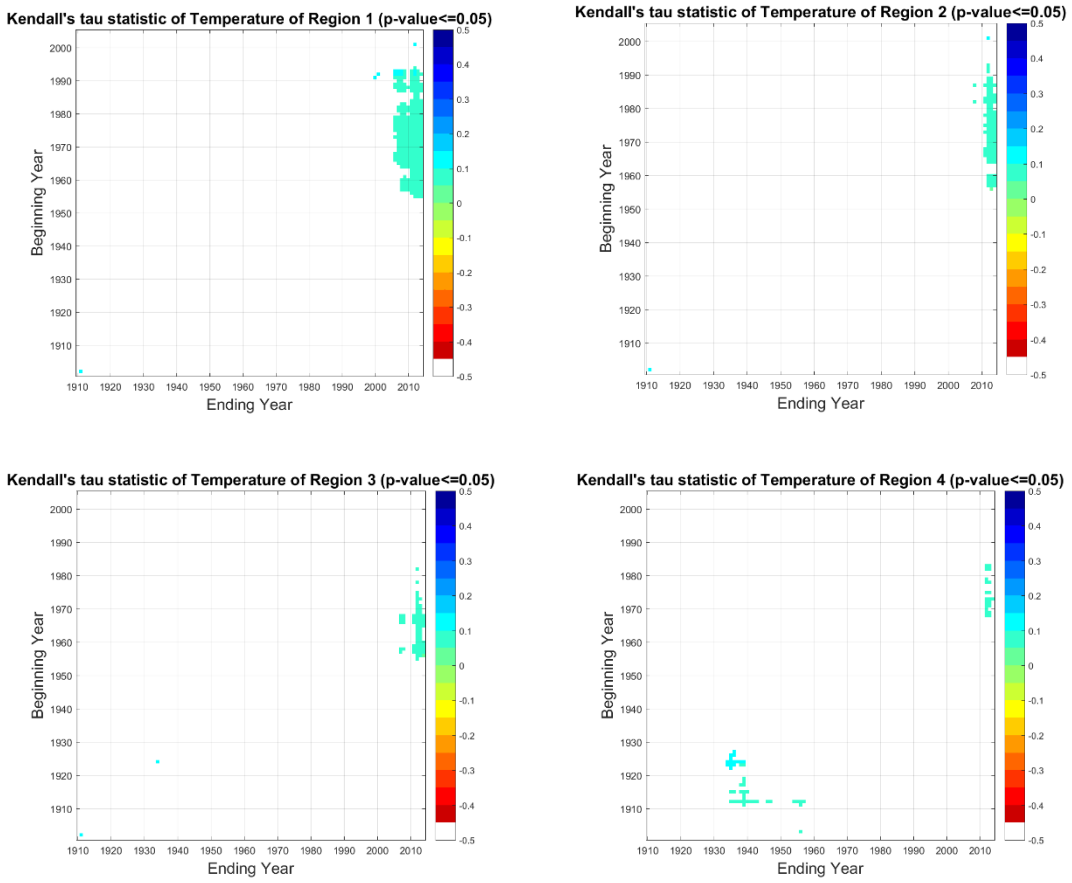

Figure 4.13 Kendall's tau statistic to test for trends in temperature for all time periods longer than 10 years. Blue colors indicate statistically significant increasing trends (warmer conditions) in temperature and red colors indicate statistically significant decreasing trends (cooler conditions). Each region in Oklahoma is shown separately.

PET based on Penman-Monteith method is a more direct variable reflecting water demand because it incorporates the information of temperature, vapor pressure, cloud cover, and wind speed. Figure 4.14 shows the Mann-Kendall test of PET for each region in Oklahoma. The PET trends are very similar to the temperature trends in each region. In recent years, PET significantly increased in all regions. Therefore, droughts in

recent years are the result of both decreases in precipitation and increases in water demand (PET). Drying trends during the 1940s to 1970s are also related with the statistically significant increase in water demand in all regions in Oklahoma. Droughts from 1920s to 1940s in the north Oklahoma (Region 4) are also related to the significant increase of PET.

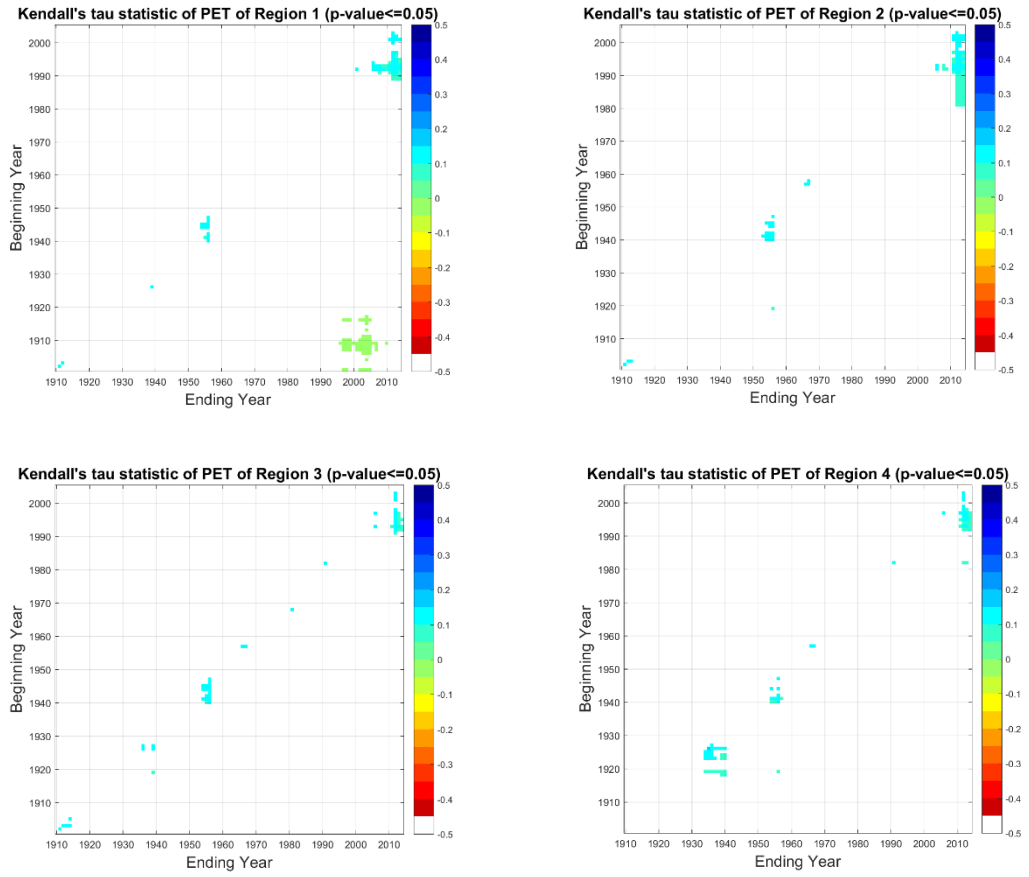

Figure 4.14 Kendall's tau statistic to test for trends in PET for all time periods longer than 10 years. Blue colors indicate statistically significant increasing trends in PET and red colors indicate statistically significant decreasing trends. Each region in Oklahoma is shown separately.

The Mann-Kendall trend tests of SPEI, precipitation, temperature, and PET at the 1-month and 3-month timescales are shown in Appendix A (Figure A.5 to A.10). There are fewer statistically significant trends than at the 6-month timescale. No statistically significant trends were found in temperature and PET at 1-month timescale in any region. Only a few significant trends were found in temperature and PET at the 3-month timescale in some regions in Oklahoma as shown in Figure A.9 and A.10.

4.4 Limitations and Conclusions

4.4.1 Limitations

In this study, we investigated the spatial and temporal patterns of agricultural drought in Oklahoma based on 1-month to 6-month SPEI from 1901 to 2014. The SPEI was calculated based on CRU precipitation and PET datasets. The CRU data provides data from 1901 to the present. Even though the spatial resolution of CRU dataset is only 0.5 degree * 0.5 degree, the CRU dataset was applied in our study because of the period of record.

The SPEI at 1-month to 6-month timescales was used in this study. Vicente-Serrano et al. (2013) found vegetation activity predominantly related to drought conditions at 2-4 month time scales. The choice of timescale will have an influence on the results. For example, we demonstrated that the trends in the 1-month SPEI are not the same as the 6-month SPEI. Therefore, future studies may also want to investigate

longer timescales (12 or 24 months) to provide more comprehensive knowledge of drought conditions in Oklahoma.

Another limitation of this study is that we chose SPEI and Z-Index for the spatial and temporal drought analysis based on the results from Chapter 3. We analyzed the spatial and temporal drought patterns based on both the SPEI and Z-Index, however, since there were no significant differences between these two indices, we only discussed the results of SPEI. SPEI is based on a water balance model. Both of the water supply and water demand are considered in SPEI. The spatial and temporal patterns of drought may change if we use a precipitation-based drought index. For example, the SPI is a widely used drought index that is solely based on precipitation. In future, it would be useful to compare the spatial and temporal variations of drought in Oklahoma based on the SPI to those based on the SPEI.

4.4.2 Conclusions

The study of spatial and temporal variations of drought is important for the evaluation of drought risk. The PCA results of indicate that Oklahoma can be divided into 4 drought regions, which are located in southeast, southwest, northeast and northwest Oklahoma. All four regions show that drought in Oklahoma has decadal-scale variability. In the 1910s, 1930s, 1950s, 1970s, and 1980s conditions were drier than other time periods. From late 1980s to the early 2000s, conditions were much wetter than normal in Oklahoma. The drought frequency results showed that droughts occur

more frequently in Region 4 (northwestern Oklahoma). Based on the seasonal analysis, drought occurs more frequently in spring than any other season.

The Mann-Kendall trend tests showed that there is a statistically significant increasing trend in the SPEI from 1901 to 2014. However, at short timescale, moisture conditions are more variable. For example, five major drought periods have occurred between 1901 and 2014. These droughts are primarily driven by decreases in precipitation. In contrast, recent droughts (e.g., 2011), were caused by both of the decreases in water supply (precipitation) and increases in water demand (PET). Due to climate change, this may be indicative of future drought conditions in Oklahoma.

Precipitation and PET are two important factors directly related with drought. Other factors such as different climate oscillations also influence drought conditions through their impact on atmospheric circulation. Relationships between multiple climate oscillations and drought will be investigated in next chapter.

CHAPTER V

IMPACTS OF MULTIPLE CLIMATE OSCILLATIONS ON DROUGHT IN OKLAHOMA[2]

5.1 Introduction

Drought is one of the most complex natural disaster that affects humans (Hagman, Beer, Bendz, & Wijkman, 1984), ecosystems (Chen, Werf, Jeu, Wang, & Dolman, 2013), water resources (Zhang et al., 2015), and agricultural productions (Q. Wang et al., 2014). Climate oscillations have been shown to be one of the factors that causes variations in drought (Mendez & Magana, 2010; Seager & Hoerling, 2014; Sutton & Hodson, 2005). A climate oscillation is defined as a slowly varying change of climate about a mean that recurs with some regularity (American Meteorological Society, 2012). An understanding of the interactions between climate oscillations and drought is vital for the prediction and mitigation of drought.

Drought occurs when precipitation is deficit considerably. A great deal of previous research has focused on how El Niño-Southern Oscillation (ENSO) affects precipitation and drought conditions. For example, Hunt (2015) performed a multi-millennial simulation with a coupled global climatic model to investigate extreme rainfall events in the Dust Bowl region, located in the southern Great Plains. This region

[2] Reprinted with permission from "Potential to improve precipitation forecasts in Texas through the incorporation of multiple teleconnections" by Liyan Tian, Zachary Leasor, and Steven M. Quiring, 2016. *International Journal of Climatology*, in press, Copyright [2016] by John Wiley and Sons.

was characterized by a persistent drought and associated dust storms during the 1930s (Schubert, Suarez, Pegion, Koster, & Bacmeister, 2004). Schubert et al. (2004) found that ENSO has a significant impact on the generation of rainfall anomalies at an interannual timescale. In contrast, Hu and Feng (2001) analyzed the effects of ENSO on the interannual variations in summer rainfall in the central United States and found that there is no persistent effect of ENSO on the summer rainfall in the central United States. The correlations between summer rainfall and tropical Pacific SSTs were strong during 1871-1916 and 1948-1978, but the relationship was weak during 1917-1947 and 1979-present. There are also studies regarding the impact of other teleconnections on precipitation and drought, such as the Atlantic Multidecadal Oscillation (AMO) (Schlesinger & Ramankutty, 1994), North Atlantic Oscillation (NAO) (Wallace & Gutzler, 1981), Pacific Decadal Oscillation (PDO) (Mantua & Hare, 2002), and Pacific-North American pattern (PNA) (Wallace & Gutzler, 1981). For example, Hurrell (1995) found that changes in the mean circulation patterns over the North Atlantic are accompanied by shifts in storms tracks and synoptic-scale eddy activity. These changes affect the transport and convergence of atmospheric moisture and consequently alter regional precipitation. Sutton and Hodson (2005) demonstrated that the boreal summer climate was affected by the AMO on multidecadal timescales during the 20th century. Kingston, Stagge, Tallaksen, and Hannah (2015) indicated the Europe-wide drought is associated with patterns of large-scale climate variations such as NAO. Leathers, Yarnal, and Palecki (1991) found that the PNA was highly correlated with regional temperature and precipitation from 1947 to 1982 for the fall, winter, and spring months when the

PNA serves as a main mode of North Hemisphere mid-tropospheric variability. McCabe, Palecki, and Betancourt (2004) demonstrated that climatic oscillations occurring at the decadal scale such as the AMO and PDO have been found to explain around half of the variance in drought frequency across the United States since the 1900s. While the AMO and PDO are important for explaining precipitation variability when considered by themselves, decadal climate oscillations also tend to modulate the impact that ENSO has on precipitation. Enfield, Mestas-Nunez, and Trimble (2001) found that the AMO has a significant impact in the Mississippi River basin, but not in the Okeechobee river basin. In Texas, the warm phases of the AMO greatly diminish the well-known positive relationship between ENSO and precipitation during the winter season (DJF). Schubert et al. (2016) investigated the relationships between sea surface temperatures (SST) and precipitation variability on a global scale. In North America, they found that SST variability in the tropical Pacific is the dominant factor that influences precipitation, with some contribution from Atlantic SSTs. Therefore, at interannual time scales, ENSO is the primary driver of precipitation variability throughout much of North and South America. At decadal time scales, the AMO and PDO are the primary drivers of precipitation variability. Cook, Smerdon, Seager, and Cook (2014) investigated the pan-continental droughts in North America over the last Millennium. They defined pan-continental drought as synchronous drought in three regions. The results showed that droughts in the Southwest and Central Plains occur in conjunction with either the Southeast or Northwest during La Niña conditions, while droughts in Central Plains, Northwest, and Southeast are primarily associated with the PDO and AMO. Mendez and

Magana (2010) also demonstrated the low frequency AMO and PDO can explain the spatial patterns of prolonged meteorological droughts in Mexico in the nineteenth century.

These studies demonstrate that climate across space and time is influenced by climate oscillations. However, because the impact of each climate oscillation does not occur in isolation, it is important to analyze the impact that multiple teleconnections jointly have on drought. Stevens and Ruscher (2014) investigated the impact of AMO, NAO, PDO and ENSO on temperature and precipitation in the Apalachicola-Chattachoochee-Flint (ACF) River Basin, which supplies water to Alabama, Georgia, and Florida. Their results showed that each of the sub-basins of the ACF are affected in a unique way by climatic oscillations, and no single climatic oscillation can adequately explain/predict the variations in meteorological conditions. Wise, Wrzesien, Dannenberg, and McGinnis (2015) analyzed the associations of cool-season precipitation patterns in the United States with teleconnection interactions, including ENSO, NAO, PNA, East Atlantic pattern (EA) and West Pacific pattern (WP). Their results emphasized the importance of considering multiple climatic oscillations when forecasting the seasonal rainfall variability. Ning and Bradley (2014) also studied the relationships between winter precipitation variability and teleconnections over the northeastern United States. Their correlation analysis showed that the first Empirical Orthogonal Function (EOF) pattern is significantly correlated with PNA and PDO, the second EOF pattern is significantly correlated with NAO and AMO, and the third EOF pattern is associated with ENSO, PNA and PDO. Therefore, multiple teleconnections

should be considered when analyzing the relationship between climate oscillations and precipitation variability. The aforementioned research has shown that ENSO, NAO, AMO, PNA and PDO are the major climate oscillations that have an impact on climate in the United States; therefore, this study will investigate the impacts of the five climate oscillations on drought in Oklahoma.

Only simultaneous relationships (zero lead time) between teleconnections and climate were evaluated in the studies described above. However, there can be significant time lags between teleconnections and drought. For example, Redmond and Koch (1991) analyzed how ENSO and PNA influence precipitation, temperature, and streamflow in the western United States. Their results indicated that June-November ENSO was strongly correlated with October-March precipitation, suggesting that the winter precipitation was related to ENSO at a six-month time lag. Harshburger, Ye, and Dzialoski (2002) also demonstrated that the state of ENSO during the fall season can be used to predict winter precipitation in the western U.S. McCabe and Dettinger (1999) investigated the relationship between ENSO during fall season and the winter precipitation. Their results indicated that the strength of the correlations between fall ENSO and winter precipitation in the western U.S. varied over space and time during the 20^{th} century. When PDO is negative, the relationship between ENSO and precipitation is strong. When PDO is positive, ENSO and precipitation are weakly correlated. Brown and Comrie (2004) studied the impact of fall ENSO on winter precipitation in the western U.S. They found significant correlations between fall ENSO and winter precipitation in the Southwest U.S. Specifically, they found that wet winters tend to

follow El Niño events, and dry winters follow La Niña. Our study will also investigate the lagged relationships between multiple teleconnections and drought.

The state of Oklahoma frequently experiences drought. Droughts in Oklahoma are caused by numerous factors, including natural atmospheric variability (i.e., climate oscillations), land-atmosphere interactions, and thermodynamic conditions (Fernando et al., 2016; Myoung & Nielsen-Gammon, 2010; Seager, Goddard, Nakamura, Henderson, & Lee, 2014). This study investigates the simultaneous and lagged relationships between Oklahoma drought and ENSO, NAO, AMO, PNA and PDO. The goals of this study are to: (1) determine which climate oscillation accounts for the greatest amount of SPEI variance in Oklahoma, (2) identify at what time lag the relationship between climate oscillations and SPEI are strongest and (3) forecast SPEI based on multiple climate oscillations using different forecast models and compare with the forecast from Climate Prediction Center (CPC).

5.2 Data and Methods

5.2.1 Climate Oscillations

Five climate oscillations are investigated in this study: ENSO, NAO, AMO, PNA, and PDO. ENSO is the most frequently studied climatic oscillation. During an El Niño event, easterly trade winds weaken or reverse and cause anomalous warming of the ocean surface, changing patterns of meteorological variables such as precipitation (Stevens & Ruscher, 2014). The NINO3.4 SST anomaly is used in this study to represent ENSO conditions. It is based on departures from the three-month running mean of SSTs

in the NINO3.4 region. Positive NINO3.4 values are associated with El Niño events, while negative values indicate La Niña events. NINO3.4 SST anomaly data from 1901 to 2011 can be downloaded from the NOAA PSD website (http://www.esrl.noaa.gov/psd/gcos_wgsp/Timeseries/Nino34/). The NINO3.4 SST index is calculated from the Hadley Centre Sea Ice and Sea Surface Temperature data set (HadISST1). It is the area averaged SST from 5°S-5°N and 170°-120°W (Rayner et al., 2003).

The NAO is an atmospheric oscillation in the North Atlantic Ocean. The NAO index from the Climate Research Unit is defined as the normalized pressure difference between a station located in the Azores and a station in Iceland (Stevens & Ruscher, 2014). The NAO index from 1901 to 2011 can be downloaded from the NOAA PSD website (http://www.esrl.noaa.gov/psd/gcos_wgsp/Timeseries/NAO/).

The AMO is a 60-85 year cycle of variable SSTs in the North Atlantic Ocean that has been shown to correlate with precipitation in the United States (Stevens & Ruscher, 2014). The AMO index is calculated using the Kaplan SST as the detrended time series of the area weighted averaged SST over the North Atlantic from 0˚ to 70˚N (Enfield et al., 2001). The smoothed AMO index from 1901 to 2011 can be downloaded from NOAA PSD (http://www.esrl.noaa.gov/psd/gcos_wgsp/Timeseries/AMO/).

The PNA index indicates the nature of atmospheric circulation in the Northern Hemisphere. A positive phase of the PNA indicates meridional flow with an enhanced jet stream while a negative phase indicates zonal flow (Henderson & Robinson, 1994). The PNA index is calculated using the 500 mb heights from the 20th Century Reanalysis

Project Version V2 dataset. Area-averaged geopotential heights from four regions in the Northern Hemisphere are combined for the PNA index (Barnston & Livezey, 1987). The PNA index data from 1901 to 2011 can be downloaded from NOAA PSD (http://www.esrl.noaa.gov/psd/data/20thC_Rean/timeseries/monthly/PNA/).

The PDO is based on monthly SST variability in the North Pacific Ocean. The PDO index is calculated based on the EOF analyses of the monthly SST anomalies in the North Pacific (Mantua, Hare, Zhang, Wallace, & Francis, 1997). The PDO index from 1901 to 2011 can be downloaded from NOAA PSD http://www.esrl.noaa.gov/psd/gcos_wgsp/Timeseries/PDO/.

Besides the climate oscillations, the 1-month SPEI from Chapter 4 will be used in this study.

5.2.2 Canonical Correlation Analysis

Canonical correlation analysis (CCA) was used to analyze the relationships between SPEI and the five teleconnections. Simultaneous (no lag) and lagged relationships (1, 3, 6, 12, and 24-month lags) were evaluated using monthly data.

CCA is a linear multivariate approach used to compare two sets of data, with each set composed of multiple arrays of variables (Thompson, 2005). Based on the CCA analysis, relationships between a set of independent variables and a set of dependent variables can be found. The linear combinations represent the weight of at least two variables from the respective set, therefore creating the two variant arrays (U_1 & V_1) seen in Equation 5.1, in which *x* represents the precipitation anomalies, *y* represents the

climate oscillations, *a* represents the coefficients for precipitation, and *b* represents the coefficients of the climate oscillations (Borga, 2001; Stevens & Ruscher, 2014).

$$U_1 = a_1x_1 + a_2x_2 + \cdots a_nx_n$$

$$V_1 = b_1y_1 + b_2y_2 + \cdots b_ny_n \qquad \text{(Equation 5.1)}$$

The loading matrices calculated using Equation 5.1 produce canonical loadings, which are linear correlations between the variables and the variate. The loadings are used to calculate the canonical cross loadings that determine the linear correlation between the independent variable and dependent variable. The canonical cross loadings of the climate oscillations are estimated using the correlation coefficient in Equation 5.2 where S_{xx} and S_{yy} are variance-covariance matrices of the respective variable and S_{xy} and S_{yx} and the covariance matrices of precipitation and the climate oscillations (Stevens & Ruscher, 2014).

$$r_cb = \left[S_{yy}\right]^{-1}\left[S_{xy}\right]\left[S_{xx}\right]^{-1}\left[S_{yx}\right]b \qquad \text{(Equation 5.2)}$$

In this study, the dependent variable set is SPEI at different lags (i.e. 0-month lag, 1-month lag, 3-month lag, 6-month lag, 12-month lag, and 24-month lag) and the independent set is the five climatic oscillations. Canonical loadings and cross loadings are two important variables about the relationships between the independent and dependent sets. This approach allows us to simultaneously examine the impacts of climatic oscillations on precipitation variations (Stevens & Ruscher, 2014).

CCA provides information about (1) the varying effects of climate oscillations in different regions, and (2) how the strength of the relationships change for each time lag.

Canonical roots that are not statistically significant at the 95% confidence level were eliminated based upon the methods used by *Stevens and Ruscher* [2014].

5.2.3 Random Forest

Random forest is an accurate and robust ensemble learning method for classification and regression (Leo Breiman, 2004; Liaw & Wiener, 2002). Decision trees are very popular in machine learning area. However, a major issue of decision trees is that they usually overfit their training data. Random forest is an effective method to overcome the overfitting issue (Leo Breiman, 2001). The difference between standard trees and random forest is that random forest add an additional layer of randomness. In standard trees, each node is split based on the best split among all variables. While, in random forest, a subset of variables are randomly selected at each node, then, each node is split based on the best split among this subset variables (Liaw & Wiener, 2002). The structure of random forest is very simple. Random forest is an ensemble of trees that are generated in the way that each tree is different in the training cases and the predictors at each node. The training set is a randomly sample from the original training set. For each random sample, a tree grows in the way that, each node is split using the best split among the randomly selected subset of variables. The tree is grown to the maximum depth until no further split is possible (Svetnik et al., 2003). For regression, a new set of predicted data is generated by averaging the predictions of the trees (Liaw & Wiener, 2002). One of the important feature of random forest is the concept of out-of-bag (OOB). In random forest, each tree is grown using a different randomly sample from the

original data set. About one third of the randomly sample is left out in the construction of each tree. This one third OOB cases can be used to get an unbiased estimate of the training set error (L Breiman, 2003).

One of the advantages of random forest is that it is robust and it does not overfit. It can run efficiently on large data sets. It can handle thousands of variables without variable deletion. It can return the importance of variables. It generate an internal unbiased estimate of the training set error (Leo Breiman, 2001).

5.2.4 Monthly SPEI Prediction

Several regression models are developed to evaluate whether climate oscillations can be used to produce skillful monthly forecasts of SPEI in Oklahoma. Based on the CCA results, a CCA-based regression model (CCA1) can be generated based on all of the five teleconnections at 1 month lag for each region in each month. The linear regression model uses weights for each of the climate oscillations calculated as the dividend between the canonical loadings and the dependent and independent arrays. Since the CCA results can illustrate the relationships between SPEI and each teleconnection at different lags for each region in each month, a CCA-based regression model (CCA2) can be developed using another strategy. For each region and each month, only the teleconnections at different lags that has significant correlations with SPEI are used in the regression model. Random forest (RF) is also used for the SPEI forecast. Then, a set of ensemble models are generated for the SPEI forecast, including the averaged prediction of CCA1 and CCA2 models (ensemble12), the averaged

prediction of CCA1 and RF models (ensemble13), the averaged prediction of CCA2 and RF models (ensemble23), and the averaged prediction of CCAs and RF models (ensemble123). The forecast models are built using data from 1901-1980 and evaluated using data from 1981 to 2011.

The Heidke Skill Score (HSS) was used to evaluate the skill of the SPEI forecast and to facilitate comparison to the skill of the CPC monthly climate forecast. The HSS was calculated based on observed and predicted SPEI values from 1981-2010 which were grouped into three percentile ranges based upon their distribution; below normal, average, and above normal. This was done to standardize the SPEI predictions in a manner that is consistent with the methodology used by CPC. CPC provides monthly drought outlook based on the precipitation and temperature outlooks. Since the CPC precipitation and temperature forecast skill scores are based on observed and predicted precipitation and temperature data from 1981 to 2010 (CPC, 2016b), the skill score of the regression models in this study was also calculated using SPEI data from 1981 to 2010. The HSS values were calculated using Equation 5.3:

$$HSS = \frac{(NC-E)}{(T-E)} \qquad \text{(Equation 5.3)}$$

where *NC* is the number of correct forecasts, *T* is the total number of forecasts, and *E* is the number of forecasts expected to verify based upon climatology.

The CPC monthly drought outlook verification is available from July 2013 to October 2015 at a national wide scale. The monthly precipitation and temperature prediction are available from February 2004 to the present at a climate division scale. The skill scores of the regression models developed in this study are compare to evaluate

the regression models. The skill scores from the CPC drought outlook, precipitation and temperature outlooks can be a qualitative reference for the evaluations of the regression models developed in this study.

5.3 Results

5.3.1 Relationships between SPEI and Each Teleconnection

Figure 5.1 shows the correlations between each teleconnection and SPEI at different lags for each month in each region of Oklahoma. These regions are based on the PCA results from Chapter 4. Only correlations that are statistically significant at the 95% confidence level are shown. NAO has the most statistically significant correlations with SPEI, followed by ENSO, PNA, PDO, and AMO. There are a total of 288 month/region/lags combinations (12 months * 4 regions * 6 lags), and there is a statistically significant correlation between NAO and SPEI in 32 of the 288 cases (11.1%). There is a statistically significant correlation between ENSO and SPEI in 10.8% of these combinations. PNA, PDO, and AMO have statistically significant correlations in 10.1%, 6.3%, and 1.7% of these 288 combinations, respectively. Statistically significant correlations between ENSO and SPEI are mainly at shorter time lags in most months, except in summer. For NAO, correlations with SPEI are statistically significant at shorter time lags in November to March. In the warmer months of May to September, correlations between NAO and SPEI are mainly at longer time lags (e.g., longer than 6 months). Previous studies of the relationship between ENSO/NAO and climate in the United States have shown that the impacts of

ENSO/NAO on precipitation and temperature are most pronounced during the winter (Durkee et al., 2008; Hu & Feng, 2001). Therefore, it is not surprising that the correlations between ENSO/NAO and SPEI have pronounced seasonality.

Correlations between PNA and SPEI are mainly at shorter time lags. There are fewer statistically significant correlations between PDO and SPEI. Correlations between PDO and SPEI are significant at different time lags for different regions and months. No seasonal trends are evident. Correlations between AMO and SPEI are only significant in Region 4 in September.

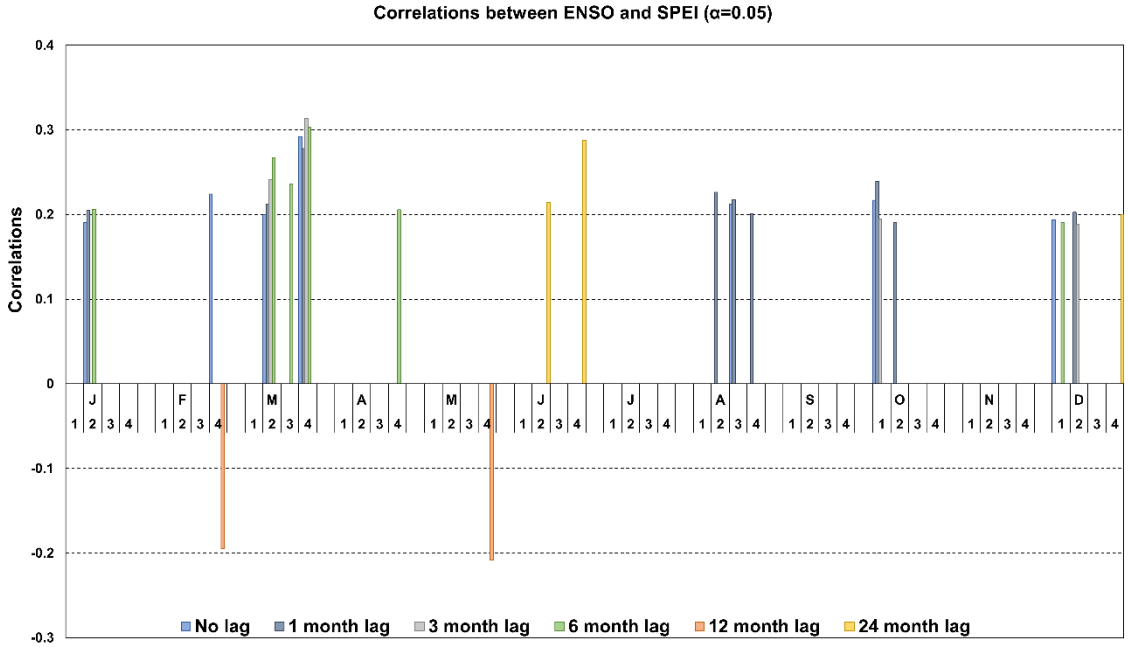

Figure 5.1 Correlations between each teleconnection and SPEI from 1901-2011 in each region with different lags: (a) ENSO; (b) NAO; (c) PNA; (d) PDO; (f) AMO.

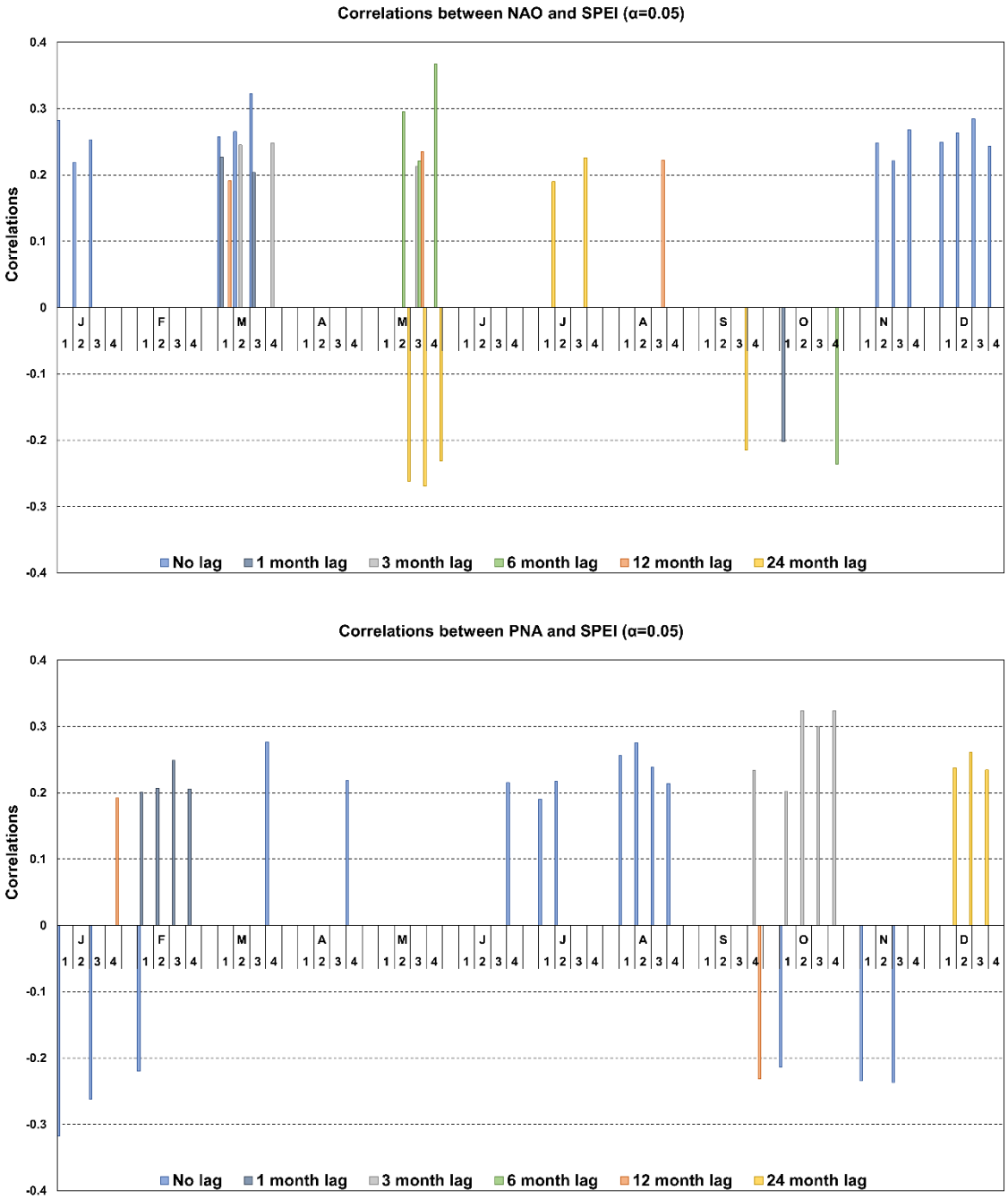

Figure 5.1 Continued

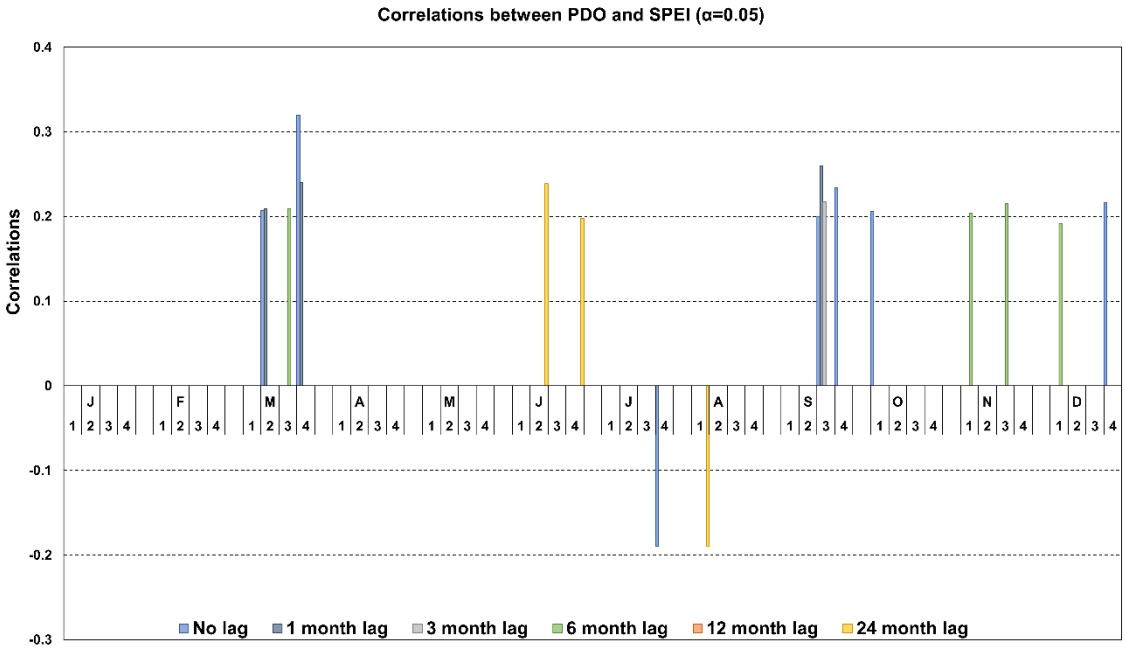

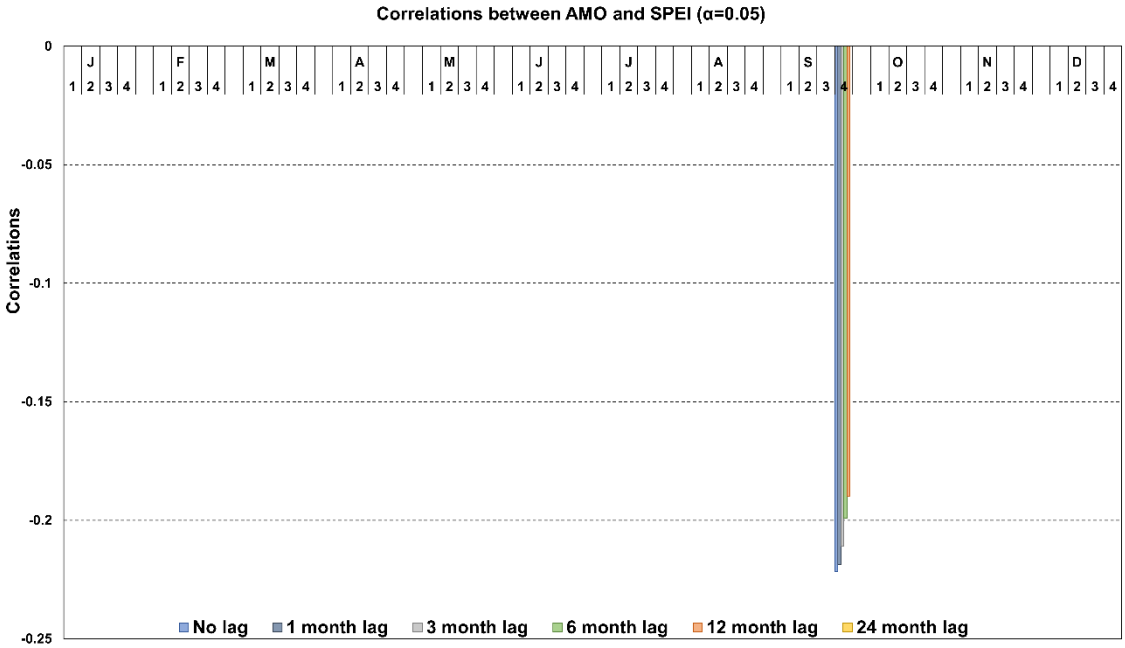

Figure 5.1 Continued

5.3.2 Relationships between SPEI and Multiple Teleconnection

Figure 5.2 shows how the correlations between multiple climate oscillations and SPEI vary by month and region at different lags. The correlations between multiple climate oscillations and SPEI are the dependent cross loadings between the observed dependent variable (i.e., SPEI) and the opposite canonical variate, which is the linear combination of the correlations with the five climate oscillations. The correlations are calculated for the following combinations of climate oscillations: ENSO, ENSO/PNA, ENSO/PNA/PDO, ENSO/PNA/PDO/NAO, and ENSO/PNA/PDO/NAO/AMO. Most of the statistically significant simultaneous correlations (no lag) occur during months except April to July. The number of statistically significant correlations increases as additional climate oscillations are included. Even the AMO, which did not have many statistically significant correlations during the univariate analysis, helps to explain more of the variance in SPEI when it is included with the other climate oscillations.

Not surprisingly, our results show that the inclusion of additional climate oscillations helps to explain SPEI variability in Oklahoma. Correlations between SPEI and multiple teleconnections at different months of lags also show that the inclusion of additional climate oscillations is helpful for explaining SPEI variability in most of months and regions in Oklahoma. The number of statistically significant correlations between SPEI and multiple teleconnections decreases as the time lag increases. At a 1 month lag, there are no statistically significant correlations from April to July. At a 3 month lag, there are no statistically significant correlations from April to September. There are only a few statistically significant correlations during July to December at the

6 and 12 month time lag. At a 24 month lag, there are statistically significant correlations in June and December.

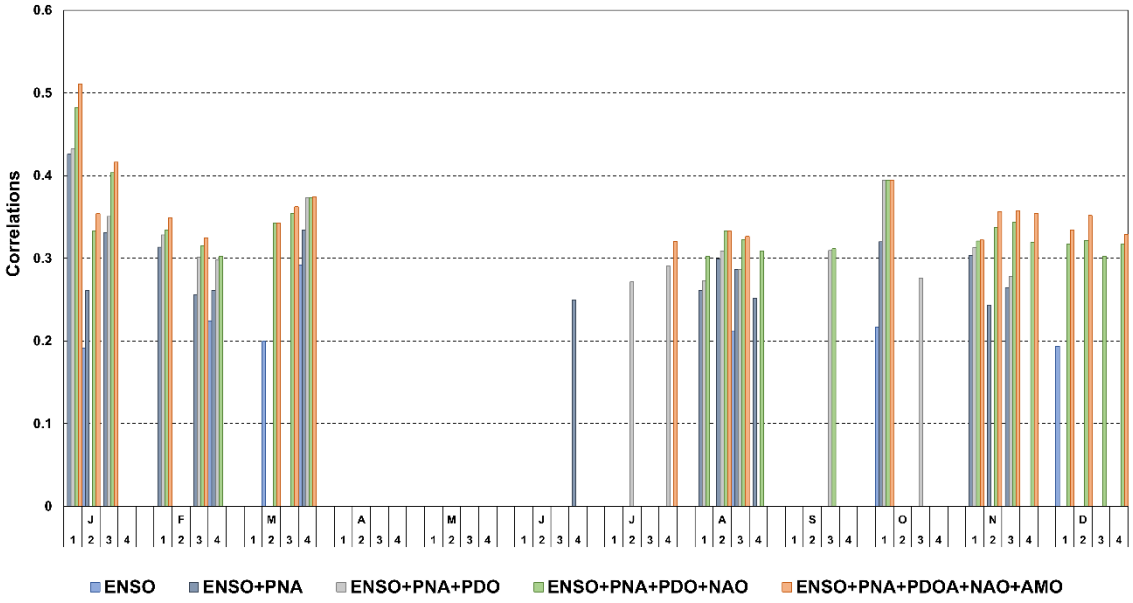

Figure 5.2 Correlations between multiple teleconnections and SPEI from 1901-2011 in each region with different lags (0 month lag, 1 month lag, 3 month lag, 6 month lag, 12 month lag, and 24 month lag).

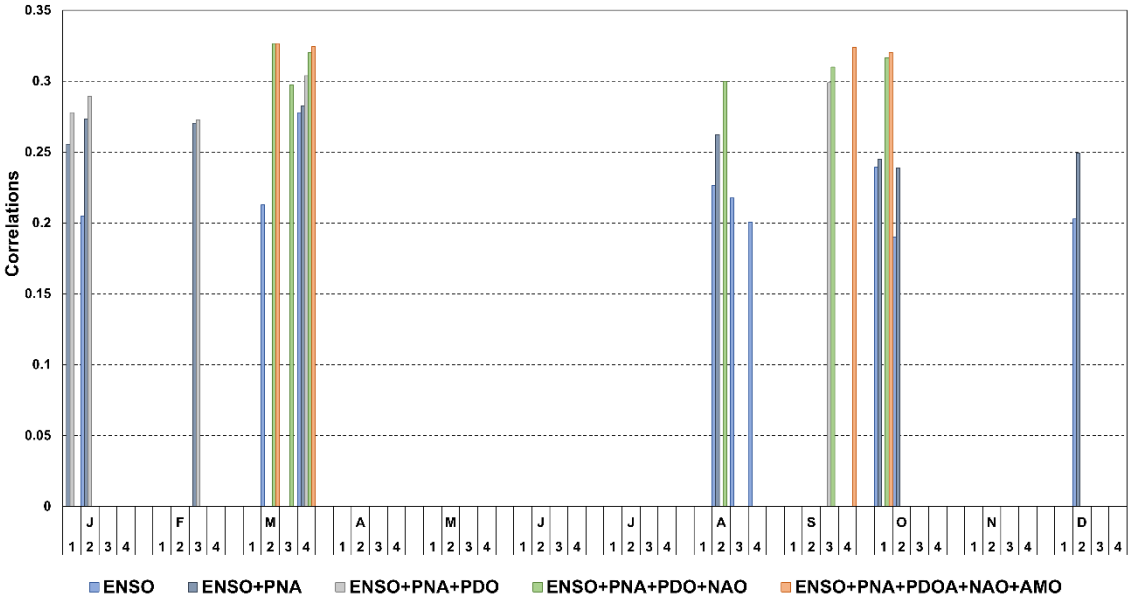

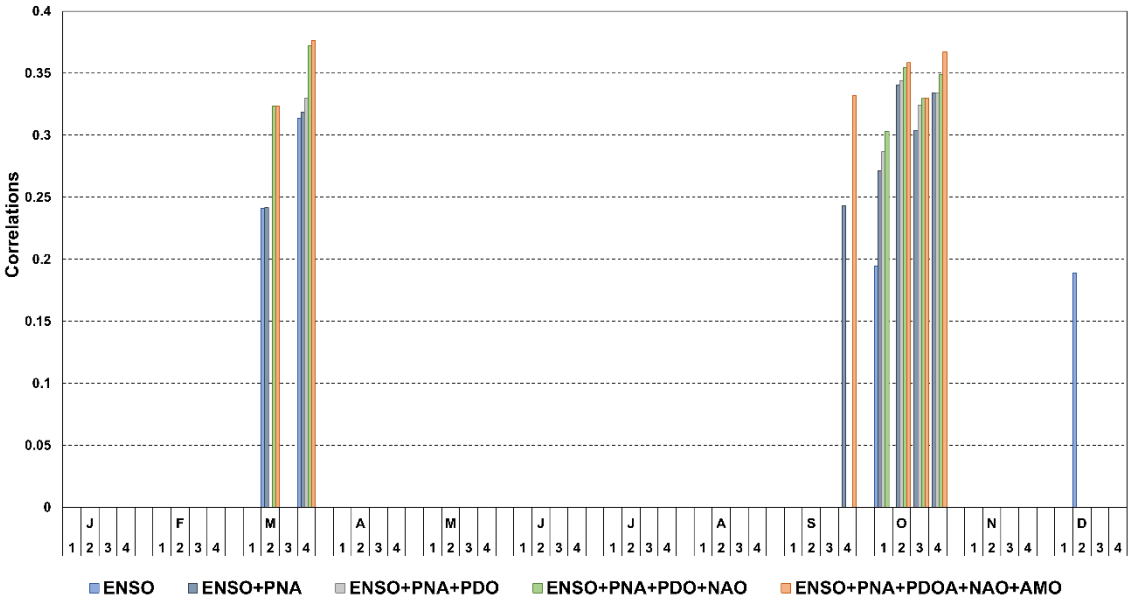

Figure 5.2 Continued

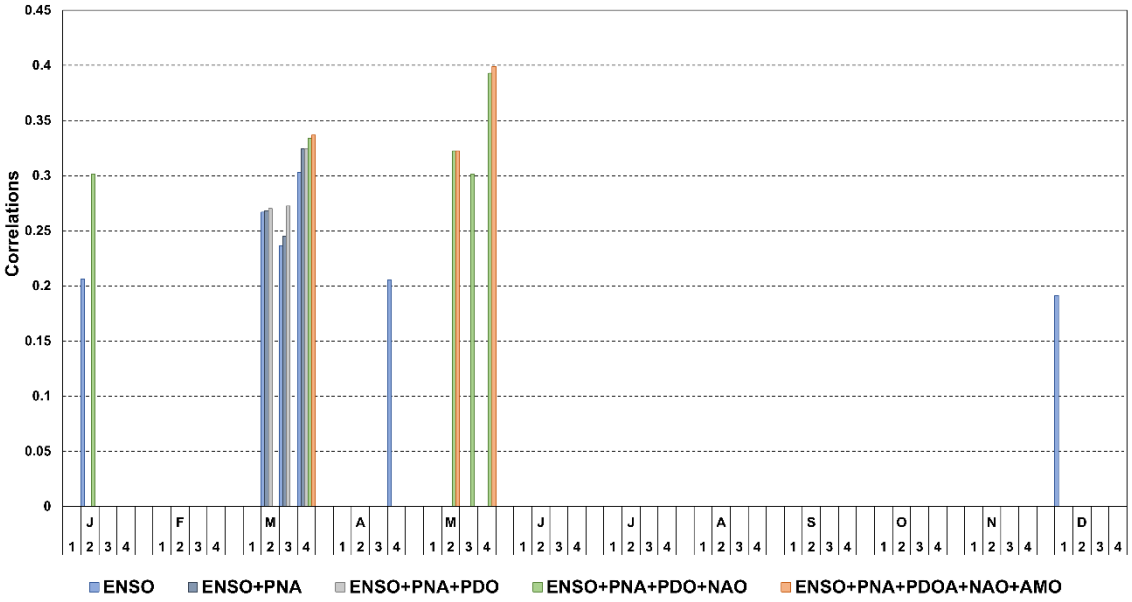

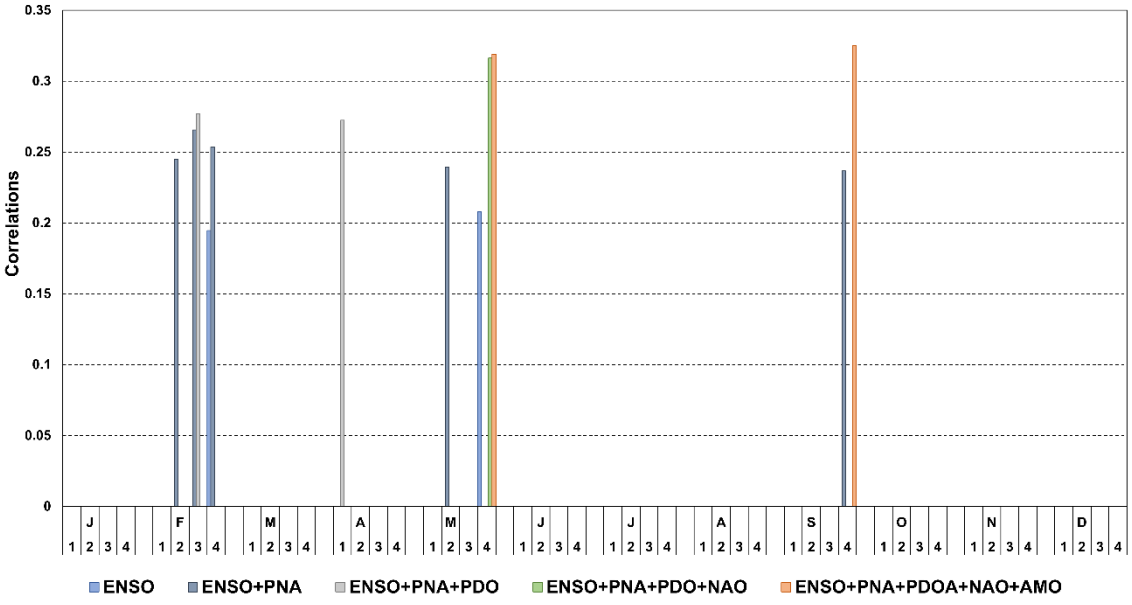

Figure 5.2 Continued

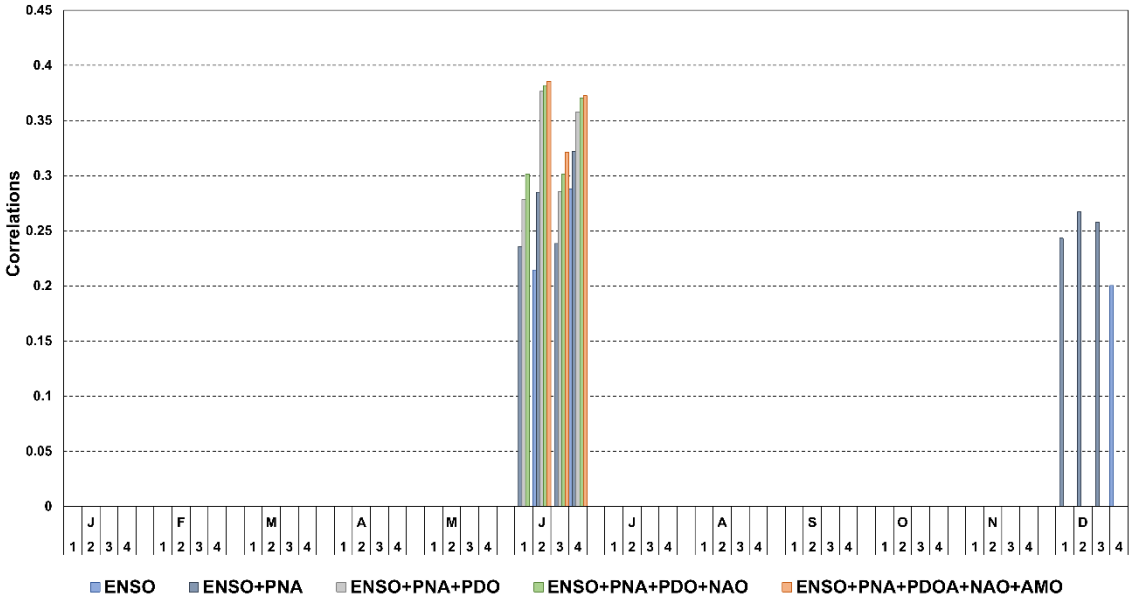

Figure 5.2 Continued

5.3.3 SPEI Forecast

As described above, two CCA-based linear regression models and a random forest model are developed to evaluate whether the climate oscillations can be used to produce skillful monthly forecasts of SPEI in Oklahoma. According to Figure 5.2, the number of statistically significant correlations between SPEI and multiple teleconnections decreases as the time lag increases. Therefore, a 1 month lag is used in the first CCA-based regression model (CCA1). Another reason to select a 1 month lag is that it facilitates comparison with the CPC forecast skill. The CPC forecasts precipitation and temperature at a 0-month lead and this is similar to the 1 month lag in our study. That is, climate oscillations from one month are used to forecast climate in the following

month. Therefore, the prediction can only be generated at the end of the month. Therefore, this is equivalent to the 0 month lead forecast produced by the CPC.

Another approach for forecasting the SPEI is to use multiple teleconnections at different time lags. Therefore, teleconnections which have significant correlations with SPEI in each region and month were selected based on Figure 5.1. This is the second SPEI forecast model (CCA2). However, there are no statistically significant correlations between SPEI and teleconnections for some regions are months (e.g., Region 1 in September). In these cases, multiple teleconnections at a specific lag were selected based on the correlations between SPEI and multiple teleconnections at different lags (Figure 5.2). Table 5.1 shows the combinations of teleconnections for the SPEI forecast for each region in each month. The skill of the CCA2 model will be compared to that of the CCA1 model. This comparison will show whether the accuracy of SPEI forecasts can be improved by using different lags.

A third method of forecasting the SPEI is based on random forest. In our study, the predictors that are included in the random forest model are the 5 teleconnections at 5 different lags (1 month, 3 month, 6 month, 12 month and 24 month lags). This gives a total of 25 co-variates. One of the outputs of random forest is variable importance. Therefore, the importance of each variable is weighted in the regression model. Four ensemble models from these three regression models are also analyzed in this study. The ensemble models are the average prediction of CCA1 and CCA2 models (ensemble12), the average prediction of CCA1 and RF model (ensemble13), the average prediction of

CCA2 and RF model (ensemble23), the average prediction of all of the 3 models (ensemble123).

Table 5-1 Combinations of teleconnections for SPEI forecast for each region in each month

	Region 1	Region 2	Region 3	Region 4
Jan	1m (E+P1+P2)	1m (E+P1+P2)	1m (E+P1+P2+N+A)	12m P1
Feb	1m P1	12m (E+P1)	1m (E+P1+P2)	12m (E+P1)
Mar	1m (E+P1+P2+N)	6m E+1m P2+3m N	6m E+6 P2 +1 N	3m E+1m P1+1m P2+3m N
Apr	12m (E+P1+P2)	6m (E+P1+P2+N+A)	6m (E+P1+P2+N+A)	6m E
May	6m (E+P1+P2+N+A)	6m (E+P1+P2+N)	6m (E+P1+P2+N)	6m (E+P1+P2+N+A)
Jun	24m (E+P1+P2+N)	24m (E+P1+P2+N+A)	24m (E+P1+P2+N+A)	24m (E+P1+P2+N+A)
Jul	24m N	12m (E+P1+P2+N+A)	24m N	1m P2
Aug	1m P1 +24m P2	1m (E+P1+P2+N)	1m E+1m P1+12m N	1m (E+P1+P2+N)
Sep	1m (E+P1+P2+N+A)	1m (E+P1+P2+N+A)	1m P2+24m N	3m P1
Oct	1m E+3m P1+1m P2+1m N	1m E+3m P1	3m (E+P1+P2+N)	3m (E+P1+P2+N+A)
Nov	1m P1+6m P2	6m (E+P1+P2+N+A)	1m P1+6m P2+1m N	6m (E+P1+P2+N+A)
Dec	6m E+24m P1+6m P2+1m N	1m E+24m P1+1m N	24m P1+1m N	24m E+1m P2

(*Note: *n*m means n month lag; E means ENSO; P1 means PNA; P2 means PDO; N means NAO; and A means AMO)

The HSS, correlation coefficient, and correlation coefficient at 80% significance level are used to evaluate model performance for each region in each month. Figure 5.3 shows the HSS of the models. Only HSSs that are great than zero are shown. In January, the highest HSS is in Region 4 based on the CCA2 model and the ensemble23 model. In

February, the highest HSS is in Region 2 based on the CCA2 model. In March, the highest HSS is in Region 4 based on the CCA2 model and ensemble 23 model. In April, the highest HSS is in Region 4 based on CCA2 model, ensemble 23 model, and ensemble123 model. In May, the highest HSS is in Region 4 based on ensemble 23 model. In June, the highest HSS is in Region 2 based on CCA2 model. In July, the highest HSS is in Region 2 based on ensemble 12 model. In August, the highest HSS is in Region 1 based on CCA1 model. In September, the highest HSS is in Region 3 based on the RF model, ensemble13 model, and ensemble 123 model. In October, the highest HSS is in Region 1 based on the ensemble12 model. In November, the highest HSS is in Region 1 based on the ensemble23 model. In December, the highest HSS is in Region 3 based on the CCA2 model and the ensemble23 model.

Figure 5.4 shows the correlation coefficients of different prediction models. The correlation coefficient of CCA2 model is higher than the correlation coefficient of ensemble23 model in January and Region 4. In March and April, the CCA2 model also has a higher correlation coefficient than the ensemble models. In September, the correlation coefficient of RF model is higher than the correlations coefficient of the ensemble models. In December, the CCA2 model also has a higher correlation coefficient than the ensemble models. Table 5.2 shows the best SPEI-teleconnection regression model based on HSS and correlation coefficient. CCA2 is the best model in 6 of 12 cases. Overall, the SPEI forecasts are more skillful in western Oklahoma (Region 2 and 4) than in eastern Oklahoma (Region 1 and 3).

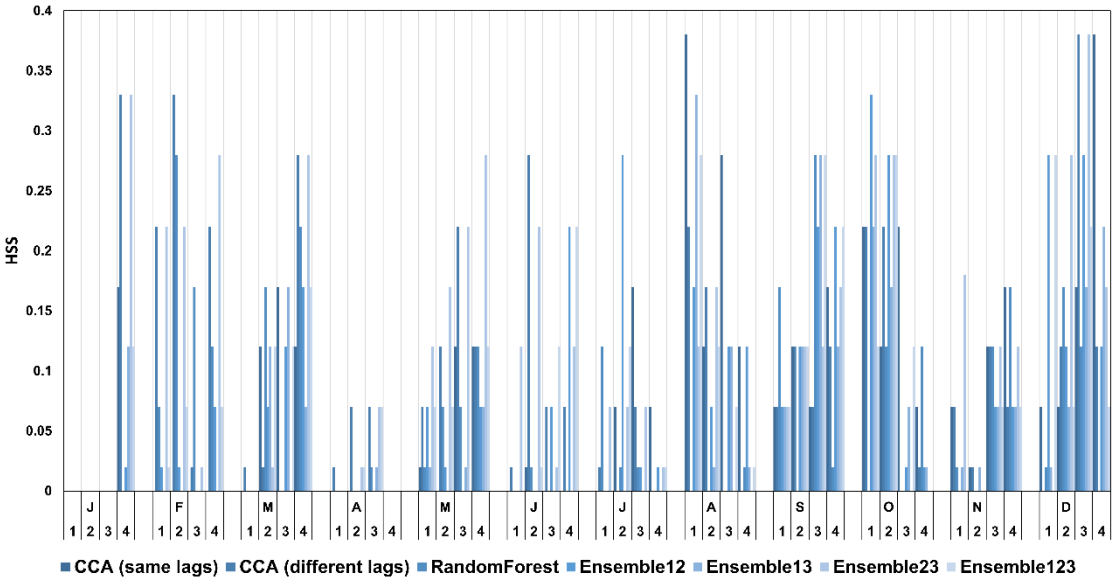

Figure 5.3 HSSs of different prediction models.

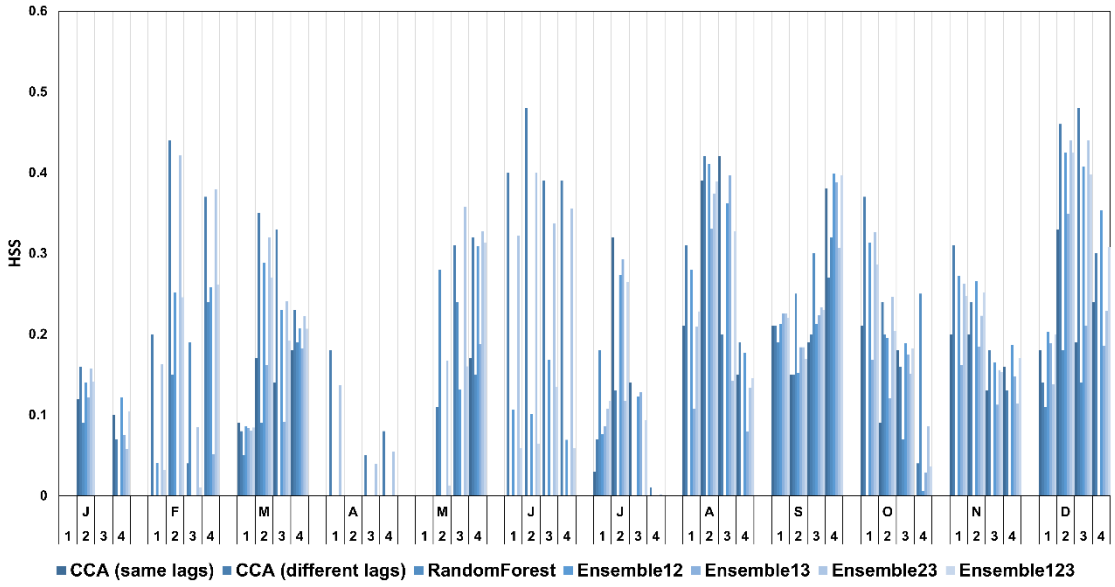

Figure 5.4 Correlation coefficient of different prediction models.

Table 5-2 Regression model for the region in each month with highest HSS

	Jan	Feb	Mar	Apr	May	Jun
Region	4	2	4	4	4	2
Model	CCA2	CCA2	CCA2	CCA2	Ensembles23	CCA2
	Jul	Aug	Sep	Oct	Nov	Dec
Region	2	1	3	1	1	3
Model	Ensembles 12	CCA1	RF	Ensembles 12	Ensembles 23	CCA2

The results of the model evaluation suggest that using a prediction model based on multiple teleconnections at different lags can produce somewhat better predictions of the SPEI than a model based on multiple teleconnections at same lag. The highest HSS of the regression models is 0.38. The HSSs are low in some cases, and the regression models are not statistically significant in some cases, as shown in Figure 5.5. This indicates that the regression models cannot accurately predict the magnitude of the SPEI. However, it is not uncommon that the skill of monthly to seasonal forecasts is relatively low (Barnston, Thiao, & Kumar, 1996; McCabe & Dettinger, 1999). Therefore, we also compare the climate oscillation-based forecasts developed in this study to the CPC forecasts.

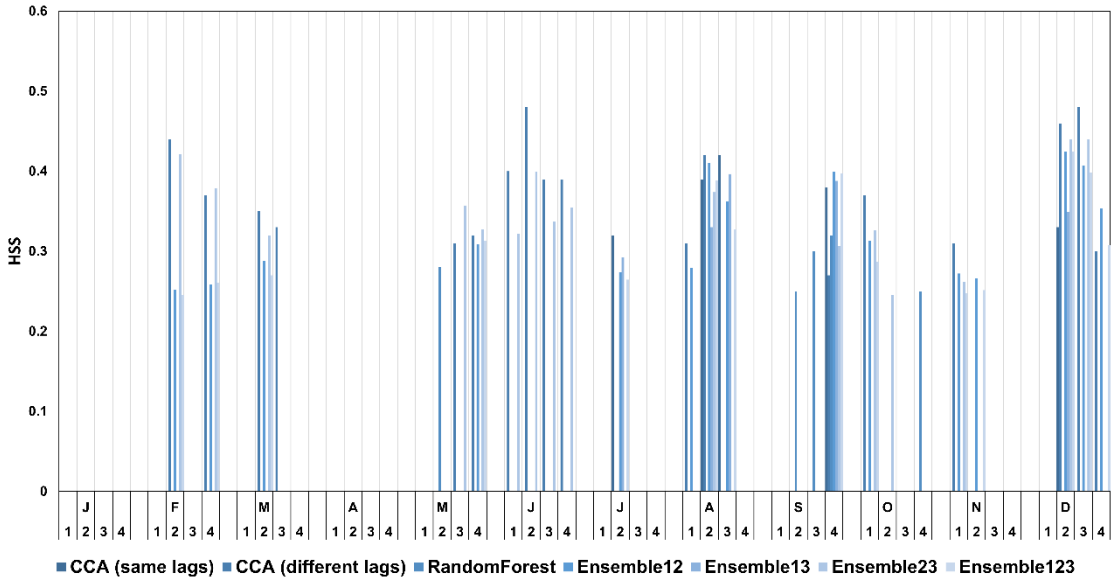

Figure 5.5 Correlation coefficient of different prediction models with 80% significance level.

5.3.4 Comparing Forecast Skill to CPC

The CPC provides monthly drought outlooks at a national scale. The monthly drought outlook is based on CPC monthly precipitation and temperature forecasts, and some other precipitation and temperature forecasts at shorter timescales (CPC, 2017b). The monthly drought outlook is a gridded national product. The outlook verification skill score is the difference between the drought outlook verification score and the persistence forecast score. The drought outlook verification score is the ratio of number of grids forecast successfully to the total number of grids (CPC, 2014). The drought outlook verification is only available from July 2013 to October 2015. Therefore, the CPC drought forecast skill score is only used here for a qualitative analysis.

Since the drought outlook is based on CPC monthly precipitation and temperature forecast, the forecast skill of monthly precipitation and temperature are also used for the qualitative analysis. The CPC provides monthly precipitation and temperature forecasts at a 0-month lead. The 0-month lead of precipitation/temperature forecast is created and updated the last day of the month for the following month. Therefore, all data in the initial month are used to predict precipitation/temperature in the subsequent month. Our SPEI forecast is similar to this 0-month lead CPC monthly precipitation/temperature forecast. All of the regression models developed in this study and the CPC forecast model utilize all antecedent climate data from the first month to predict climate in the following month. The CPC precipitation/temperature forecast is primarily based on a dynamical model (CPC, 2016a). The dynamical model uses a set of current climate variable observations and equations describing the physical behavior of the climate variable system to predict the climate variable in a short time future. Then, the predicted climate variables are used as the initial condition for a subsequent prediction for the next time-step until the future prediction time is reached. The CPC reports the Heidke Skill Score for various regions (Figure 5.6) (CPC, 2017a). The regions that are used by CPC do not match the regions that were defined in this study using PCA analysis, and the years used by the CPC do not match the years of our study. Therefore, only a qualitative comparison of the HSSs of our regression model and the CPC HSSs is shown here.

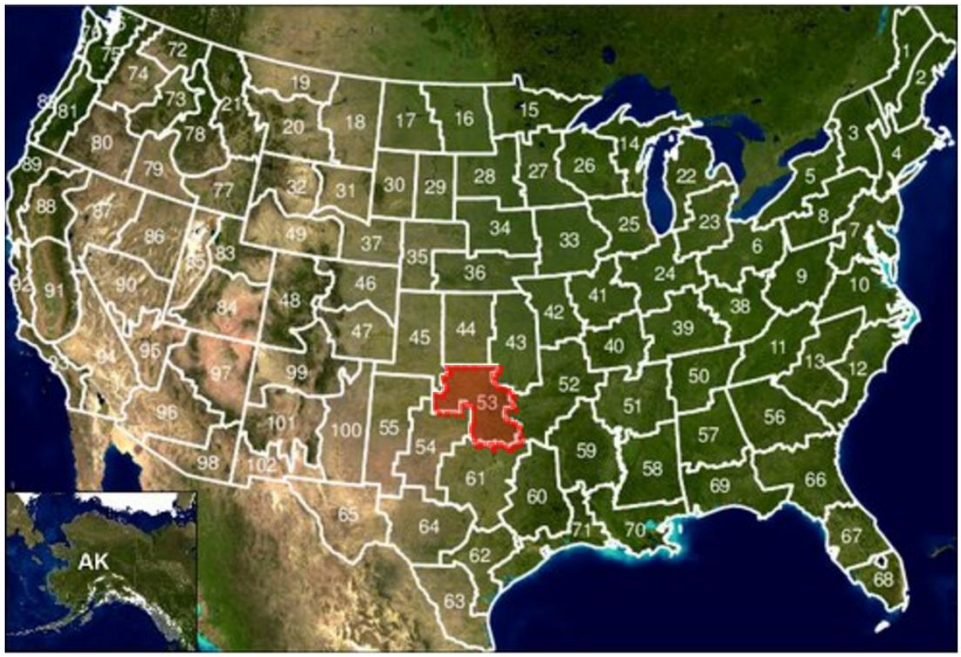

Figure 5.6 Map of CPC climate divisions with region in Oklahoma highlighted in red shade (Adapted from CPC, 2017).

Table 5.3 shows the monthly skill score of our regression model, CPC monthly drought outlooks, and CPC monthly precipitation and temperature forecast. The HSS from this study is the mean HSSs of all models for each month in Oklahoma and the highest HSSs from the seven regression models for one region in Oklahoma. The mean HSS based on all of the regression models averaged over the entire state is compared to the CPC monthly drought outlooks (MDO). The results show that in 10 out of 12 cases the mean HSS of our regression models is positive. For the CPC MDO, only 5 out of 12 cases have a positive skill score.

Since the purpose of this study is to find the best regression model for SPEI forecast in each region and month, the best model (i.e., the one with the highest HSS) is

compared to the HSS of the CPC precipitation and temperature forecasts. The results show that in 7 out of 12 cases our models have a higher HSS than the HSS of both CPC precipitation and temperature forecasts. In 2 out of 12 cases, the HSS of our regression model is lower than the HSS of both the CPC precipitation and temperature forecasts. In the other 3 cases, the HSS of our regression model is between the CPC precipitation and temperature forecast skill scores. These results provide some evidence to suggest that the skill of our models is at least equivalent to that of the CPC. Therefore, the models can provide useful SPEI forecasts at a 0-month lead in most regions and seasons in Oklahoma. Obviously, a more thorough direct comparison of forecast skill is necessary before stronger conclusions can be drawn.

Table 5-3 Forecast skill scores of models in this study comparing to CPC climate forecast

	Averaged-regression models	Highest-regression model	MDO	Precipitation (%)	Temperature (%)
Jan	-0.05	0.33	-2.05	27.27	18.18
Feb	0.05	0.33	-4.95	29.17	29.17
Mar	0.06	0.28	-8.50	45.83	-12.50
Apr	-0.08	0.07	-6.25	16.67	33.33
May	0.08	0.28	1.55	18.18	4.55
Jun	0.00	0.28	10.40	31.82	13.64
Jul	0.01	0.28	-8.60	40.91	31.82
Aug	0.08	0.38	1.80	13.64	-18.18
Sep	0.13	0.28	3.67	0.00	18.18
Oct	0.11	0.33	5.30	-40.91	59.09
Nov	0.05	0.18	-1.85	9.09	-9.09
Dec	0.15	0.38	-13.65	22.73	9.09

5.4 Limitations and Conclusions

Correlations between the five climate oscillations and SPEI indicated that NAO and ENSO account for the greatest amount of variance in the SPEI in Oklahoma. Many previous studies have also shown that NAO and ENSO are important factors that affect the climate system and can provide monthly-to-seasonal predictability (Barnston et al., 1996; Aiguo Dai & Wigley, 2000). However, across nearly every month and region, the correlations between the climate oscillations and SPEI were stronger when the combined impact of multiple teleconnections was considered. This result is consistent with previous studies such as Stevens and Ruscher (2014), Wise et al. (2015),] and Ning and Bradley (2014). For example, Stevens and Ruscher (2014) indicated that the sub-basins of the ACF are affected differently by multiple climatic oscillations, and no particular climatic oscillation can explain surface meteorological variation.

Using this knowledge, CCA was used to identify the months, regions, and time lags where the relationships between teleconnections and SPEI are the strongest. Dependent cross loadings were used to provide a means for quantifying the relationship between the five combined teleconnections and SPEI at various time lags. The results of the CCA analysis were generally in agreement with the correlation results. The strongest correlations occurred during the colder months and there were also more time lags that were statistically significant during this time. These results agree with studies such as Hu and Feng (2001) and Leathers et al. (1991) which suggest that teleconnections have a stronger impact on North American climate during the fall, winter, and spring. Statistically significant relationships were found for longer time lags (> 6 months)

during the warm months, while most of the statistically significant relationships were found at shorter time lags (< 6 months) during the cold months. These findings are supported by previous studies that observed the strongest relationships between precipitation and teleconnections during the winter months (Leathers et al., 1991; Ning & Bradley, 2014; Sutton & Hodson, 2005; Wise et al., 2015).

Several forecast models were developed to predict the SPEI using these five climate oscillations. The regression models include a CCA-based model using multiple climate oscillations at a 1 month lag, a CCA-based model using multiple climate oscillations at different lags, a random forest regression model, and four ensemble models. The results show that the CCA-based models developed in this study have forecast skill that was similar, and in some cases, better than the CPC. The comparison of the seven regression models developed in this study shows that the performance of the regression models varies from months and regions. In general, the CCA-based model using multiple climate oscillations at different lags is better than other regressions models in most of cases. The qualitative forecast skill comparison with CPC climate oscillation suggests that the statistical methods used in this study have forecast skill that is comparable to the dynamical models used by the CPC. Since one of the objectives of this study was to determine the value of considering multiple teleconnections, the correlations between the teleconnections and SPEI shows the multiple teleconnections can explain more of SPEI variance. Overall, the results demonstrate that using multiple teleconnections is valuable for explaining and predicting SPEI in Oklahoma. The relative importance of these teleconnections varies by region, month, and time lag. The

results presented here suggest that the regression model using multiple teleconnections is able to adequately forecast SPEI in Oklahoma. One of the limitations of the CCA-based regression model is the relationships among the input variables. For example, both of the ENSO and PNA are considered in the regression model, however, ENSO and PNA share some of common variance. In the future, PCA should be used to generate orthogonal input variables before they are used in the regression model.

Further research will evaluate whether including additional teleconnections can improve the accuracy of SPEI forecasts. In addition, it may also be useful to explore other statistical modeling approaches such as weighted multiple linear regression model using canonical weights to improving the forecasts. Finally, the skill of the regression model was evaluated over a multi-year period. It may be more helpful to evaluate how forecast skill changes during years when there are strong ENSO or NAO events. It is likely that the skill of the model varies significantly over time and that it is strongest during ENSO events and that the forecasts are less skillful when there is not strong remote forcing.

Oklahoma is a region where there are relatively strong relationships between teleconnections and SPEI, particularly NAO and ENSO. However, the analysis employed in this study can be applied to diagnose the impacts of multiple teleconnections on SPEI in other regions around the world. While the regression models can effectively predict SPEI with skill comparable to the CPC, climate oscillations only explain around half of the SPEI. While the purpose of this study was to observe the impact teleconnections have on SPEI at various time lags, the seasonal forecasting of

SPEI could improve with the additional consideration of variables not related to teleconnections. Including the influence of antecedent temperature, precipitation, and soil moisture may help to further improve these forecast. For example, land-based hydrological processes have been show to influence drought (Koster & Suarez, 1995; Koster, Suarez, & Heiser, 2000). Precipitation is also an important indicator of drought. Koster and Suarez (1995) investigated the impacts of sea surface temperatures and land surface hydrological state to the annual and seasonal precipitation variability. They found that the land surface impacts on precipitation variability are greatest during summer when the precipitation processes are sensitive to evaporation. Koster et al. (2000) indicated precipitation anomalies can be amplified by land surface processes. A positive precipitation anomaly can lead to an evaporation anomaly through land-atmospheric feedback, which in turn leads to additional precipitation through water recycling. Since evaporation is related with soil moisture and temperature, soil moisture and temperature can be used to improve the drought forecast. These types of studies are useful for examining other areas which could improve drought forecasts, while this study focuses primarily on identifying the strength and nature of the relationship between SPEI and various teleconnections in Oklahoma.

CHAPTER VI

CONCLUSIONS

6.1 Summary and Conclusions

This dissertation provided a comprehensive analysis of drought in Oklahoma. A new drought index, Precipitation Evapotranspiration Difference Condition Index (PEDCI) was developed in Chapter 2. PEDCI is based on SPEI and VCI. SPEI is a drought index based on a simple water balance model (difference between precipitation and potential evapotranspiration). However, SPEI is sensitive to the calculation of PET, and a probability distribution function is needed for the SPEI calculation. PEDCI overcomes the shortcomings of the SPEI by using the Penman-Monteith based PET and using the algorithm of VCI to normalize the monthly PEDCI values. Penman-Monteith-based PET is better than using temperature-based methods such as Thornthwaite. Unlike SPEI, the calculation of PEDCI is based on a simple normalization method rather than probability distribution which is complex to select the most suitable distribution and the calculation of the distribution parameters are complex. The normalization of difference between precipitation and potential evapotranspiration can avoid the differences between short-term weather-related water balance fluctuation and the influence of long-term ecosystem changes.

In Chapter 3, we compared six widely used drought indices and the new PEDCI for agricultural drought monitoring in Oklahoma. Soil moisture from Oklahoma Mesonet and crop yields from USDA were applied for the drought indices comparison. The

results indicated the relationship between soil moisture and drought indices is stronger during the warm season and weaker during the cool season. The correlations between soil moisture and drought indices during the warm season demonstrated that SPEI and PEDCI were most representative of soil moisture conditions.

The relationship between crop yield and drought indices indicated that the performance of drought indices varies from month to month during the crop growing period. For the comparison with crop yield, we applied two strategies. The first one is using all of the data, and the other excludes the middle 40% of data. The purpose of the second strategy is to investigate which drought indices perform best when crop yield and climate conditions are both well above- or below-normal. Overall, the comparison of drought indices based on the first strategy indicated that SPEI and Z-index are better than other indices for monitoring crop yield. The results based on second strategy indicated that drought indices that are solely based on precipitation, such as percent normal and SPI, are better during the early part of the winter wheat growing season, while water balance-based drought indices, such as the Z-index and PEDCI, are better closer to harvest. Since the second strategy is sensitive to the record length, it might not be the most robust approach for identifying the best drought indices when the period of record is relatively short.

Based on the results from Chapter 3, the spatial and temporal patterns of drought in Oklahoma were analyzed using the SPEI. SPEI at 1-month, 3-month and 6-month time scales were used in this anaysis since these are suitable for agricultural drought monitoring. The results at a 6-month scale showed that drought in Oklahoma has

decadal-scale variability. In the 1910s, 1930s, 1950s, 1970s, and 1980s Oklahoma was drier than normal. From the late 1980s to the early 2000s, Oklahoma experienced wetter than normal conditions. In recent years the SPEI has been decreasing, which suggests that another dry cycle may be starting.

The drought frequency analysis showed that drought occurs more frequently in northwestern Oklahoma. The seasonal drought frequency showed that droughts are more frequent during the spring. The Mann-Kendall trend tests showed that the SPEI significantly increased from 1901 to 2014. However, at shorter time periods, conditions are variable. There were five major drought periods between 1901 and 2014. These were primarily caused by significant decreases in precipitation. However, the recent 2011 drought is related to both decreases in water supply (precipitation) and increases in water demand (PET).

The goal of Chapter 5 was to identify the factors that are responsible for causing drought in Oklahoma. The results indicated that NAO, ENSO and PNA are the primary climate oscillations that influence the climate of Oklahoma. They also showed that the inclusion of multiple climate oscillations can enhance the relationship between climate oscillations and drought. Based on the relationships between climate oscillations and SPEI at different lags, two CCA-based regression model were developed for monthly SPEI forecast. The correlations between SPEI and multiple teleconnections decrease as the time lag increases. Therefore, a CCA-based regression model using multiple teleconnections at 1-month lag was developed. In the second strategy, a CCA-based regression model using multiple teleconnections at different lags was developed. The

skill scores show that the performance of these regression models varies from months and regions. In general, CCA-based regression model using multiple teleconnections at different lags is the most skillful approach for forecasting SPEI.

6.2 Future Research

Soil moisture is a key variable in the land-atmosphere interaction and hydroclimate system. A lot of effort has been done devoted to soil moisture monitoring. Given the challenges in estimating and measuring soil moisture, drought indices are potentially a useful method for estimating soil moisture conditions.

There are also opportunities to apply the results of the relationships between drought indices and winter wheat yield to improve the crop yield modeling. Statistical models based on weather conditions and mechanistic models based on fundamental mechanisms of plant and soil processes are two major types of crop simulation models. Assimilating the drought conditions in the mechanistic models can be promising method to improve the crop yield modeling.

Drought forecast is vitally important for drought assessment and mitigation. Droughts are caused by numerous factors such as natural atmospheric variability (i.e., climate oscillations), land-atmosphere interactions, and thermodynamic conditions. The regression models in this study demonstrate that this method has promise for providing drought early warning in Oklahoma. However, the skill of the regression models are lower than the skill of CPC drought forecast in some months and regions. It is necessary

to do further research to improve the drought forecast skill by integrating more factors into consideration.

REFERENCES

Alley, W. M. (1984). The Palmer Drought Severity Index - Limitations and Assumptions. *Journal of Climate and Applied Meteorology, 23*(7), 1100-1109.

Alley, W. M. (1985). The Palmer Drought Severity Index as a measure of hydrologic drought. *Journal of the American Water Resources Association, 21*(1), 105-114.

American Meteorological Society. (1997). Policy statement: Meteorological drought. *Bulletin of the American Meteorological Society, 78*, 847-849.

American Meteorological Society. (2004). AMS statement on meteorological drought. *Bulletin of the American Meteorological Society, 85*, 771-773.

American Meteorological Society. (2012). "Climatic Cycle". Glossary of Meteorology. (http://glossary.ametsoc.org/wiki/Climatic cycle).

Barnston, A. G., & Livezey, R. E. (1987). Classification, seasonality and persistence of low-frequency atmospheric circulation patterns. *Monthly Weather Review, 115*(6), 1083-1126.

Barnston, A. G., Thiao, W., & Kumar, V. (1996). Long-lead forecasts of seasonal precipitation in Africa using CCA. *Weather and Forecasting, 11*(4), 506-520.

Bayazit, M., & Onoz, B. (2007). To prewhiten or not to prewhiten in trend analysis? *Hydrological Sciences Journal, 52*(4), 611-624.

Belmans, C., Wesseling, J., & Feddes, R. A. (1983). Simulation model of the water balance of a cropped soil: SWATRE. *Journal of Hydrology, 63*(3-4), 271-286.

Borga, M. (2001). Canonical correlation: a tutorial (http://people.imt.liu.se/magnus/cca). *4*, 5.

Breiman, L. (2001). Random forests. *Machine learning*, *45*(1), 5-32.

Breiman, L. (2003). Manual--setting up, using, and understanding random forests V4. 0. (https://www.stat.berkeley.edu/~breiman/Using_random_forests_v4.0.pdf).

Breiman, L. (2004). Consistency for a simple model of random forests (https://www.stat.berkeley.edu/~breiman/RandomForests/consistencyRFA.pdf).

Brock, F. V., Crawford, K. C., Elliott, R. L., Cuperus, G. W., Stadler, S. J., & et al. (1995). The Oklahoma Mesonet: a technical overview. *Journal of Atmospheric and Oceanic Technology*, *12*(1), 5-19.

Brown, D. P., & Comrie, A. C. (2004). A winter precipitation 'dipole'in the western United States associated with multidecadal ENSO variability. *Geophysical Research Letters*, *31*(9).

Bryant, S., Arnell, N., & Law, F. (1992). *The long-term context for the current hydrological drought.* Paper presented at the Proceedings of the IWEM Conference on the Management of Scarce Water Resources.

Chen, T., Werf, G., Jeu, R., Wang, G., & Dolman, A. (2013). A global analysis of the impact of drought on net primary productivity. *Hydrology and Earth System Sciences*, *17*(10), 3885-3894.

Cook, B. I., Smerdon, J. E., Seager, R., & Cook, E. R. (2014). Pan-continental droughts in North America over the last millennium*. *Journal of Climate*, *27*(1), 383-397.

CPC. (2014). Explanation of Drought Outlook Verificatio (http://www.cpc.ncep.noaa.gov/products/expert_assessment/sdo_verification/DO-verif-explanation.shtml).

CPC. (2016a). 30-Day Outlook Discussion (http://www.cpc.ncep.noaa.gov/products/predictions/30day/).

CPC. (2016b). CPC Verification Summary (http://www.cpc.ncep.noaa.gov/products/verification/summary/index.php?page=tutorial).

CPC. (2017a). CPC Verification Web Tool (http://www.vwt.ncep.noaa.gov/).

CPC. (2017b). Discussion for the Monthly Drought Outlook (http://www.cpc.ncep.noaa.gov/products/expert_assessment/mdo_discussion.php).

Dai, A. (2011). Characteristics and trends in various forms of the Palmer Drought Severity Index during 1900-2008. *Journal of Geophysical Research: Atmospheres, 116*(D12).

Dai, A., Trenberth, K. E., & Qian, T. T. (2004). A global dataset of Palmer Drought Severity Index for 1870-2002: Relationship with soil moisture and effects of surface warming. *Journal of Hydrometeorology*, *5*(6), 1117-1130.

Dai, A., & Wigley, T. (2000). Global patterns of ENSO-induced precipitation. *Geophysical Research Letters, 27*(9), 1283-1286.

Daly, C., Halbleib, M., Smith, J. I., Gibson, W. P., Doggett, M. K., & et al. (2008). Physiographically sensitive mapping of climatological temperature and precipitation across the conterminous United States. *International Journal of Climatology, 28*(15), 2031.

Denmead, O., & Shaw, R. H. (1962). Availability of soil water to plants as affected by soil moisture content and meteorological conditions. *Agronomy Journal, 54*(5), 385-390.

Dracup, J. A., Lee, K. S., & Paulson, E. G. (1980). On the definition of droughts. *Water Resources Research, 16*(2), 297-302.

Drobyshev, I., Niklasson, M., & Linderholm, H. W. (2012). Forest fire activity in Sweden: Climatic controls and geographical patterns in 20th century. *Agricultural and Forest Meteorology, 154*, 174-186.

Durkee, J., Frye, J., Fuhrmann, C., Lacke, M., Jeong, H., & et al. (2008). Effects of the North Atlantic Oscillation on precipitation-type frequency and distribution in the eastern United States. *Theoretical and Applied Climatology, 94*(1-2), 51-65.

Ek, M., Xia, Y., Wood, E., Sheffield, J., Luo, L., & et al. (2011). North American Land Data Assimilation System Phase 2 (NLDAS-2): Development and applications. *GEWEX News, 2*, 6-8.

Enfield, D. B., Mestas-Nunez, A. M., & Trimble, P. J. (2001). The Atlantic multidecadal oscillation and its relation to rainfall and river flows in the continental U. S. *Geophysical Research Letters, 28*(10), 2077-2080.

FAO Land and Water division. (2015). Crop Water Information: Wheat (http://www.fao.org/land-water/databases-and-software/crop-information/wheat/en/).

Fernando, D. N., Mo, K. C., Fu, R., Pu, B., Bowerman, A., & et al. (2016). What caused the spring intensification and winter demise of the 2011 drought over Texas? *Climate Dynamics*, 1-14.

Field, C. B. (2012). *Managing the risks of extreme events and disasters to advance climate change adaptation: special report of the intergovernmental panel on climate change*: Cambridge University Press.

Ford, T., & Labosier, C. F. (2014). Spatial patterns of drought persistence in the Southeastern United States. *International Journal of Climatology, 34*(7), 2229-2240.

Ge, Y., Apurv, T., & Cai, X. (2016). Spatial and temporal patterns of drought in the Continental US during the past century. *Geophysical Research Letters, 43*(12), 6294-6303.

Gibbs, W. J. (1967). *Rainfall deciles as drought indicators*: Melbourne: Bureau of Meteorology.

Gommes, R., & Petrassi, F. (1996). Rainfall variability and drought in sub-Saharan Africa. *Environmental and Natural Resources Services, FAO Agrometeorology Series Working Paper No. 9*.

Graumann, A., Lott, N., McCown, S., & Ross, T. (1998). *Climatic extremes of the summer of 1998*: U.S. Department of Commerce, National Oceanic and Atmospheric Administration, National Environmental Satellite, Data and Information Service, National Climatic Data Center.

Hagman, G., Beer, H., Bendz, M., & Wijkman, A. (1984). *Prevention better than cure. Report on human and environmental disasters in the Third World. 2*: Stockholm: Swedish Red Cross.

Hamlet, A. F., Mote, P. W., Clark, M. P., & Lettenmaier, D. P. (2007). Twentieth-century trends in runoff, evapotranspiration, and soil moisture in the western United States. *Journal of Climate, 20*(8), 1468-1486.

Hannachi, A., Jolliffe, I., & Stephenson, D. (2007). Empirical orthogonal functions and related techniques in atmospheric science: A review. *International Journal of Climatology, 27*(9), 1119-1152.

Harris, I., Jones, P. D., Osborn, T. J., & Lister, D. H. (2014). Updated high-resolution grids of monthly climatic observations - the CRU TS3.10 Dataset. *International Journal of Climatology, 34*(3), 623-642.

Harshburger, B., Ye, H., & Dzialoski, J. (2002). Observational evidence of the influence of Pacific SSTs on winter precipitation and spring stream discharge in Idaho. *Journal of Hydrology*, *264*(1), 157-169.

Hartmann, D., Tank, A., & Rusticucci, M. (2013). IPCC fifth assessment report, climate change 2013: The physical science basis. *IPCC AR5*, 31-39.

Heim, R. R. (2002). A review of twentieth-century drought indices used in the United States. *Bulletin of the American Meteorological Society*, *83*(8), 1149-1165.

Henderson, K. G., & Robinson, P. J. (1994). Relationships between the pacific/north american teleconnection patterns and precipitation events in the south-eastern USA. *International Journal of Climatology*, *14*(3), 307-323.

Hu, Q., & Feng, S. (2001). Variations of teleconnection of ENSO and interannual variation in summer rainfall in the central United States. *Journal of Climate, 14*(11), 2469-2480.

Huang, J., Tian, L., Liang, S., Ma, H., Becker-Reshef, I., & et al. (2015). Improving winter wheat yield estimation by assimilation of the leaf area index from Landsat TM and MODIS data into the WOFOST model. *Agricultural and Forest Meteorology, 204*, 106-121.

Hunt, B. (2015). Rainfall variability and predictability issues for North America. *Climate Dynamics*, 1-19.

Hurrell, J. W. (1995). Decadal trends in the North Atlantic Oscillation: regional temperatures and precipitation. *Science, 269*(5224), 676-679.

Illston, B. G., Basara, J. B., & Crawford, K. C. (2004). Seasonal to interannual variations of soil moisture measured in Oklahoma. *International Journal of Climatology, 24*(15), 1883-1896.

Kempes, C., Myers, O., Breshears, D., & Ebersole, J. (2008). Comparing response of Pinus edulis tree-ring growth to five alternate moisture indices using historic meteorological data. *Journal of Arid Environments, 72*(4), 350-357.

Keyantash, J. A., & Dracup, J. A. (2002). The quantification of drought: an evaluation of drought indices. *Bulletin of the American Meteorological Society, 83*(8), 1167.

Keyantash, J. A., & Dracup, J. A. (2004). An aggregate drought index: assessing drought severity based on fluctuations in the hydrologic cycle and surface water storage. *Water Resources Research, 40*(9).

Kingston, D. G., Stagge, J. H., Tallaksen, L. M., & Hannah, D. M. (2015). European-Scale Drought: Understanding Connections between Atmospheric Circulation and Meteorological Drought Indices. *Journal of Climate, 28*(2), 505-516.

Kogan, F. N. (1995). Application of vegetation index and brightness temperature for drought detection. *Advances in Space Research, 15*(11), 91-100.

Koster, R. D., & Suarez, M. J. (1995). Relative contributions of land and ocean processes to precipitation variability. *Journal of Geophysical Research: Atmospheres, 100*(D7), 13775-13790.

Koster, R. D., Suarez, M. J., & Heiser, M. (2000). Variance and predictability of precipitation at seasonal-to-interannual timescales. *Journal of Hydrometeorology, 1*(1), 26-46.

Kumar, M. N., Murthy, C. S., Sai, M. V. R. S., & Roy, P. S. (2012). Spatiotemporal analysis of meteorological drought variability in the Indian region using standardized precipitation index. *Meteorological Applications, 19*(2), 256-264.

Kumar, S., Merwade, V., Kam, J., & Thurner, K. (2009). Streamflow trends in Indiana: effects of long term persistence, precipitation and subsurface drains. *Journal of Hydrology, 374*(1), 171-183.

Kwitt, R., & Hofmann, U. (2006). *Robust methods for unsupervised PCA-based anomaly detection.* Paper presented at the Proc. IEEE/IST Workshop Monitoring, Attack Detection Mitigation.

Leathers, D. J., Yarnal, B., & Palecki, M. A. (1991). The Pacific/North American teleconnection pattern and United States climate. Part I: Regional temperature and precipitation associations. *Journal of Climate, 4*(5), 517-528.

Liaw, A., & Wiener, M. (2002). Classification and regression by randomForest. *R news, 2*(3), 18-22.

Lobell, D. B., Schlenker, W., & Costa-Roberts, J. (2011). Climate trends and global crop production since 1980. *Science, 333*(6042), 616-620.

Lorenz, E. N. (1956). *Empirical orthogonal functions and statistical weather prediction*: Massachusetts Institute of Technology, Department of Meteorology.

Lorenzo-Lacruz, J., Vicente-Serrano, S. M., López-Moreno, J. I., Beguería, S., García-Ruiz, J. M., & et al. (2010). The impact of droughts and water management on various hydrological systems in the headwaters of the Tagus River (central Spain). *Journal of Hydrology, 386*(1), 13-26.

Mahrt, L., & Ek, M. (1984). The influence of atmospheric stability on potential evaporation. *Journal of Climate and Applied Meteorology, 23*(2), 222-234.

Mantua, N. J., & Hare, S. R. (2002). The Pacific decadal oscillation. *Journal of oceanography, 58*(1), 35-44.

Mantua, N. J., Hare, S. R., Zhang, Y., Wallace, J. M., & Francis, R. C. (1997). A Pacific interdecadal climate oscillation with impacts on salmon production. *Bulletin of the American Meteorological Society, 78*(6), 1069-1079.

Masih, I., Maskey, S., Mussa, F. E. F., & Trambauer, P. (2014). A review of droughts on the African continent: a geospatial and long-term perspective. *Hydrology and Earth System Sciences, 18*(9), 3635-3649.

McCabe, G. J., & Dettinger, M. D. (1999). Decadal variations in the strength of ENSO teleconnections with precipitation in the western United States. *International Journal of Climatology, 19*(13), 1399-1410.

McCabe, G. J., Palecki, M. A., & Betancourt, J. L. (2004). Pacific and Atlantic Ocean influences on multidecadal drought frequency in the United States. *Proceedings of the National Academy of Sciences, 101*(12), 4136-4141.

McCabe, G. J., & Wolock, D. M. (2002). A step increase in streamflow in the conterminous United States. *Geophysical Research Letters*, *29*(24).

McKee, T. B., Doesken, N. J., & Kleist, J. (1993). *The relationship of drought frequency and duration to time scales.* Paper presented at the Proceedings of the 8th Conference on Applied Climatology.

Mendez, M., & Magana, V. (2010). Regional aspects of prolonged meteorological droughts over Mexico and Central America. *Journal of Climate, 23*(5), 1175-1188.

Meyer, S. J., Hubbard, K. G., & Wilhite, D. A. (1993). A crop-specific drought index for corn: I. Model development and validation. *Agronomy Journal, 85*(2), 388-395.

Mishra, A., & Desai, V. (2005). Spatial and temporal drought analysis in the Kansabati river basin, India. *International Journal of River Basin Management, 3*(1), 31-41.

Mishra, A. K., & Singh, V. P. (2010). A review of drought concepts. *Journal of Hydrology, 391*(1-2), 204-216.

Myoung, B., & Nielsen-Gammon, J. W. (2010). The convective instability pathway to warm season drought in Texas. Part I: The role of convective inhibition and its modulation by soil moisture. *Journal of Climate, 23*(17), 4461-4473.

NASS, U. (2010). Field Crops: Usual Planting and Harvesting Dates. *USDA National Agricultural Statistics Service, Agricultural Handbook*(628).

Navarra, A., & Simoncini, V. (2010). Empirical Orthogonal Functions *A Guide to Empirical Orthogonal Functions for Climate Data Analysis* (pp. 39-67): Springer.

Niemeyer, S. (2008). New drought indices. *Water Management, 80*, 267-274.

Ning, L., & Bradley, R. S. (2014). Winter precipitation variability and corresponding teleconnections over the northeastern United States. *Journal of Geophysical Research-Atmospheres, 119*(13).

Oklahoma Climatological Survey. (2014). Oklahoma Climatological Survey (http://climate.ok.gov/index.php/climate/map/map_of_oklahoma_climate_divisions).

Oklahoma Water Resources Board, Oklahoma Climatological Survey, & (U.S.), G. S. (2012). Hydrologic drought of water year 2011: a historical context (https://www.owrb.ok.gov/supply/drought/pdf_dro/DroughtFactSheet2011.pdf).

Palmer, W. C. (1965). *Meteorological drought* (Vol. 30): US Department of Commerce, Weather Bureau Washington, DC, USA.

Palmer, W. C. (1968). Keeping track of crop moisture conditions, nationwide: The new crop moisture index. *Weatherwise, 21*(4), 156-161.

Potopova, V., Boroneant, C., Boincean, B., & Soukup, J. (2016). Impact of agricultural drought on main crop yields in the Republic of Moldova. *International Journal of Climatology, 36*(4), 2063-2082.

Quiring, S. M. (2009). Developing Objective Operational Definitions for Monitoring Drought. *Journal of Applied Meteorology and Climatology, 48*(6), 1217-1229.

Quiring, S. M. (2009). Monitoring drought: an evaluation of meteorological drought indices. *Geography Compass, 3*(1), 64-88.

Quiring, S. M., Ford, T. W., Wang, J. K., Khong, A., Harris, E., & et al. (2016). The North American soil moisture database: development and applications. *Bulletin of the American Meteorological Society, 97*(8), 1441-1459.

Quiring, S. M., & Goodrich, G. B. (2008). Nature and causes of the 2002 to 2004 drought in the southwestern United States compared with the historic 1953 to 1957 drought. *Climate Research, 36*(1), 41-52.

Quiring, S. M., & Papakryiakou, T. N. (2003). An evaluation of agricultural drought indices for the Canadian prairies. *Agricultural and Forest Meteorology, 118*(1-2), 49-62.

Rayner, N., Parker, D. E., Horton, E., Folland, C., Alexander, L., & et al. (2003). Global analyses of sea surface temperature, sea ice, and night marine air temperature since the late nineteenth century. *Journal of Geophysical Research: Atmospheres (1984–2012), 108*(D14).

Redmond, K. T., & Koch, R. W. (1991). Surface climate and streamflow variability in the western United States and their relationship to large‐scale circulation indices. *Water Resources Research, 27*(9), 2381-2399.

Rushton, K., Eilers, V., & Carter, R. (2006). Improved soil moisture balance methodology for recharge estimation. *Journal of Hydrology, 318*(1), 379-399.

Saadat, S., Khalili, D., Kamgar-Haghighi, A. A., & Zand-Parsa, S. (2013). Investigation of spatio-temporal patterns of seasonal streamflow droughts in a semi-arid region. *Natural Hazards, 69*(3), 1697-1720.

Schlesinger, M. E., & Ramankutty, N. (1994). An oscillation in the global climate system of period 65-70 years. *Nature, 367*(6465), 723-726.

Schneider, U., Becker, A., Finger, P., Meyer-Christoffer, A., Ziese, M., & et al. (2014). GPCC's new land surface precipitation climatology based on quality-controlled in situ data and its role in quantifying the global water cycle. *Theoretical and Applied Climatology, 115*(1-2), 15-40.

Schubert, S. D., Stewart, R. E., Wang, H., Barlow, M., Berbery, E. H., & et al. (2016). Global Meteorological Drought: A Synthesis of Current Understanding with a Focus on SST Drivers of Precipitation Deficits. *Journal of Climate, 29*(11), 3989-4019.

Schubert, S. D., Suarez, M. J., Pegion, P. J., Koster, R. D., & Bacmeister, J. T. (2004). On the cause of the 1930s Dust Bowl. *Science, 303*(5665), 1855-1859.

Scott, R. L., Shuttleworth, W. J., Keefer, T. O., & Warrick, A. W. (2000). Modeling multiyear observations of soil moisture recharge in the semiarid American Southwest. *Water Resources Research, 36*(8), 2233-2247.

Seager, R., Goddard, L., Nakamura, J., Henderson, N., & Lee, D. E. (2014). Dynamical Causes of the 2010/11 Texas–Northern Mexico Drought*. *Journal of Hydrometeorology, 15*(1), 39-68.

Seager, R., & Hoerling, M. (2014). Atmosphere and ocean origins of North American droughts. *Journal of Climate, 27*(12), 4581-4606.

Sheffield, J., Wood, E. F., & Roderick, M. L. (2012). Little change in global drought over the past 60 years. *Nature, 491*(7424), 435-438.

Song, X., Li, L., Fu, G., Li, J., Zhang, A., & et al. (2014). Spatial-temporal variations of spring drought based on spring-composite index values for the Songnen Plain, Northeast China. *Theoretical and Applied Climatology, 116*(3-4), 371-384.

Spinoni, J., Naumann, G., Carrao, H., Barbosa, P., & Vogt, J. r. (2014). World drought frequency, duration, and severity for 1951-2010. *International Journal of Climatology, 34*(8), 2792-2804.

Staff National Drought Mitigation Center. (2000). United States Drought Monitor maps (http://droughtmonitor.unl.edu/MapsAndData/MapArchive.aspx).

Stevens, K. A., & Ruscher, P. H. (2014). Large scale climate oscillations and mesoscale surface meteorological variability in the Apalachicola-Chattahoochee-Flint River Basin. *Journal of Hydrology, 517*, 700-714.

Stotts, D. (2011). Oklahoma Agricultural Losses from Drought More Than $1.6 Billion. . Retrieved from http://water.okstate.edu/news-events/news/acs/oklahoma-agricultural-losses-from-drought-more-than-1.6-billion

Sutton, R. T., & Hodson, D. L. (2005). Atlantic Ocean forcing of North American and European summer climate. *Science, 309*(5731), 115-118.

Svetnik, V., Liaw, A., Tong, C., Culberson, J. C., Sheridan, R. P., & et al. (2003). Random forest: a classification and regression tool for compound classification and QSAR modeling. *Journal of chemical information and computer sciences, 43*(6), 1947-1958.

Svoboda, M., LeComte, D., Hayes, M., Heim, R., Gleason, K., & et al. (2002). The drought monitor. *Bulletin of the American Meteorological Society, 83*(8), 1181-1190.

Tan, C., Yang, J., & Li, M. (2015). Temporal-spatial variation of drought indicated by SPI and SPEI in Ningxia Hui Autonomous region, China. *Atmosphere, 6*(10), 1399-1421.

Thompson, B. (2005). Canonical correlation analysis *Encyclopedia of statistics in behavioral science*: John Wiley & Sons, Inc.

Trenberth, K. E., Dai, A., van der Schrier, G., Jones, P. D., Barichivich, J., & et al. (2014). Global warming and changes in drought. *Nature Climate Change, 4*(1), 17-22.

Van Rooy, M. (1965). A rainfall anomaly index independent of time and space. *Notos, 14*(43), 6.

Vicente-Serrano, S. M. (2006). Spatial and temporal analysis of droughts in the Iberian Peninsula (1910–2000). *Hydrological Sciences Journal, 51*(1), 83-97.

Vicente-Serrano, S. M., Begueria, S., & Lopez-Moreno, J. I. (2010). A Multiscalar Drought Index Sensitive to Global Warming: The Standardized Precipitation Evapotranspiration Index. *Journal of Climate, 23*(7), 1696-1718.

Vicente-Serrano, S. M., Begueria, S., Lopez-Moreno, J. I., Angulo, M., & El Kenawy, A. (2010). A new global 0.5 gridded dataset (1901ق | ô2006) of a multiscalar drought index: comparison with current drought index datasets based on the Palmer Drought Severity Index. *Journal of Hydrometeorology, 11*(4), 1033-1043.

Vicente-Serrano, S. M., Beguería, S., Lorenzo-Lacruz, J., Camarero, J. J., López-Moreno, J. I., & et al. (2012). Performance of drought indices for ecological, agricultural, and hydrological applications. *Earth Interactions, 16*(10), 1-27.

Vicente-Serrano, S. M., Gouveia, C., Camarero, J. J., Begueria, S., Trigo, R., & et al. (2013). Response of vegetation to drought time-scales across global land biomes. *Proceedings of the National Academy of Sciences, 110*(1), 52-57.

Von Storch, H. (1999). Misuses of statistical analysis in climate research *Analysis of Climate Variability* (pp. 11-26): Springer.

Wallace, J. M., & Gutzler, D. S. (1981). Teleconnections in the geopotential height field during the Northern Hemisphere winter. *Monthly Weather Review, 109*(4), 784-812.

Wang, H., Rogers, J. C., & Munroe, D. K. (2015). Commonly Used Drought Indices as Indicators of Soil Moisture in China. *Journal of Hydrometeorology*(2015).

Wang, Q., Wu, J., Lei, T., He, B., Wu, Z., & et al. (2014). Temporal-spatial characteristics of severe drought events and their impact on agriculture on a global scale. *Quaternary International, 349*, 10-21.

Westerhoff, R. (2015). Using uncertainty of Penman and Penmanق | ôMonteith methods in combined satellite and ground-based evapotranspiration estimates. *Remote Sensing of Environment, 169*, 102-112.

Wilhite, D. A. (1996). A methodology for drought preparedness. *Natural Hazards, 13*(3), 229-252.

Wilhite, D. A. (2000). Drought as a Natural Hazard: Concepts and Definitions *Drought: A Global Assessment* (pp. 3–18): London: Routledge.

Wise, E. K., Wrzesien, M. L., Dannenberg, M. P., & McGinnis, D. L. (2015). Cool-Season Precipitation Patterns Associated with Teleconnection Interactions in the United States. *Journal of Applied Meteorology and Climatology, 54*(2), 494-505.

Xie, H., Ringler, C., Zhu, T., & Waqas, A. (2013). Droughts in Pakistan: a spatiotemporal variability analysis using the Standardized Precipitation Index. *Water International, 38*(5), 620-631.

Xu, K., Yang, D., Yang, H., Li, Z., Qin, Y., & et al. (2015). Spatio-temporal variation of drought in China during 1961-2012: a climatic perspective. *Journal of Hydrology, 526*, 253-264.

Yarnal, B. (1993). *Synoptic climatology in environmental analysis: a primer*: Belhaven.

Yevjevich, V. M. (1967). An objective approach to definitions and investigations of continental hydrologic droughts. *Hydrology papers (Colorado State University), 23*.

Yuan, S., & Quiring, S. M. (2014). Drought in the US Great Plains (1980–2012): A sensitivity study using different methods for estimating potential evapotranspiration in the Palmer Drought Severity Index. *Journal of Geophysical Research: Atmospheres, 119*(19), 10,996-911,010.

Yue, S., & Wang, C. Y. (2002). Applicability of prewhitening to eliminate the influence of serial correlation on the Mann-Kendall test. *Water Resources Research, 38*(6).

Zargar, A., Sadiq, R., Naser, B., & Khan, F. I. (2011). A review of drought indices. *Environmental Reviews, 19*, 333-349.

Zhang, Z., Chen, X., Xu, C.-Y., Hong, Y., Hardy, J., & et al. (2015). Examining the influence of river-lake interaction on the drought and water resources in the Poyang Lake basin. *Journal of Hydrology, 522*, 510-521.

Zhu, L., & Quiring, S. M. (2013). Variations in tropical cyclone precipitation in Texas (1950 to 2009). *Journal of Geophysical Research: Atmospheres, 118*(8), 3085-3096.

APPENDIX A

FIGURES

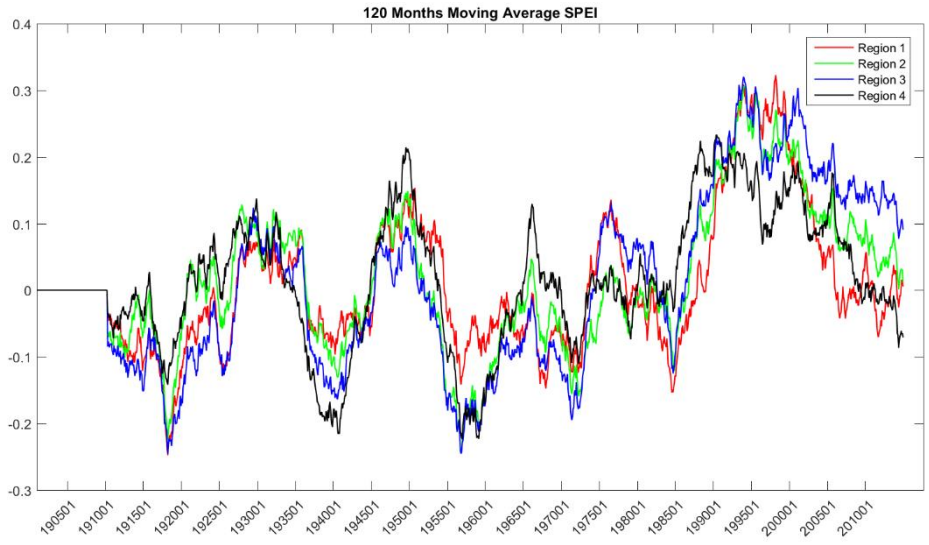

Figure A.1 1-month SPEI (SPEI1) for each region in Oklahoma from 1901 to 2014. Data have been smoothed with a 120-month moving average.

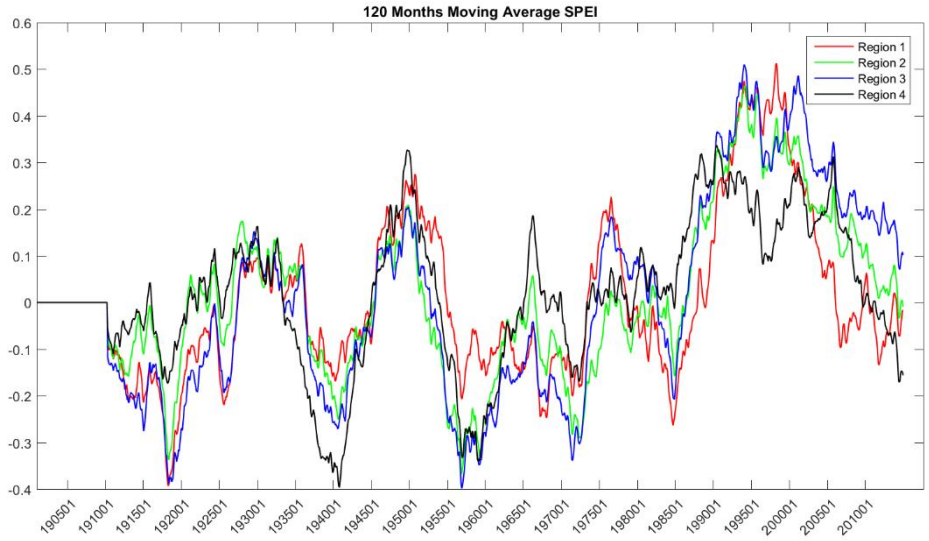

Figure A.2 3-month SPEI (SPEI3) for each region in Oklahoma from 1901 to 2014. Data have been smoothed with a 120-month moving average.

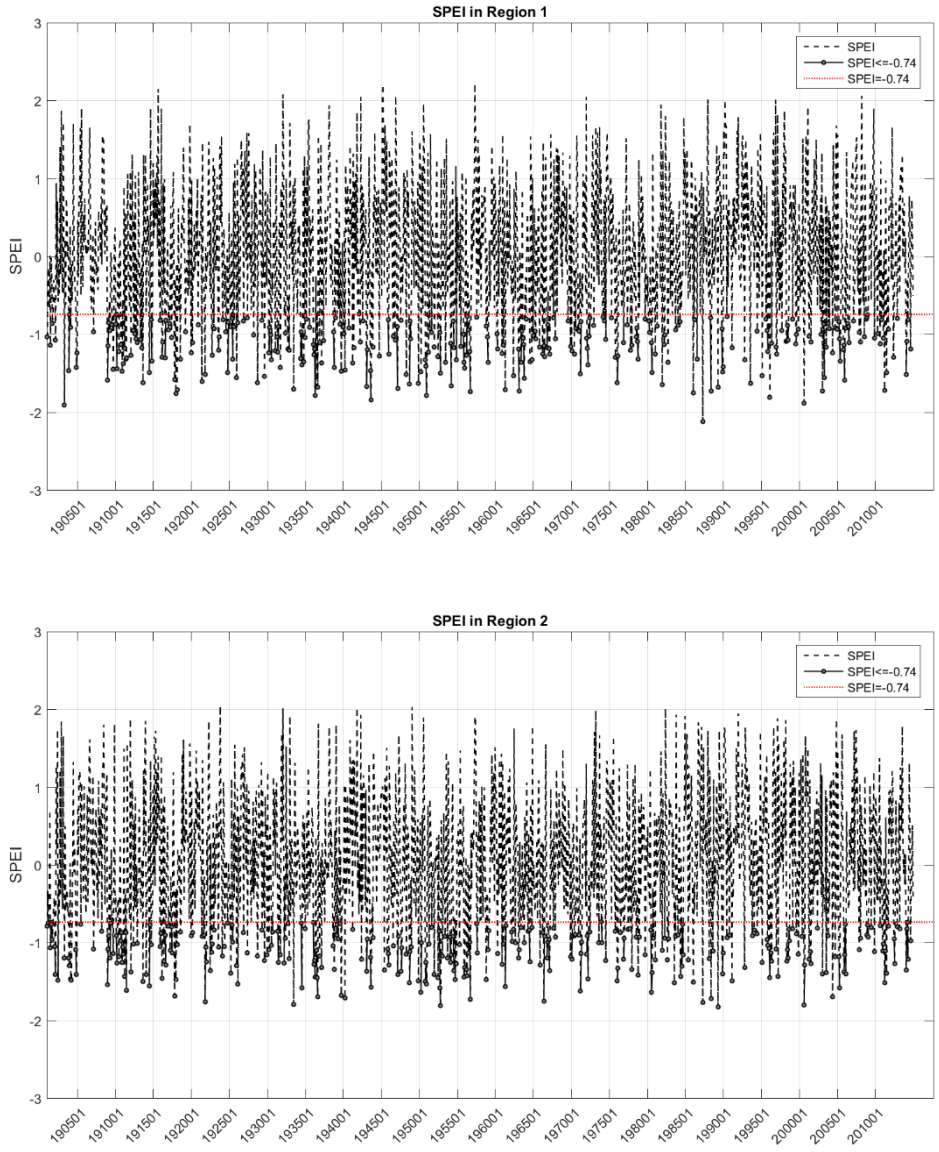

Figure A.3 SPEI values for each region in Oklahoma from 1901 to 2014 (SPEI1).

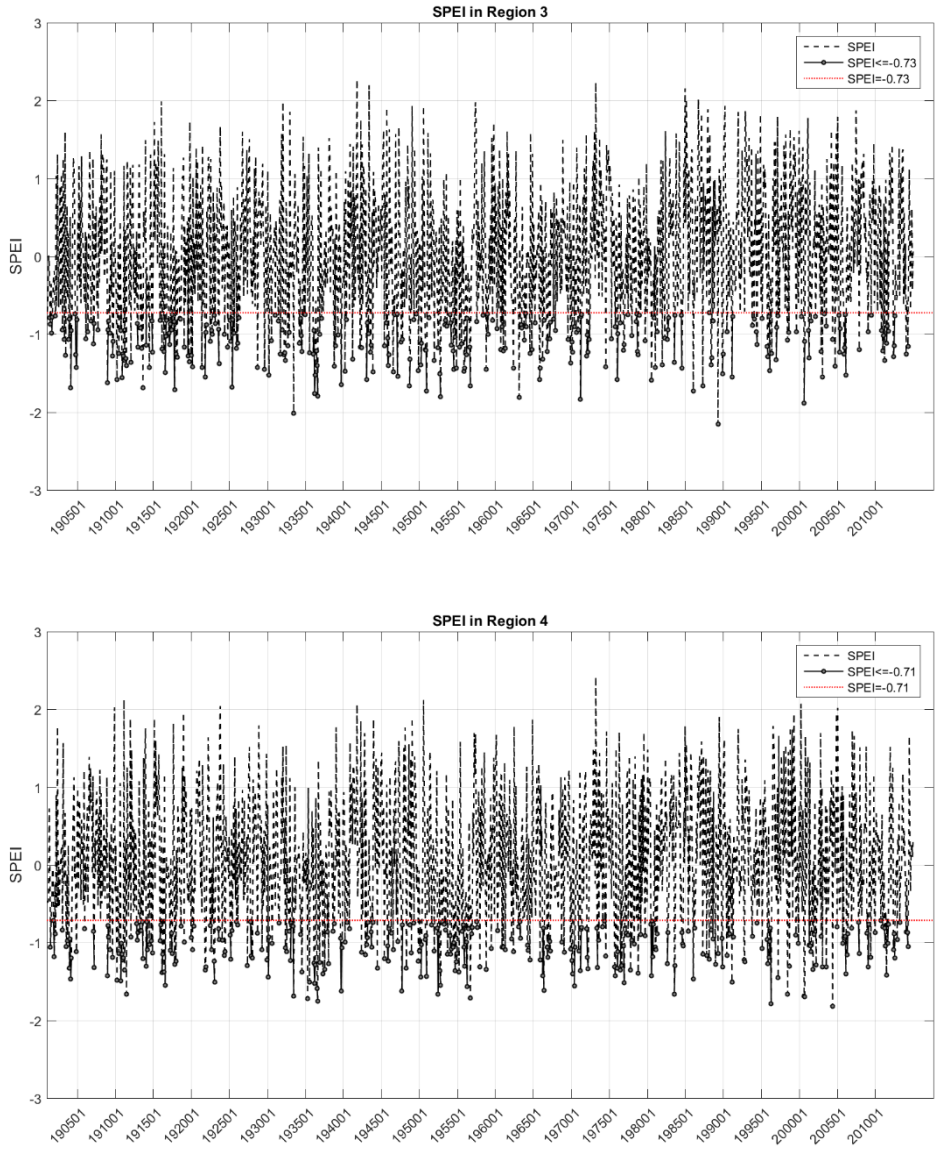

Figure A.3 Continued

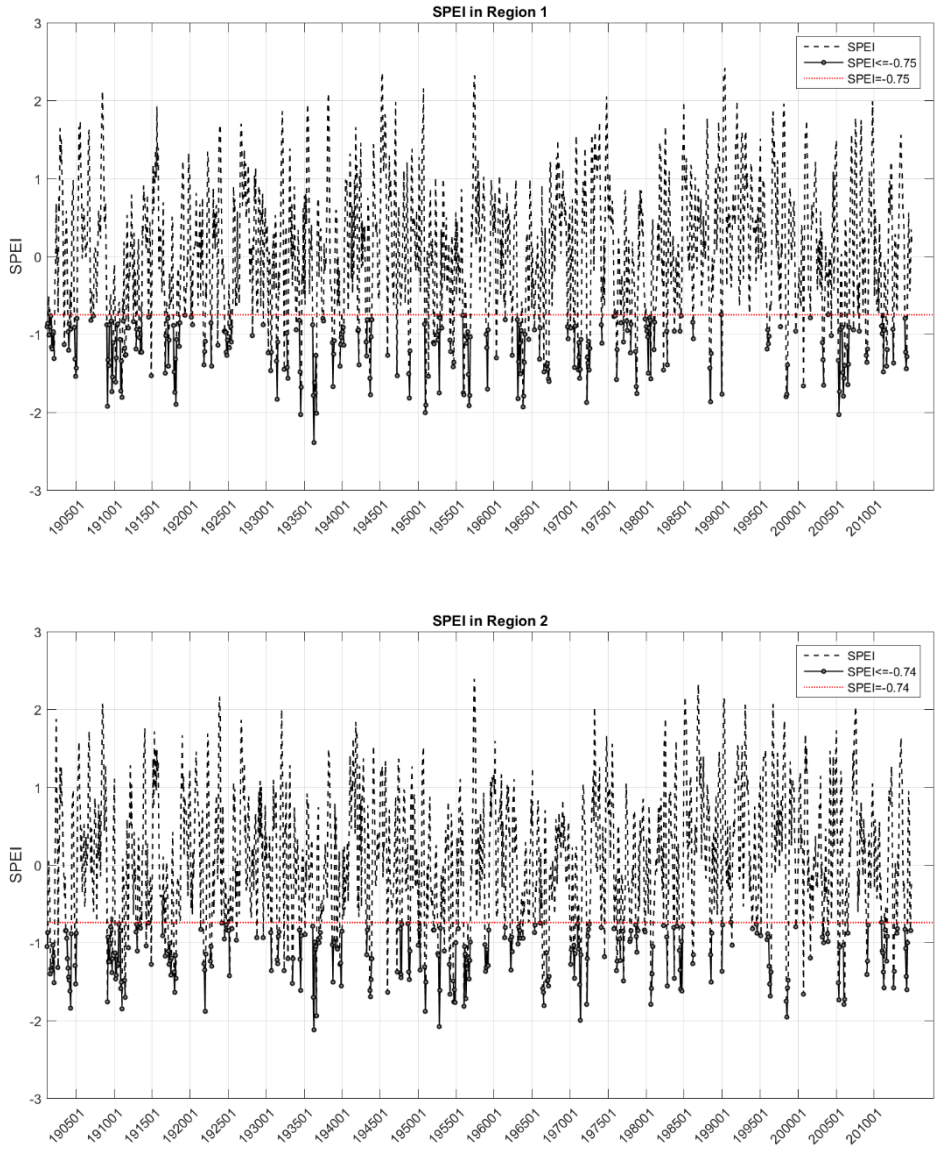

Figure A.4 SPEI values for each region in Oklahoma from 1901 to 2014 (SPEI3).

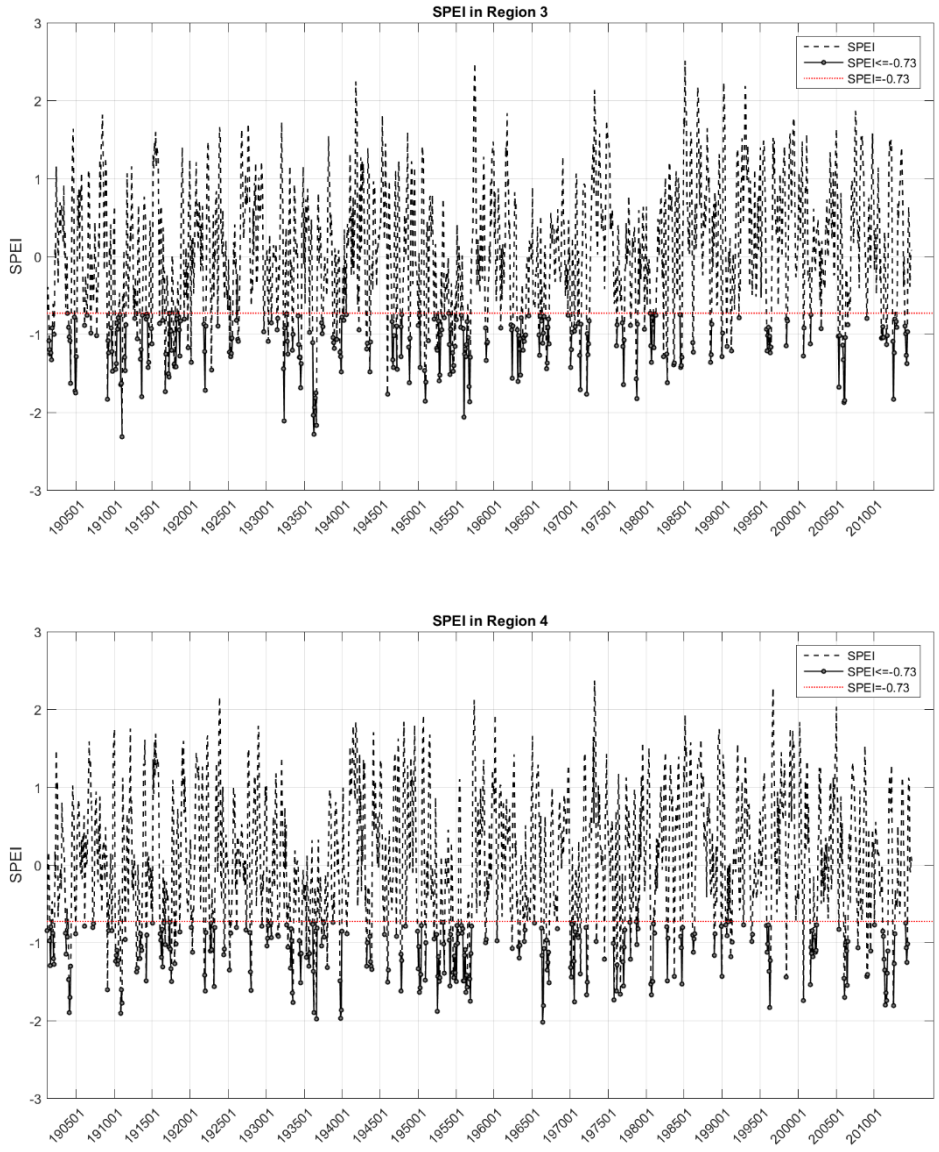

Figure A.4 Continued

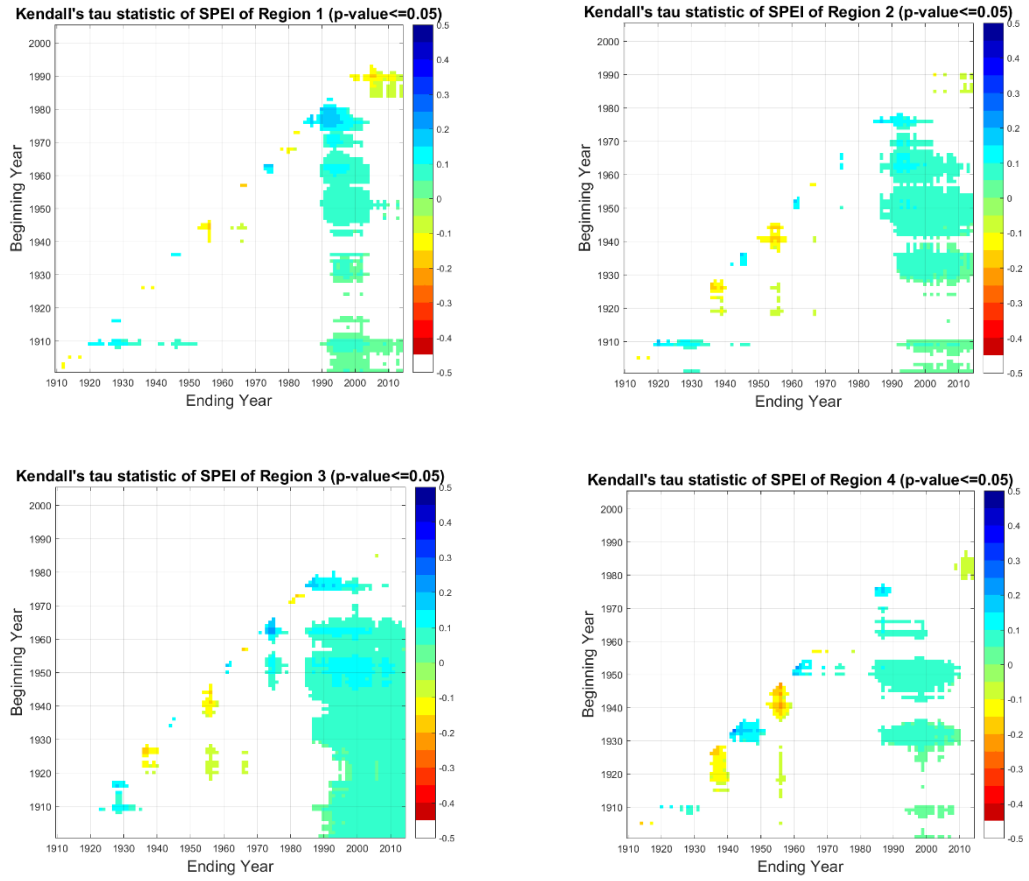

Figure A.5 Kendall's tau statistic to test for trends in the 1-month SPEI for all time periods longer than 10 years. Blue colors indicate statistically significant increasing trends (wetter conditions) in the SPEI and red colors indicate statistically significant decreasing trends (drier conditions). Each region in Oklahoma is shown separately.

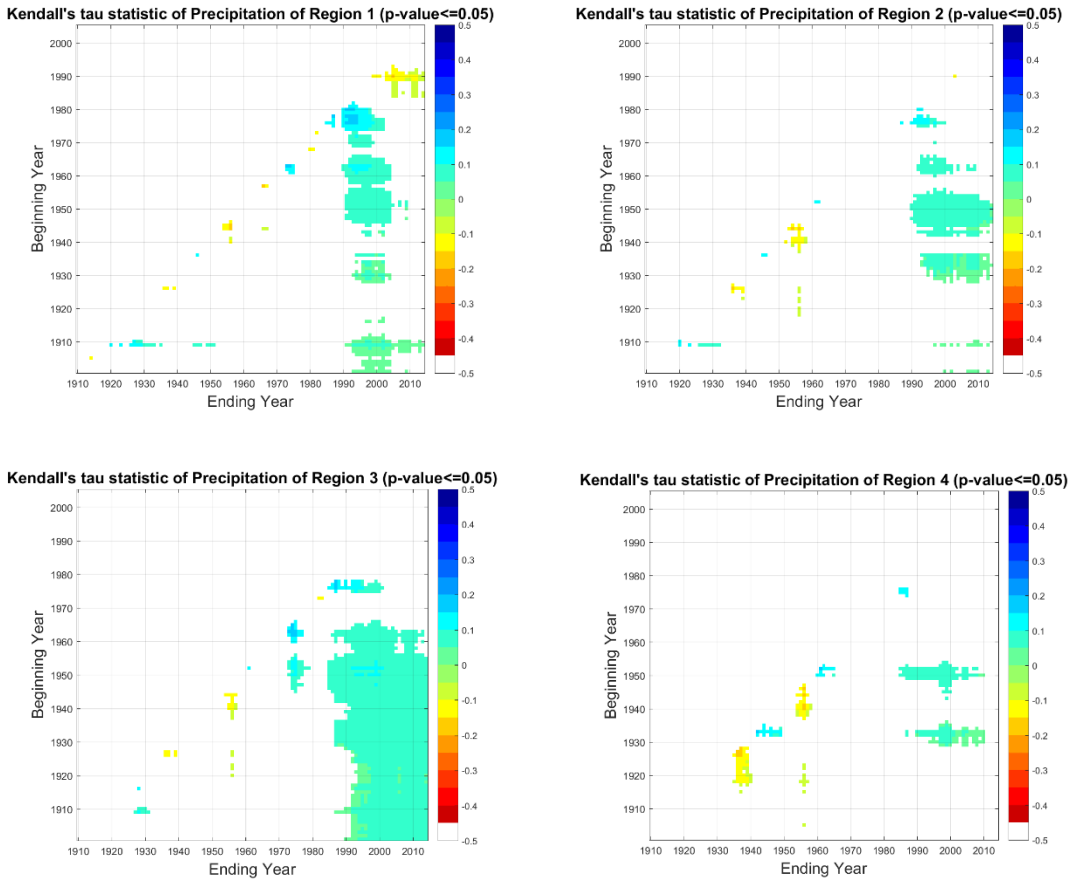

Figure A.6 Kendall's tau statistic to test for trends in the precipitation at 1 month scale for all time periods longer than 10 years. Blue colors indicate statistically significant increasing trends (wetter conditions) in the precipitation and red colors indicate statistically significant decreasing trends (drier conditions). Each region in Oklahoma is shown separately.

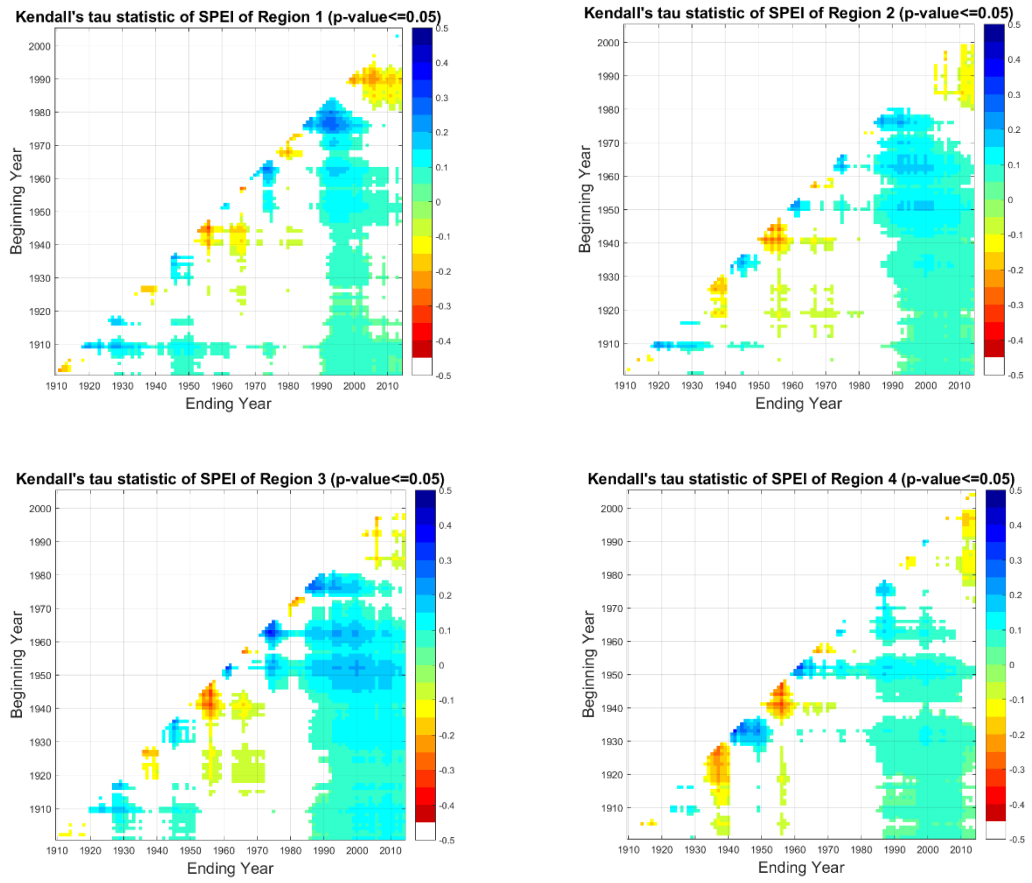

Figure A.7 Kendall's tau statistic to test for trends in the 3-month SPEI for all time periods longer than 10 years. Blue colors indicate statistically significant increasing trends (wetter conditions) in the SPEI and red colors indicate statistically significant decreasing trends (drier conditions). Each region in Oklahoma is shown separately.

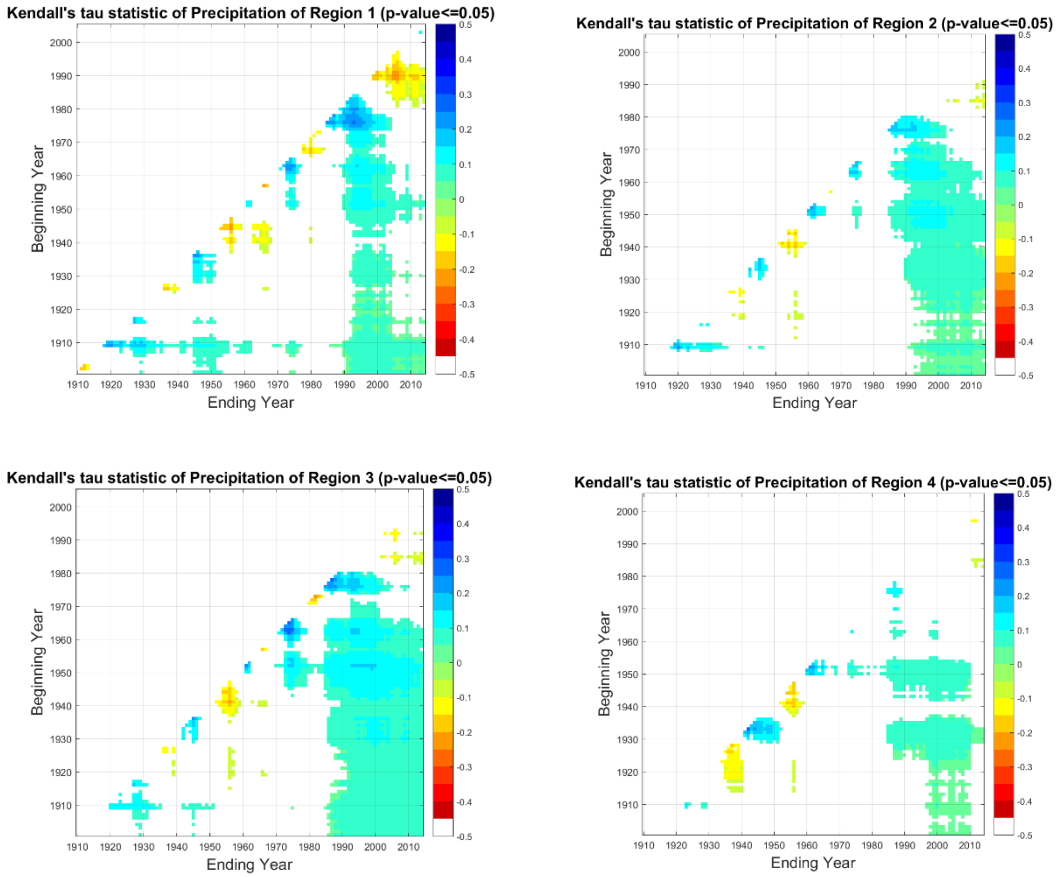

Figure A.8 Kendall's tau statistic to test for trends in the precipitation at 3 month scale for all time periods longer than 10 years. Blue colors indicate statistically significant increasing trends (wetter conditions) in the precipitation and red colors indicate statistically significant decreasing trends (drier conditions). Each region in Oklahoma is shown separately.

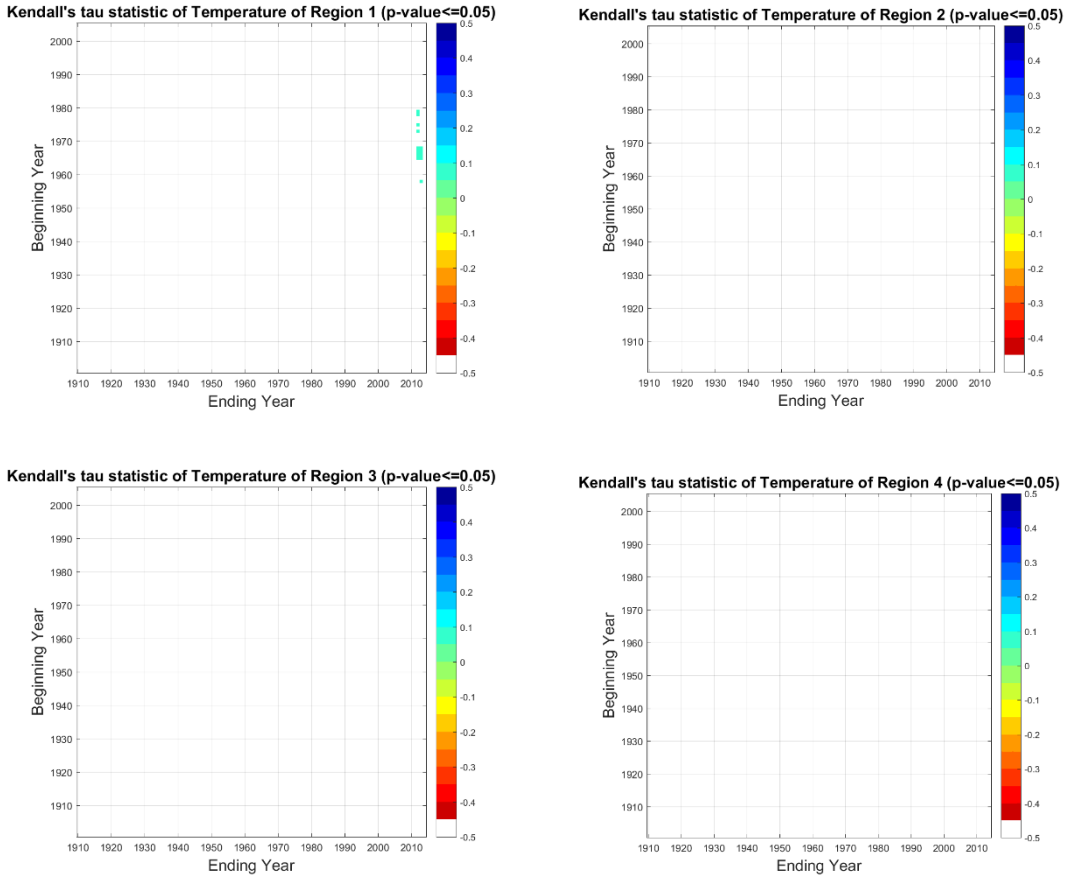

Figure A.9 Kendall's tau statistic to test for trends in the temperature at 3 month scale for all time periods longer than 10 years. Blue colors indicate statistically significant increasing trends (warmer conditions) in the temperature and red colors indicate statistically significant decreasing trends (cooler conditions). Each region in Oklahoma is shown separately.

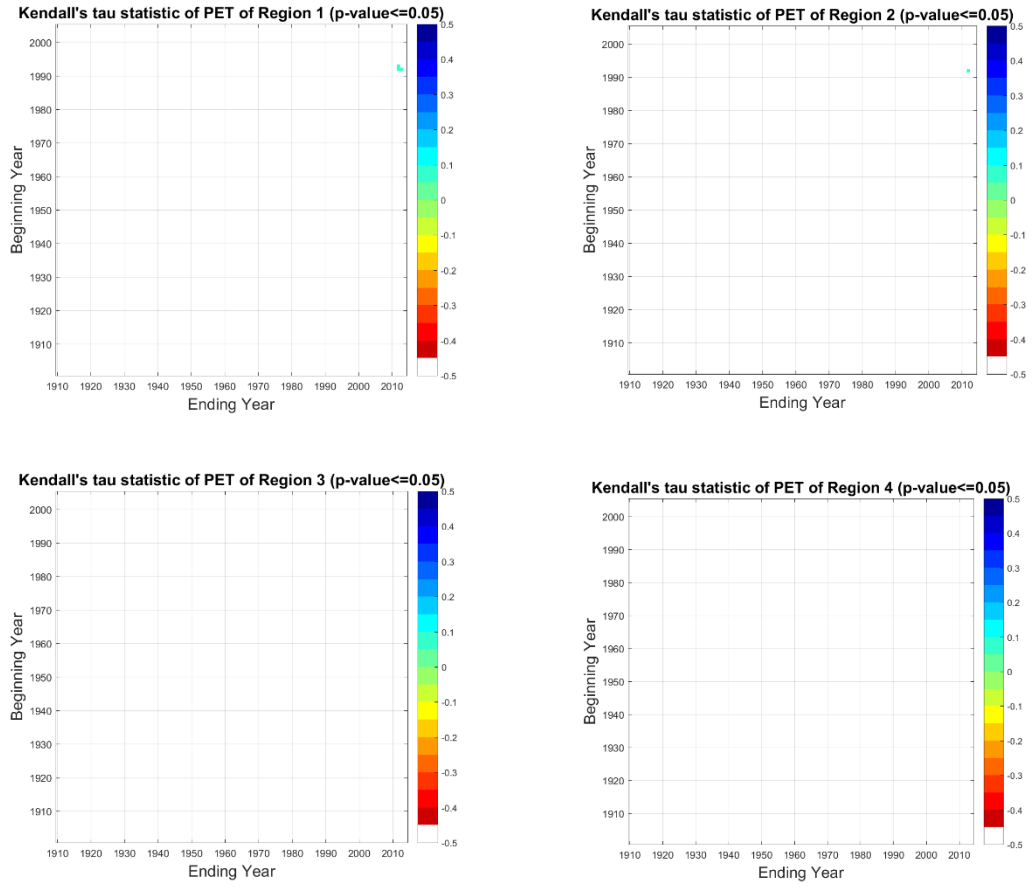

Figure A.10 Kendall's tau statistic to test for trends in the PET at 3 month scale for all time periods longer than 10 years. Blue colors indicate statistically significant increasing trends in the PET and red colors indicate statistically significant decreasing trends (drier conditions). Each region in Oklahoma is shown separately.